TURKISH LRFD LIVE LOAD DESIGN PARAMETERS FOR CABLE STAYED BRIDGE WITH CONCRETE DECK ON STEEL GIRDER

A THESIS SUBMITTED TO
THE GRADUATE SCHOOL OF NATURAL AND APPLIED SCIENCES
OF
MIDDLE EAST TECHNICAL UNIVERSITY

BY

YUSUF DÖNMEZ

IN PARTIAL FULFILLMENT OF THE REQUIREMENTS FOR
THE DEGREE OF MASTER OF SCIENCE IN
CIVIL ENGINEERING

JUNE 2015

Approval of the thesis:

TURKISH LRFD LIVE LOAD DESIGN PARAMETERS
FOR
CABLE STAYED BRIDGE WITH CONCRETE DECK ON STEEL GIRDER

submitted by **YUSUF DÖNMEZ** in partial fulfillment of the requirements for the degree of **Master of Science in Civil Engineering Department, Middle East Technical University** by,

Prof. Dr. Gülbin Dural Ünver
Dean, Graduate School of **Natural and Applied Sciences** _____

Prof. Dr. Ahmet Cevdet Yalçıner
Head of Department, **Civil Engineering** _____

Assoc. Prof. Dr. Alp Caner
Supervisor, **Civil Engineering Dept., METU** _____

Examining Committee Members:

Prof. Dr. Ahmet Türer
Civil Engineering Dept., METU _____

Assoc. Prof. Dr. Alp Caner
Civil Engineering Dept., METU _____

Assoc. Prof. Dr. Afşin Sarıtaş
Civil Engineering Dept., METU _____

Assoc. Prof. Dr Eray Baran
Civil Engineering Dept., METU _____

Asst. Prof. Dr. Burcu Güldür
Civil Engineering Dept., Hacettepe University _____

Date: 09.06.2015

I hereby declare that all information in this document has been obtained and presented in accordance with academic rules and ethical conduct. I also declare that, as required by these rules and conduct, I have fully cited and referenced all material and results that are not original to this work.

Name, Last Name : Yusuf DÖNMEZ

Signature :

ABSTRACT

TURKISH LRFD LIVE LOAD DESIGN PARAMETERS
FOR
CABLE STAYED BRIDGE WITH CONCRETE DECK ON STEEL GIRDER

Dönmez, Yusuf
M.S., Department of Civil Engineering
Supervisor: Assoc. Prof. Dr. Alp Caner

June 2015, 121 pages

In Turkey, bridge design procedure has been followed from a modified version of the AASHTO LFD (Load Factor Design) or ASD (Allowable Stress Design) requirements until now. The recent switch of the US bridge codes to LRFD method also necessitates the calibration of the new design of the Turkish bridges according to the LRFD system. The main aim of this study is to develop the load and resistance factors to be implemented in the design of steel composite I-girders of cable-stayed bridges (span lengths 420 m to 550 m) for the basic gravity load combination. Moreover, the performance of new type of live (truck) load of Turkish LRFD, namely, AYK-45 is evaluated. In such studies, usually a target reliability index is selected to reflect the safety level of current design practice based on the uncertainties associated with the design parameters. For the basic gravity load combination, which includes the dead and live loads, a minimum target reliability of 4.30 is selected, instead of 3.50 that have been used in US. In the statistical computations of the reliability index, the quantification of uncertainties is made based on local data supplemented by information compiled from relevant international literature.

Keywords: Reliability Analysis, Reliability Index, Target Reliability Level, Long Span Bridge Live Load Models, Cable Stayed Bridge Girders, Load and Resistance Factor Calibration, LRFD.

ÖZ

GERGİN EĞİK ASKILI KÖPRÜLER İÇİN
HAREKETLİ YÜK TASARIM PARAMETRELERİNİN
TÜRK LRFD METHODU İÇİN BELİRLENMESİ

Dönmez, Yusuf
Yüksek Lisans, İnşaat Mühendisliği
Tez Yöneticisi: Doç. Dr. Alp Caner

Haziran 2015, 121 sayfa

Türk köprü tasarım pratiğinde AASHTO limit durum tasarım kılavuzunun değiştirilmiş versiyonu ve emniyet gerilmeleri tasarım yöntemleri uygulana gelmiştir. Günümüzde ise Amerikan köprü şartnamelerinin limit durum tasarımdan, yük ve dayanım katsayıları tasarım yöntemine geçmesi Türkiye'de de yeni yük ve dayanım katsayıları tasarım yönteminin geliştirmesi ihtiyacını doğurmuştur. Bu çalışmadaki esas amaç çelik kompozit I-kirişli gergin eğik askılı köprülerin (420m'den 550m'ye açıklığa sahip) tasarımında kullanılacak hareketli yüklere uygun yük ve dayanım katsayısı belirlemektir. Dahası, bu çalışmada Türk LRFD şartnamesinin yeni hareketli yük modeli olan AYK-45 kamyonun performansı da irdelenecektir. Bu tür çalışmalarda, genellikle mevcut köprülerin güvenirlik durumları tasarım parametrelerinin belirsizlikleri üzerinden değerlendirilerek bir hedef güvenirlik indisi belirlenir. Ölü ve hareketli yükleri barındıran temel düşey yük kombinasyonu için asgari hedef güvenirlik indisi Amerika'da 3.50 seçilmesine karşın, bu çalışmada 4.30 olarak seçilmiştir. Güvenirlik indisinin istatistiki hesaplarının içerdiği belirsizlikler yerel kaynaklardan elde edilen verilere göre belirlenmiş olup, elde edilemeyen yerel bilgiler için uluslararası ilgili çalışmalardan yararlanılmıştır.

Anahtar Kelimeler: Güvenirlik Analizi, Güvenirlik Endeksi, Hedef Güvenirlik Seviyesi, Uzun Açıklı Köprü Hareketli Yük Modelleri, Gergin Eğik Askılı Köprü Kirişleri, Yük ve Dayanım Katsayısı Kalibrasyonu, LRFD.

To My Wife and Parents,

ACKNOWLEDGMENTS

The author deeply appreciates his supervisor Assoc. Prof. Dr. Alp Caner for the continuous guidance and constructive criticism he has provided throughout the preparation of the thesis. Without his encouragement and patience, this thesis would not have been completed.

I would also like to express my sincere thanks to Prof. Dr. Ahmet Türer, Assoc. Prof. Dr. Afşin Sarıtaş, Assoc. Prof. Dr. Eray Baran, and Asst. Prof. Dr. Burcu Güldür for their suggestions and contributions during my thesis defense.

The author also would like to thank Turkish General Directorate of Highways for providing data and guidance in this study and all specialists and researchers who involved in TUBITAK 110G093 project.

I should also thank my dearest friends Mustafa Berk Duygu, Mehmet Kemal Ardoğa, Çağın Çetinyürek, Ömer Kevran and Bahadır Tunç for their great friendship and for giving moral and academic support.

The last but not least, the author wants to express his sincere thanks to his wife, Meltem Dönmez and his parents Gürcan Dönmez and Nazife Dönmez for the encouragement and love they have given him not only throughout the completion of this thesis but also his whole life.

TABLE OF CONTENTS

LIST OF TABLES

TABLES

LIST OF FIGURES

FIGURES

CHAPTER 1

INTRODUCTION

Bridges are one of the most important components of highway and railway network system and need to be designed and constructed to meet serviceability and ultimate limit state requirements of the specifications.

In Turkish engineering practice, Load Factor Design (LFD) based design approach is typically used to design highway bridges. LFD based design approach is an adapted version of "AASHTO Standard Specifications for Highway Bridges", which was terminated in US designs after 2010. Since design trend changed from LFD concept to LRFD concept in the world, General Directorate of Highways (KGM) of Turkey has started an extensive research program to shift the design concept from LFD to LRFD (probability-based design method).

Load and resistance are two basic components of the calibration process. Calibration of load and resistance factors was performed based on experience gained from Allowable Stress Design (ASD) and judgment in the LFD method. However, in the LRFD method, calibration of load and resistance factors is performed based on study of statistical parameters of the load and resistance. The major aim of LRFD method is to provide a uniform and steady safety margin for different types of structures. The study of calibration of AASHTO LRFD method was done by using statistical parameters belonging to design and construction practices in the US. Hence, the same calibration process to develop the LRFD method shall also be repeated based on uncertainties of Turkish engineering practices and construction techniques.

The first and the most basic rule of design is that resistance should be higher than the loads acting on the structure. However, due to uncertainties there is always a possibility that the loads acting on structure may be higher than the resistance. The load factors and resistance factors are calibrated in such a way that probability of failure is indirectly quantified in design. Developing a design method based on probabilistic approach needs to investigate the uncertainties of loads and resistance.

Reliability index, β, is the most popular bridge safety measurement tool in probabilistic approach. β is an indicator of probability of survival as well as probability of failure. Calibration process aims to reach the chosen target reliability index with suitable load and resistance factors.

1.1 Aim

The main aim of this study is the calibration of load and resistance factors for the design of composite steel plate girder of cable stayed bridges at positive moment region by considering uncertainties of Turkish engineering practice using probabilistic methods to determine a uniform safety. Another purpose of this study is to compare the new live load model of Turkish LRFD suggested by Koç (2013) which is AYK-45 with other live load models.

AASHTO LRFD Strength I limit state is considered for calibration of cable-stayed bridges with a main span of 420m to 550m considering uncertainties of the design and construction practices in Turkey. However, international literature have been used for locally unavailable uncertainty data.

For live load models used in this study, statistical parameters are calculated using truck survey data belonging to years 2005, 2006 and 2013 obtained from the Division of Transportation and Cost Studies of the General Directorate of Highways of Turkey.

When the total expected cost of a structure is minimized, then optimum target reliability is determined. The total expected cost involves the cost of project design and construction, and also the expected cost of failure. The cost of failure involves both the cost of replacement or repair and the cost of shortage of use. Moreover, legal costs (liability in case of injuries) are included in the cost of failure. Therefore, considering the economy, it is reasonable to separate the bridge components into two as primary and secondary elements. Target reliability index for primary components is higher than that for secondary components.

As the main consideration of this study, girders are the primary and repairable components of cable-stayed bridges (Nowak and Szerszen, 2000). As target reliability index 4.30 is aimed for composite girders of cable-stayed bridges at positive flexural region. In the calibration of AASHTO LRFD in the US, reliability index is targeted as 3.50.

In this study, flexural designs and analyses of four cable-stayed bridge composite steel girders having span length varying from 420 m to 550m are performed for four different live load models, namely, AYK-45, HL-93, H30-S24 and grouped survey truck load. As design process, AASHTO LRFD specification requirements have been followed. Reliability indices are evaluated for different sets of resistance factors by using MVFOSM (Mean Value First Order Second Moment).

1.2 Scope

Reliability index analysis for a variation of load and resistance factors to be used in live load and dead load strength design of cable stayed bridges is gathered in seven chapters.

In Chapter 2 literature is reviewed. Live load models for long-span bridges throughout world is stated. Calibration procedures of AASHTO LRFD and Turkish LRFD for different types of bridges are presented. Moreover, other load and resistance factor calibration researches are summed up.

In Chapter 3, statistical parameters of loads are presented. AYK-45, HL-93, H30-S24 and grouped truck obtained from surveyed data live load models are explained. The maximum live load impact is obtained with projection of results to 75-year by using the extreme value theory. In addition, for dead loads and dynamic load, statistical parameters are stated.

In Chapter 4, statistical parameters of resistance are presented for uncertainties pertaining to Turkish engineering and construction practice. These uncertainties are used in reliability index analysis.

In Chapter 5, nominal positive flexural resistance capacity of composite steel girder is stated based on AASHTO LRFD Bridge Design Specifications. Besides, all structural analyses and design results presented.

In Chapter 6, used reliability analysis method is introduced. Furthermore, reliability analysis of girders designed and analyzed for all live load models are presented. Reliability indices are given with respect to span length and also with respect to resistance factors. The comparison of results are discussed within this chapter.

Finally, main findings of the study are presented in Chapter 7. Conclusions are drawn and further studies to be conducted in future are recommended.

1.3 Studied Bridge Properties

In this study, a real life cable-stayed bridge which is Cooper River Bridge in South Carolina is selected as reference bridge design. Original bridge has a main span length of 470 meters and 195 meters edge spans. From original bridge type by modifying the span dimensions other three bridges are obtained to increase the span length range of the study. The bridge dimensions and some properties are tabulated in Table 1-1 for all four different studied bridges. Moreover, in Figure 1-1 and Figure 1-2 side view of Cooper River Bridge and typical section for main span of Cooper River Bridge are presented, respectively.

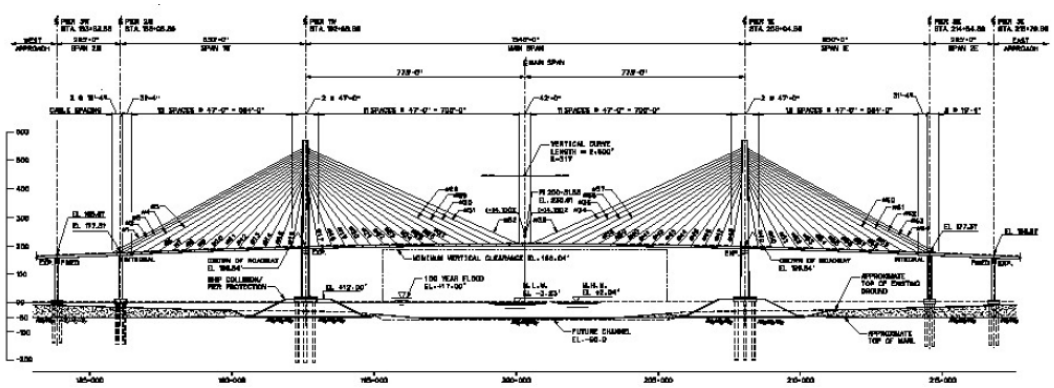

Figure 1-1 Side View of Cooper River Bridge (Abrahams et al.)

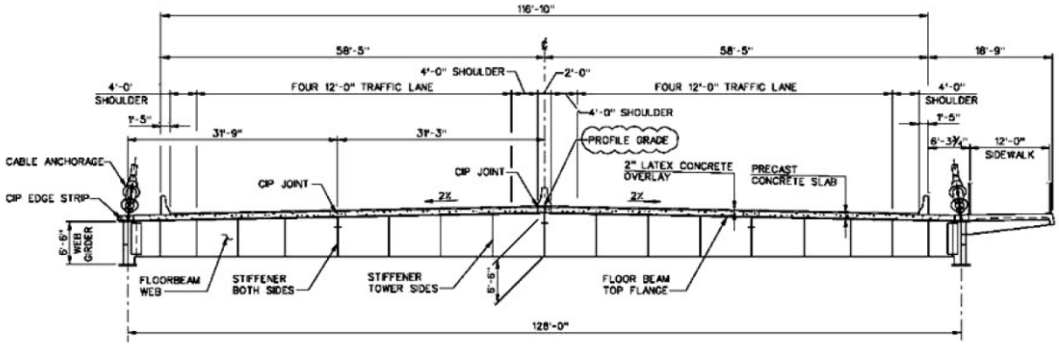

Figure 1-2 Typical Section for Main Span of Cooper River Bridge (Abrahams et al.)

Table 1-1 Some Important Bridge Dimensions and Properties

Bridge Number	Main Span Length (m)	Edge Span Length (m)	Width (m)	Lane Number	Cable Spacing (m)
Bridge #1	420	195	39	6	14.65
Bridge #2 (Original)	470	195	39	6	14.65
Bridge #3	500	205	39	6	14.65
Bridge #4	550	210	39	6	14.65

In this study, only positive moment region at mid-span will be investigated because positive moment is more critical than the negative moment. Moment diagram of a live load moving on the bridge and dead load for main span are presented in Figure 1-3 and Figure 1-4, respectively.

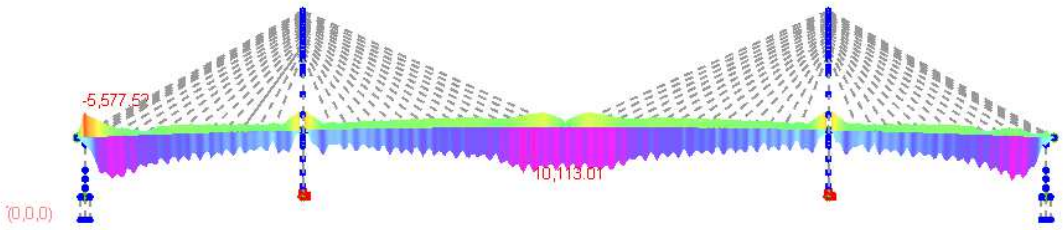

Figure 1-3 Moment Diagram of a Cable Stayed Bridge for Moving Load

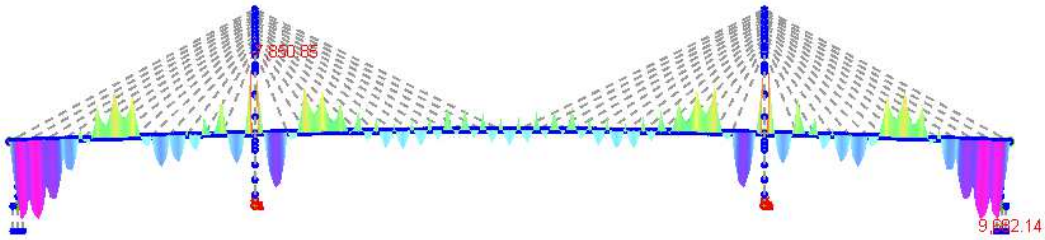

Figure 1-4 Moment Diagram of a Cable Stayed Bridge for Dead Load

1.4 Chapter Summary

In this chapter, the major aims of study, scope and bridge properties are discussed. There are two important points that writer wants to investigate. The first one is to calibrate the load & resistance factors for the design of composite steel plate girder of cable stayed bridges at positive moment region by considering local conditions of Turkey and probabilistic methods (LRFD). The second one is to compare the performance of new live load model of Turkish LRFD, suggested by Koç (2013) which is AYK-45, with other well-known live load models. In this study, four different cable-stayed bridge models are used having main span length of 420m to 550m. In following chapter, the literature is reviewed about the topic of this study which is load and resistance factors calibration and live load models for long-span bridges.

CHAPTER 2

LITERATURE REVIEW

2.1 Literature Survey

Bridge designs made by Allowable Stress Design and Load Factor Design methods do not usually provide a uniform safety level for design of different bridges. Hence, to be able to obtain a uniform safety level different and new bridge design method which is based on probabilistic approach, namely, LRFD is developed.

The study conducted by Nowak, namely, “Report 368: Calibration of LRFD Bridge Design Code” which is a report of National Cooperative Highway Research Program describes the LRFD calibration process for loads and resistance (Nowak, 1999). The main parts of this report are calibration process, load and resistance models, reliability analysis and load and resistance factor development. In this thesis, Report 368: Calibration of LRFD Bridge Design Code is utilized as the main guideline.

Calibration Report describes six main steps for calibration procedure. These steps are as follows;

- Selection of bridges
- Preparing the statistical database for load and resistance parameters
- Establishing the load and resistance models
- Development of the reliability analysis procedure
- Choosing of the target reliability index
- Calculation of load and resistance factors

For LRFD calibration study, about 200 newly constructed bridges are chosen from different places of the US. Load effects like moments, shears, tensions and compressions were determined for about 200 bridges and their members. Moreover, load carrying capacities were calculated for each of them. The database is obtained for loads and resistance by using local conducted surveys, material property tests, and field measurements. This study assumed that loads and resistance were random variables. Therefore, they were described in terms of cumulative distribution

functions (CDF). Then, live load and resistance (bridge girders) models were introduced. Live load model were constructed by considering multiple presence of trucks, dynamic load of trucks and two trucks side-by-side. After that, structural reliability was evaluated in terms of reliability index (β). Reliability index was calculated by an iterative procedure. The procedure was defined by Rackwitz and Fiessler. Then, a target reliability index (β_T) was selected. β_T is adequately selected by considering existing structures' reliability level. As final step, load and resistance factors were calculated with achieving target reliability index (Nowak, 1999).

Reliability analysis was performed by using average daily truck traffic (ADTT) = 5000 in the Calibration Report at final stage. By using ADTT equals to 5000, AASHTO LRFD uses the design equation below as Strength Limit State I.

$$1.25\,x\,D\ +1.50\,x\,D_A\ +1.75\,x\,(1\ +I)\,x\,L\ <\emptyset R \qquad (2\text{-}1)$$

in which D is load effect due to factory made elements and cast-in place concrete, D_A is load effect due to the wearing surface and miscellaneous weight, and (1+I)L is load effect due to live load including impact factor.

Kun and Qilin (2012) conducted a research in China for calibration of resistance factor and for determining target reliability index of steel highway bridges. This study was conducted for two commonly used steel grades in China bridges (Q235q and Q345qD). In this research, different type of failure modes are investigated. These are flexure γ_{R1}, shear γ_{R2}, axial tensile γ_{R3}, axial compression γ_{R4}, and eccentric compression γ_{R5}. The main purpose of this study was to prepare a new design guideline for steel highway bridges in China by using load and resistance local database. As a result of the research, recommended target reliability indices are tabulated in Table 2-1 (Kun and Qilin, 2012).

Table 2-1 Recommended Target Reliability Indices (Kun and Qilin, 2012)

Load Combination	Safety of structure					
	Class I		Class II		Class III	
	Ductile failure	Brittle failure	Ductile failure	Brittle failure	Ductile failure	Brittle failure
Primary	5.7	7.2	5.2	6.7	4.7	6.2
Adjunctive	4.2	5.7	3.7	5.2	3.2	4.7

In Table 2-2 resistance factors are presented for different load combinations and steel grades and failure modes of members, i.e. axial tension, axial compression, eccentric compression, flexural, and shear. The basic design equation for the following table is $M_n/\gamma \geq M_u$ where M_n is resistance capacity, M_u is ultimate demand and γ is resistance factor.

Table 2-2 Recommended Resistance Factors (Kun and Qilin, 2012)

Steel	Load Combination	Resistance factor, γ_{Ri}				
		γ_{R1}	γ_{R2}	γ_{R3}	γ_{R4}	γ_{R5}
Q235q	Primary	1.2687	1.2996	1.3431	1.3592	1.8895
	Adjunctive	1.2034	1.2273	1.3027	1.3150	1.8009
Q345qD	Primary	1.2629	1.3804	1.3654	1.3656	2.1806
	Adjunctive	1.2049	1.3194	1.3217	1.3248	2.1302

In 2010, Argınhan studied a thesis having the title of “Reliability Based Safety Level of Turkish Type Precast Pre-stressed Concrete Bridge Girders Designed in accordance with LRFD”. In his study, four different types of precast concrete girders are considered varying span lengths of 25 to 40 m. Load and resistance statistical parameters were obtained from local database and relevant international literature where necessary. He used different sets of load and resistance factors in design process of girders to investigate the change in reliability indices. As live load models, Turkish live load, H30S24 and AASHTO LRFD live load, HL93 were used in his study. He calculated reliability indices for each of the designed girders. In Figure 2-1, reliability analyses results of girders for HL93 loading by 15 different sets of load and resistance factors are presented.

Koç (2013) conducted a study on steel bridge design and his analysis approach is very similar to Argınhan's study (2010) where pre-stressed concrete bridges are investigated. Koç (2013) considered the bridges varying span lengths of 50 to 80 m. As live load models, AASHTO LRFD live load, HL93 and a newly suggested live load model by Koç, AYK-45 were used in his study. In Table 2-3, reliability analyses results of girders for AYK-45 loading by 15 different sets of load and resistance factors were tabulated.

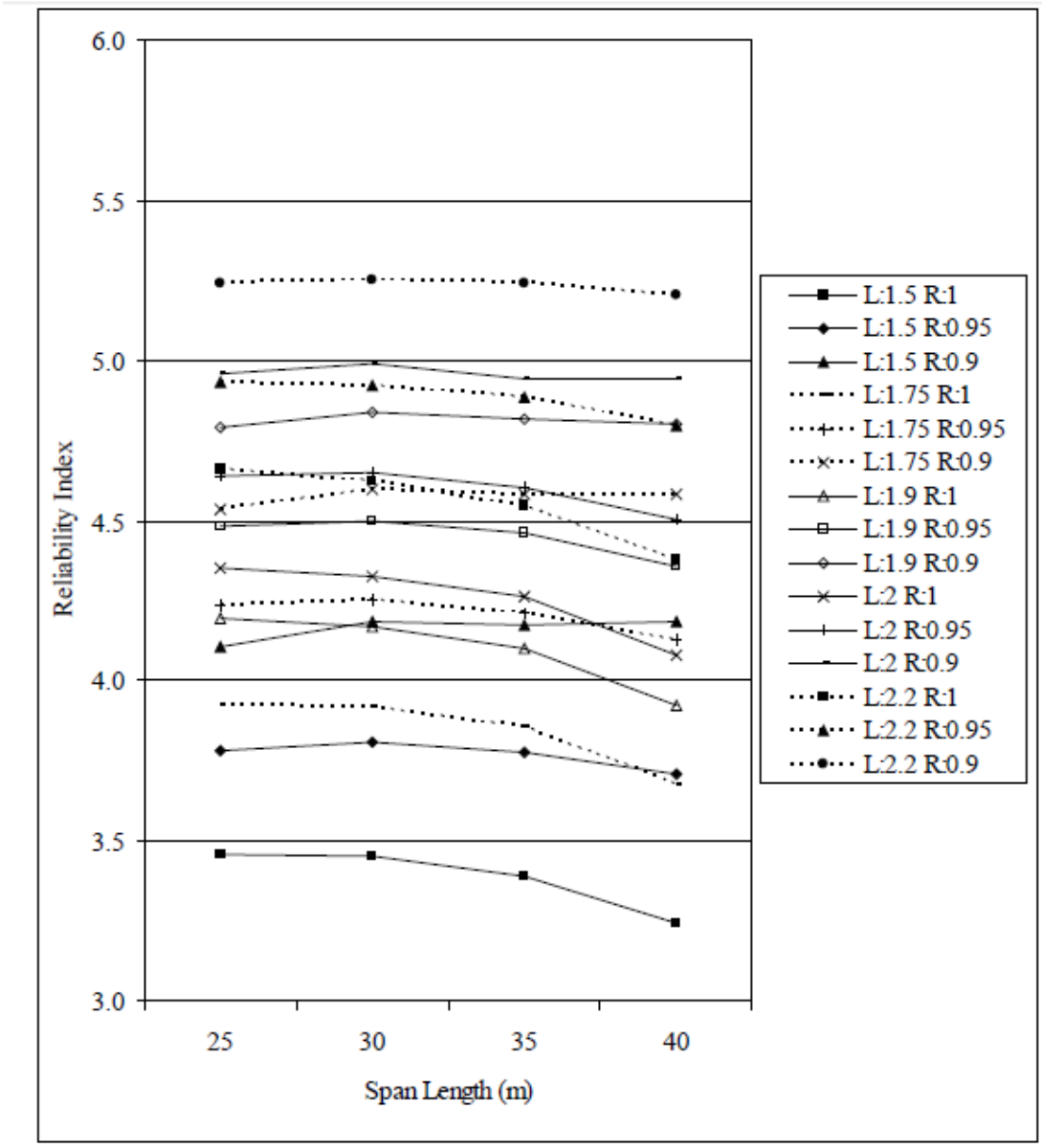

Figure 2-1 Reliability Indices for Different Sets of Load and Resistance Factors (HL93) (Argınhan, 2010)

Wang and et al. (2014) summarized the traffic load in current design codes for long-span suspension bridges. This case study discusses the traffic loads for long-span bridges defined in BS5400, AASHTO LRFD, Sweden TK BRO, Great Belt (East) Bridge Design Basis, the Superstructure Design of Honshu-Shikoku Bridge of Japan, and the Highway Bridge Design Code of China. The live load models of mentioned design codes are summarized.

Table 2-3 Reliability Indices for Different Sets of Load and Resistance Factors (AYK45) (Koç, 2013)

Live Load (LL) and	Span Length (m)				Average
Resistance (R) Factors	50	60	70	80	β
LL: 1.50; R: 0.90	4.53	4.41	4.40	4.29	4.41
LL: 1.50; R: 0.95	4.31	4.14	4.11	3.99	4.14
LL: 1.50; R: 1.00	4.02	3.86	3.83	3.69	3.85
LL: 1.75; R: 0.90	4.89	4.74	4.74	4.60	4.74
LL: 1.75; R: 0.95	4.63	4.49	4.46	4.32	4.48
LL: 1.75; R: 1.00	4.39	4.23	4.19	4.03	4.21
LL: 2.00; R: 0.90	5.20	5.20	5.03	4.89	5.08
LL: 2.00; R: 0.95	4.97	4.80	4.77	4.62	4.79
LL: 2.00; R: 1.00	4.73	4.56	4.51	4.34	4.54
LL: 2.25; R: 0.90	5.47	5.48	5.30	5.14	5.35
LL: 2.25; R: 0.95	5.26	5.24	5.05	4.88	5.11
LL: 2.25; R: 1.00	5.03	4.84	4.80	4.62	4.82
LL: 2.50; R: 0.90	5.71	5.73	5.54	5.37	5.59
LL: 2.50; R: 0.95	5.51	5.50	5.30	5.12	5.36
LL: 2.50; R: 1.00	5.30	5.27	5.06	4.88	5.13

BS5400 Part 2: BS 5400 has offered a load model for long-span bridges shown in Figure 2-2. This model include dynamic impact. The curve of the model has two equations for 0-50 meters span length and 50-1600 meters span length.

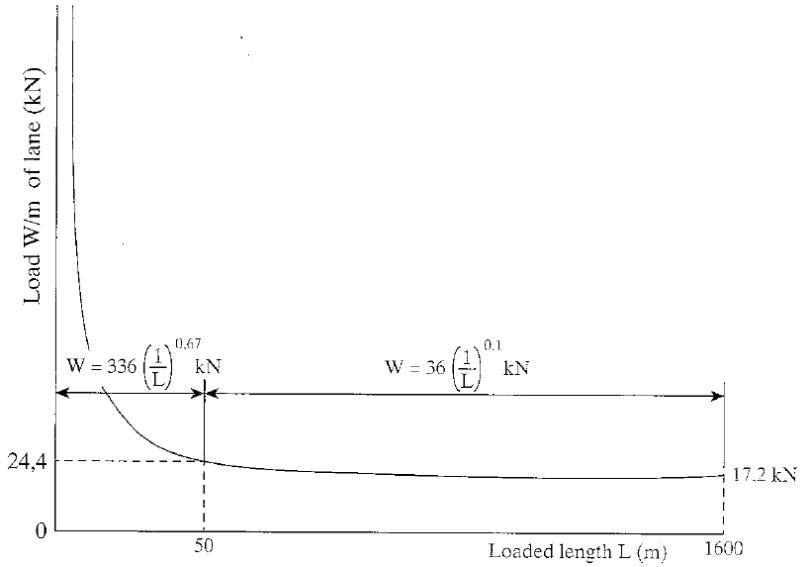

Figure 2-2 The Loading Curve of HA UDL of BS5400 (BS5400 Part-2)

AASHTO Code 2007: AASHTO 2007 code has provided a load model composed of a design truck load and a lane load. However, there is no limitation for span length of the bridge. Moreover, in this model dynamic load effect and multiple presence are considered separately with applying some other pre-defined coefficients. The load model is shown in Figure 2-3.

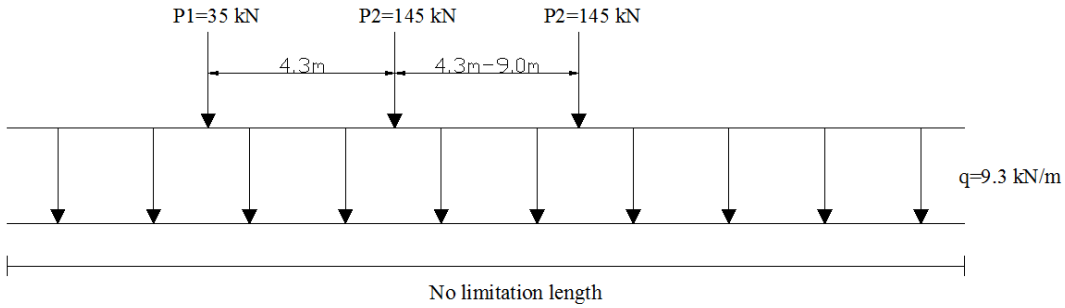

Figure 2-3 The Load Model of AASHTO 2007 (AASHTO LRFD 2007)

Swedish Code TK BRO 2009: In this code, there is a live load model for bridges having span length larger than 200 meters. The load model and its load values are presented in Figure 2-4 and Table 2-4 below.

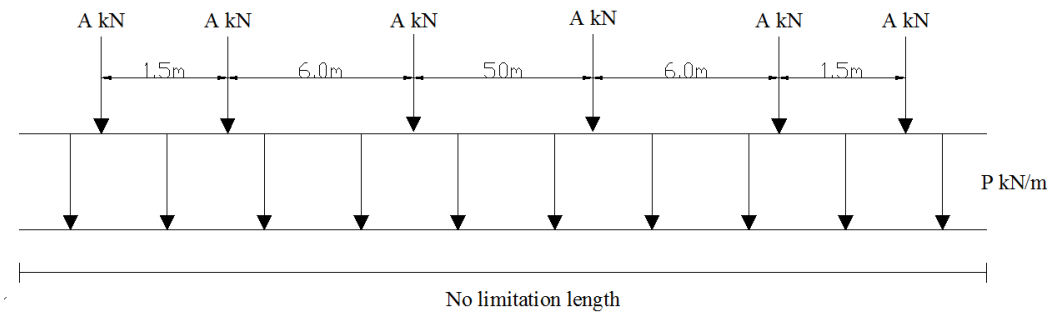

Figure 2-4 Swedish Traffic Load of Bridge when its main span is larger than 200m (Swedish Code TK BRO 2009)

Table 2-4 The UDL and KEL of Swedish Code TK Bro (Swedish Code TK BRO 2009)

Number of Lanes	Linear meter load P (kN/m)	Concentrated load A (kN)
First lane	12	250
Second lane	9	170
Third and subsequent lane	6	0

Great Belt (East) Bridge Design Basis: Great Belt Bridge design basis was prepared based on probabilistic modeling and statistics. The load model is presented in Figure 2-5 and Figure 2-6.

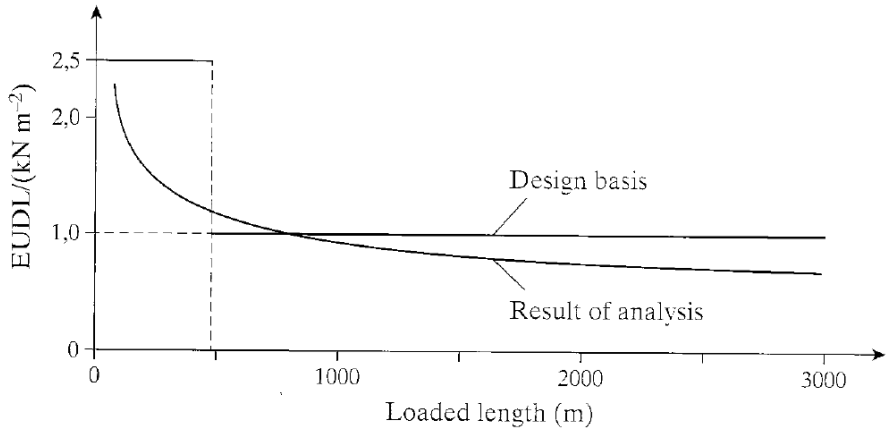

Figure 2-5 UDL (Uniform Distributed Load) in the second direction as function of loaded length of the positive influence (Great Belt Bridge Design Basis)

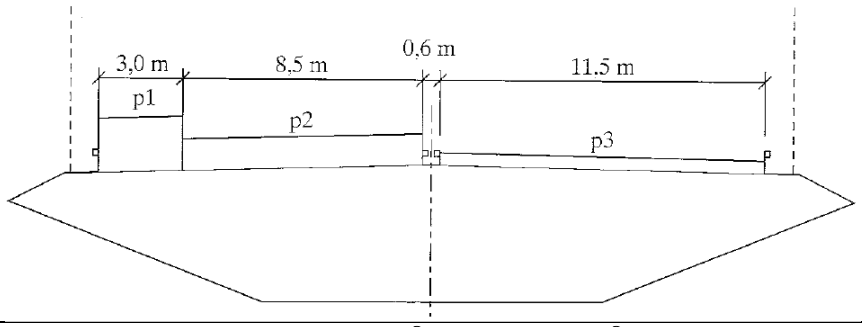

P1=5.0 kN/m^2, P2=2.5 kN/m^2
P3=2.5 kN/m^2 when the loaded length is less than 500m
P3=1.0 kN/m^2 when the loaded length is not less than 500m

Figure 2-6 Equivalent UDL of Great Belt Bridge (Great Belt Bridge Design Basis)

The Highway Bridge Design Code of China: This Chinese code has provided a load model composed of a concentrated load and a uniformly distributed load. However, there is no limitation for span length of the bridge. Moreover, in this live load model reduction and multiple presence are considered separately with applying some other pre-defined coefficients by multiplying the obtained internal forces due to live load model. The load model is presented in Figure 2-7 and Tables 2-5 and 2-6 below.

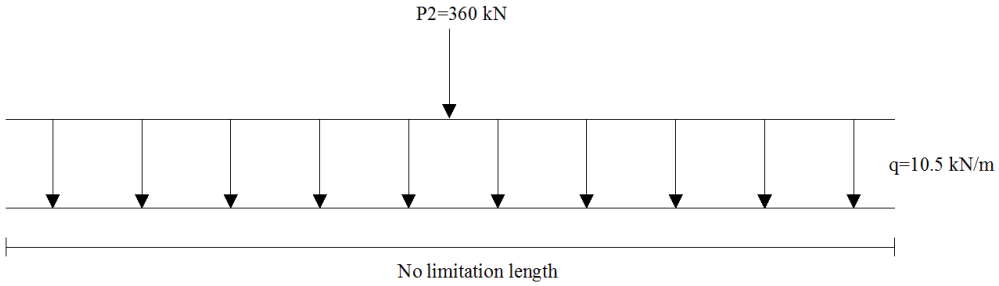

Figure 2-7 The Load Model of the Chinese Highway (The Highway Bridge Design Code of China)

Table 2-5 Multiple Presence Factors (The Highway Bridge Design Code of China)

# of lanes	**2**	**3**	**4**	**5**	**6**	**7**	**8**
Lanes factor	1.0	1.0	0.85	0.65	0.65	0.65	0.60

Table 2-6 Longitudinal Reduction Factors (The Highway Bridge Design Code of China)

Loaded Length	**150<L<400 (m)**	**400≤L<600 (m)**	**600≤L<800 (m)**	**800≤L<1000 (m)**	**L≥1000 (m)**
Reduction factor	0.97	0.96	0.95	0.94	0.93

Superstructure Design of Honshu-Shikoku Bridge of Japan: The load model of this code is described in Table 2-7 below.

Table 2-7 The Equivalent Load Model of Honshu-Shikoku Bridge of Japan (Superstructure Design of Honshu-Shikoku Bridge of Japan)

Load Type		**Main Span L (m)**	**The equivalent load**
Primary traffic load (width=5.5m)	Linear meter traffic load P_1 (kN/m)	130<L≤1000	111.0+0.012L
		1000<L	118.0+0.005L
	Uniform distributed traffic load p_1 (kN/m^2)	L≤80	3.5
		80<L≤130	4.3-0.01L
		130<L≤500	3.0
		500<L	3.0x(0.57+300/(200+L))
Secondary traffic load	Linear meter traffic load P_2 (kN/m)	-	2.50
	Uniform distributed traffic load p_2 (kN/m^2)	-	1/2 x p_1

2.2 Chapter Summary

In chapter 2, both national and international literature is reviewed for load and resistance factor calibration procedure and live load models of long span bridges. Live load models of different specifications from different countries like China, Japan, USA and Sweden are presented. AASHTO LRFD calibration report by Nowak (1999) describes the load and resistance factor calibration procedure. Furthermore, two national sources, Argınhan (2010) and Koç (2013), are reviewed for load and resistance factors calibration. Argınhan had studied on the load and resistance factor calibration for pre-stressed concrete girder bridges and Koç had studied on the load and resistance factor calibration for steel plate composite girder bridges including local uncertainties and engineering practice. In chapter 3, statistics of loads, i.e. dead and live, are determined.

CHAPTER 3

STATISTICS OF LOADS

One of the main components of structural design is the loads which will/may act on a structure within its service life. For highway bridges, most common design load types are live load (static and dynamic), dead load, environmental loads (wind, earthquake, temperature) and other loads (emergency breaking, collision). Modeling the loads is done by using the available statistical data, surveys and observations. Considering these load components as random variables, and defining them by their statistical distribution, bias factor (mean value/nominal value) and coefficient of variation are determined.

AASHTO LRFD involves different load combinations but they can be classified in to two main limit states which are strength limit state and service limit state. Strength I limit state is the main load combination relating to vehicular use of the bridge without wind (AASHTO LRFD 3.4.1). Strength I limit state load combination is cited as the following.

$$Q = 1.25 \text{ x } DC + 1.50 \text{ x } DW + 1.75 \text{ x } LL \text{ x } (1 + IM) \text{ x } GDF \qquad (3\text{-}1)$$

where DC is dead load of structural and non-structural components, DW is dead load of wearing surface, LL is vehicular live load, IM is dynamic impact factor, and GDF is girder distribution factor.
In this study, structural design of bridges are performed with respect to this load combination.

3.1 Dead Loads

The dead loads consists of four components:

D_1 - Weight of factory made elements
D_2 - Weight of cast-in-place concrete
D_3 - Weight of wearing surface
D_4 - Weight of miscellaneous

} In this study, (D_3+D_4) is taken as 5.8kN/m.

In this study, dead load statistical parameters are taken from Nowak's calibration report (1999). Mentioned four dead load variables are considered to be normally distributed. The parameters are listed in Table 3-1.

Table 3-1 Statistical Parameters of Dead Load

Component	Bias Factor	Coefficient of Variation
D_1	1.03	0.08
D_2	1.05	0.10
D_3	1.00	0.25
D_4	1.03-1.05	0.08-0.10

3.2 Live Loads

3.2.1 Live Load Models

In this section, four different live load models are introduced that are AASHTO LRFD HL-93, Turkish LRFD H30-S24 & AYK-45, and live load models generated by using Turkish truck survey data (Grouped Truck Loading). Moreover, the positive span moments due to the mentioned four live load models will be presented. Please note that every live load model is moved one by one on the bridge. However, it was tried that live load models were moved in consecutive manner (back to front distance 15m-80m) and the results did not change significantly. The reason of that is the basic behavior of the cable stayed bridges. Cables are placed with a spacing of 14.85 meters which is just enough for a truck only.

3.2.1.1 HL-93 Loading

AASHTO LRFD Specifications offer a live load model as design model which is HL93 loading. This live load model is comprised of a truck load and a lane load. HL-93 truck has 3 axles placed by a distance of 4.3 m from each other. To develop more critical force effects, the distance between two rear axles may be spaced up to 9.15 meters. The load value for leading axle is 35 kN and for rear axles is 145 kN. The lane load value is taken as 9.3 kN/m as uniformly distributed load. The live load model and HL-93 truck are presented in Figure 3-1 and Figure 3-2, respectively.

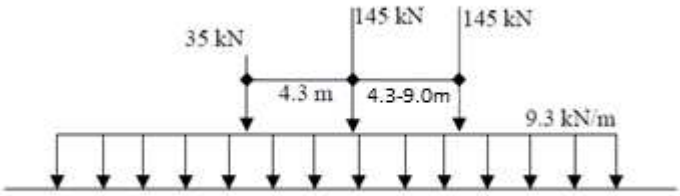

Figure 3-1 HL-93 Live Load Model

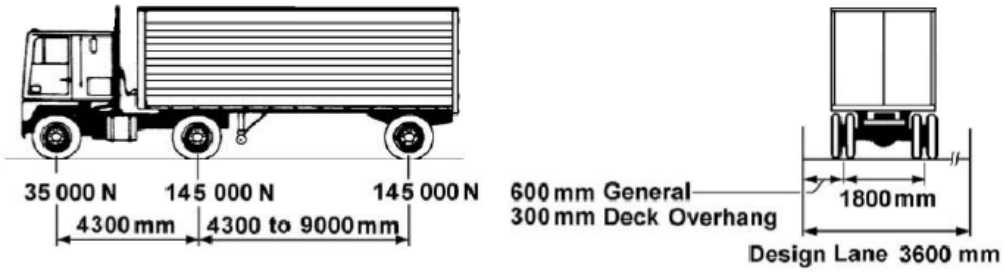

Figure 3-2 HL-93 Design Truck (AASHTO LRFD, 2010)

3.2.1.2 H30-S24 Loading

Technical Specifications for Roads and Bridges (1982) in Turkey offers a live load model as design model which is H30-S24 loading. This live load model is comprised of only a truck load. However, a uniformly distributed load of 10 kN/m is used as lane loading together with the truck load. Therefore, in this study, the live load model consists of design truck load and design lane load. H30-S24 truck has 3 axles placed by a distance of 4.25 m from each other. To create more critical force effects, the distance between two rear axles may be spaced up to 9.00 meters. The load value for leading axle is 60 kN and for rear axles is 240 kN. H30-S24 truck and the live load model are presented in Figure 3-3 and Figure 3-4, respectively.

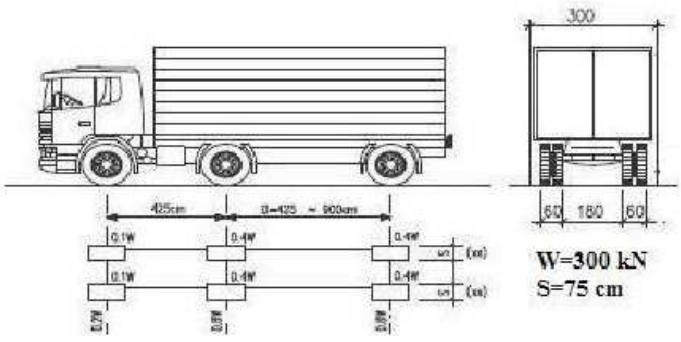

Figure 3-3 H30-S24 Design Truck (KGM 1982)

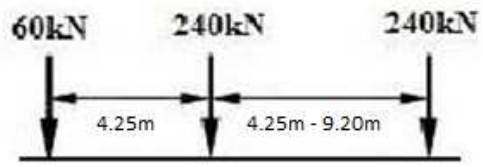

Figure 3-4 H30-S24 Live Load Model

3.2.1.3 AYK-45 Loading (KGM-45 Loading)

"In the calibration of AASHTO LRFD for Turkey, a new live load model is going to be implemented. The new model is called AYK45, in which AYK stands for "Ağır Yük Kamyonu" meaning "Heavy Load Truck" in Turkish and "45" is total weight of truck in units of ton. Similar to HL-93 truck model philosophy, AYK45 needs to be used with a uniform lane load of 10 kN/m (Koç, 2013)."

AYK-45 truck has 3 axles placed by a distance of 4.25 m from each other. The load value for leading axle is 50 kN and for rear axles is 200 kN. The lane load value is taken as 10.0 kN/m as uniformly distributed load. AYK-45 truck and the live load model are presented in Figure 3-5 and Figure 3-6, respectively.

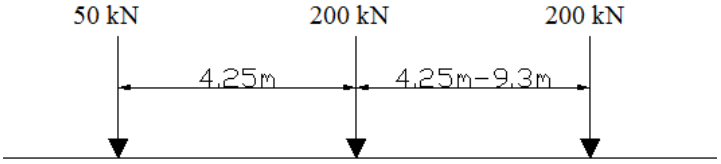

Figure 3-5 AYK-45 Design Truck

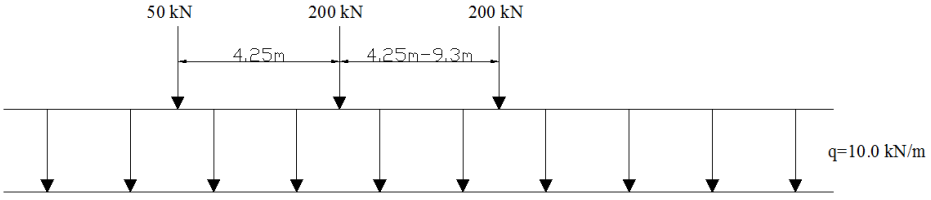

Figure 3-6 AYK-45 Live Load Model

3.2.1.4 Grouped Truck Loading

This type of live load model is generated by using Turkish truck survey data to compare the code design trucks and the real life trucks. The truck survey data was obtained from the Turkish General Directorate of Highways. In data, there are about 28,000 different truck measurements belonging the years 2005, 2006 and 2013 (axle count, axle distances and axle weights). In Table 3-2, analyzed truck survey data is presented.

Table 3-2 Summary of Truck Survey Data

Axle Count	Number of Data	Percentage (%)
2 Axles	2905	10.4
3 Axles	15084	53.8
4 Axles	7351	26.2
5 Axles	2715	9.7
Sum	**28055**	**100**

In accordance with Table 3-2, 3-axle trucks and 4-axle trucks are dominant in the real life traffic. 2-axle trucks and 5-axle trucks are very rare in the traffic when compared with the others. Considering this statistical values about occurrence of trucks in the traffic, grouped truck live load models were created. These models consist of 16 trucks (2 two-axle trucks, 8 three-axle trucks, 4 four-axle trucks and 2 five-axle trucks) placed with a 30m back to front distance. In addition, a uniformly distributed load of 10kN/m is used as lane loading together with the truck loads. 5,428 different live load models were obtained by grouping the truck survey data in a mentioned manner. One example of grouped truck loading without lane load is presented in Figure 3-7.

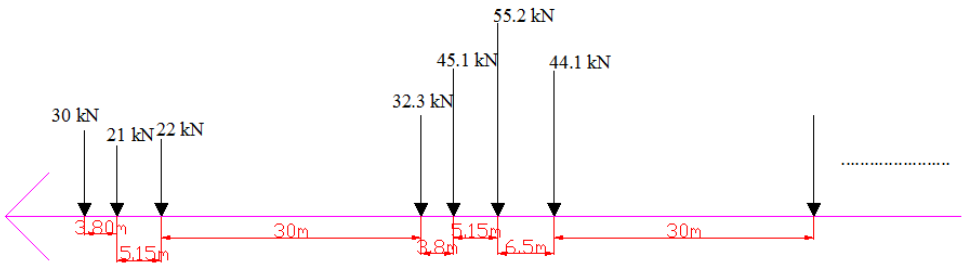

Figure 3-7 Grouped Truck Loading Example (Axle Loads in tons)

3.2.1.5 Maximum Mid-Span Moments due to Live Load Models

Maximum mid-span moments of all live load models have been calculated for span lengths of 420 meters, 470 meters, 500 meters and 550 meters. Moving load analysis (influence line) has been utilized so that position of truck on the bridge that creates maximum moment has been determined. H30-S24 loading gives around 16% higher results when compared with AYK-45 loading. HL-93 loading and grouped truck loading give nearly the same results. The results are shown in Table 3-3. The comparison is shown as a bar graph in Figure 3-8. Please note that grouped truck loading moment values (5,428 different value) are obtained for all span lengths and a single design moment value is determined in a way that this value is greater than the obtained values with a probability of 99.7%. In other words, selected design moment value is equal to ($\mu+3\sigma$) where μ is mean value of obtained moments and σ is standard deviation of obtained moment data.

Table 3-3 Maximum Moments due to Live Load Models for 6 Lanes

Span Length (m)	**Maximum Moment (kN.m)**			
	HL-93	H30-S24	AYK-45	Grouped Truck Loading
420	6518	10845	9036	6604
470	6280	10450	8735	6335
500	6850	11392	9640	7385
550	6700	11013	9321	6981

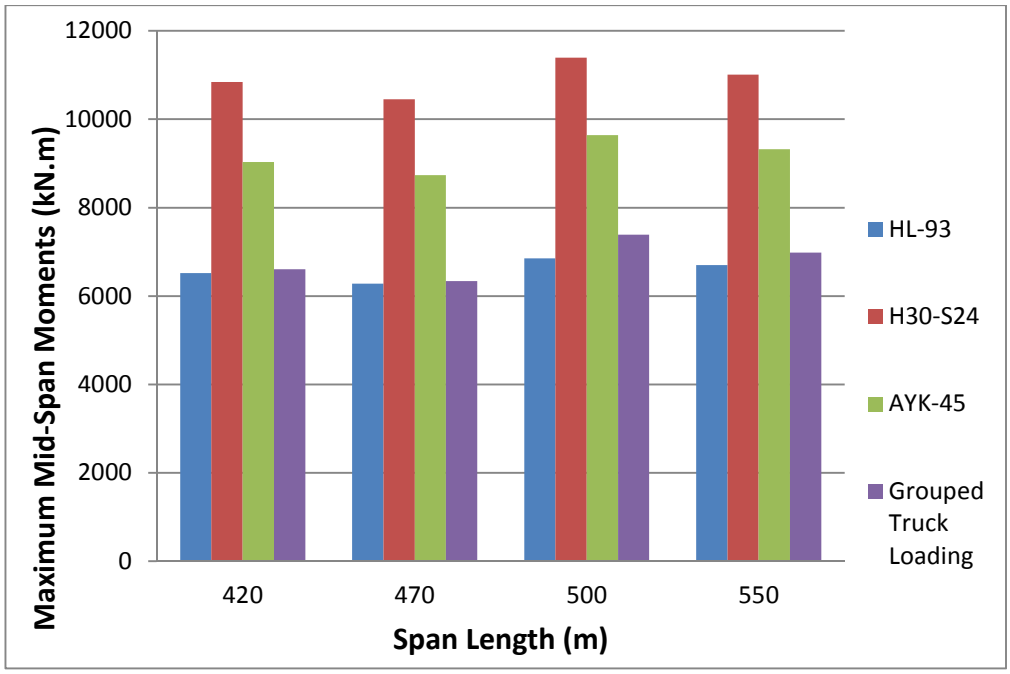

Figure 3-8 Comparison of Mid-Span Moments of Live Load Models

3.2.2 Evaluation of Truck Survey Data

To determine the statistics of live load in Turkey the truck survey data was gathered from the Turkish General Directorate of Highways. This survey was conducted in about 40 different highway measurement stations of Turkey in years between 1997-2006 and 2013. Only the years 2005,2006 and 2013 data were used in this study because the data collected between the mentioned years reflect the more recent measurements (today's traffic live loads). Turkish truck survey data consist of about 28,000 trucks' axle weights, number of axles and spacing. The years 2005 and 2006 survey data (about 11,000 different trucks) was used by Argınhan (2010) and Koç (2013) to investigate reliability-based safety level of precast pre-stressed concrete bridge girders and slab on steel plate bridge girders in Turkey, respectively. In this study, in addition to the years 2005 and 2006 survey data, survey data of the year 2013 was also used.

The maximum mid-span moments due to surveyed trucks (one-by-one) are calculated for each four different span lengths that are 420 meters, 470 meters, 500 meters and 550 meters. In Figure 3-9, frequency distribution of truck types based on axle configurations is illustrated.

In surveyed truck data, gross weights of trucks considered in calculations are varied;

- From 1.2 tons to 18.90 tons for 2-axle trucks with an average of 6.20 tons
- From 2.60 tons to 32.50 tons for 3-axle trucks with an average of 12.80 tons
- From 3.0 tons to 45.80 tons for 4-axle trucks with an average of 21.50 tons
- From 13.45 tons to 43.80 tons for 5-axle trucks with an average of 38.15 tons

Overall mean value of the gross weights is 16.85 tons for 28,000 surveyed truck data. In Figure 3-10, frequency distribution of gross vehicle weights is illustrated.

Maximum mid-span moment values due to these 28,000 trucks have been calculated for 420 meters, 470 meters, 500 meters and 550 meters span lengths. The histograms are plotted in Figure 3-11 to Figure 3-14.

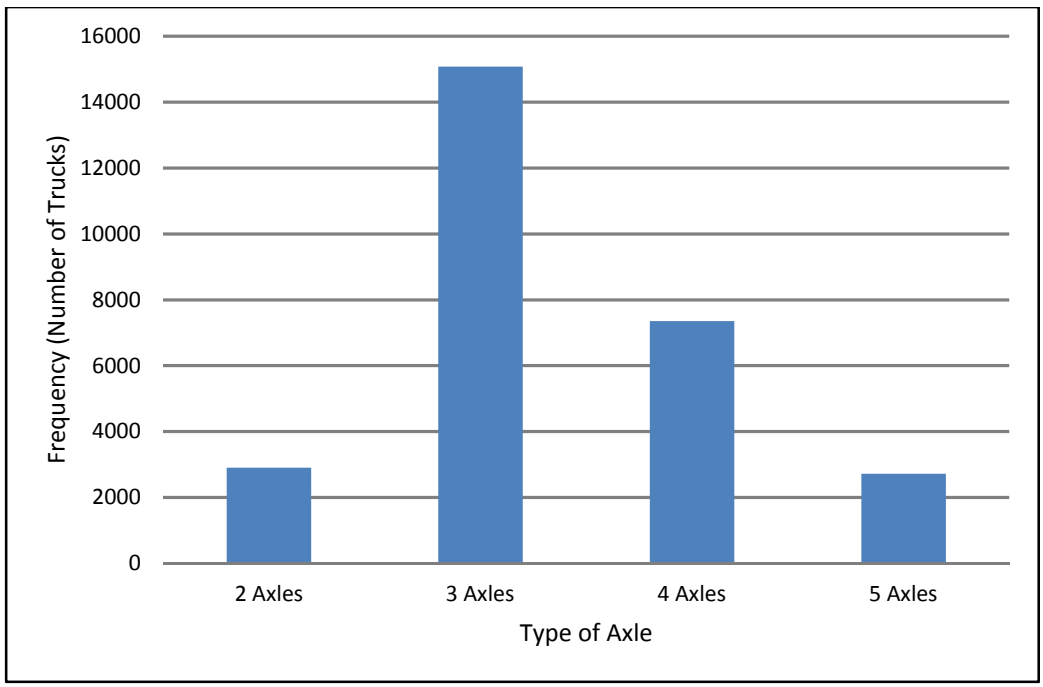

Figure 3-9 Histogram of Vehicles Based on Axle Configurations

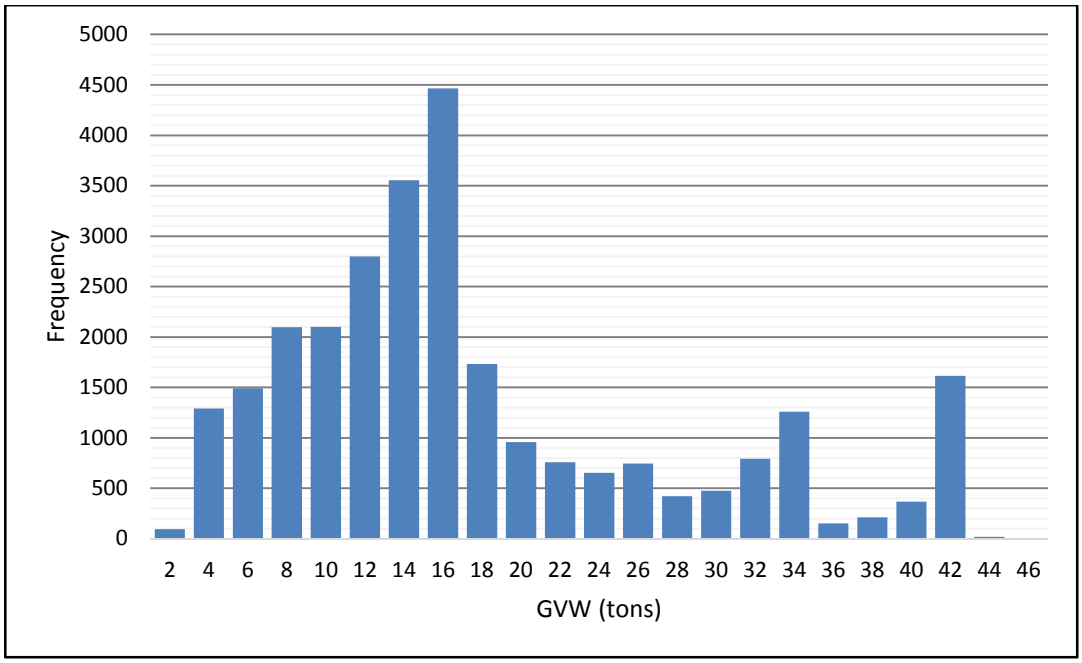

Figure 3-10 Histogram of Gross Vehicle Weights (GVW) of Surveyed Trucks

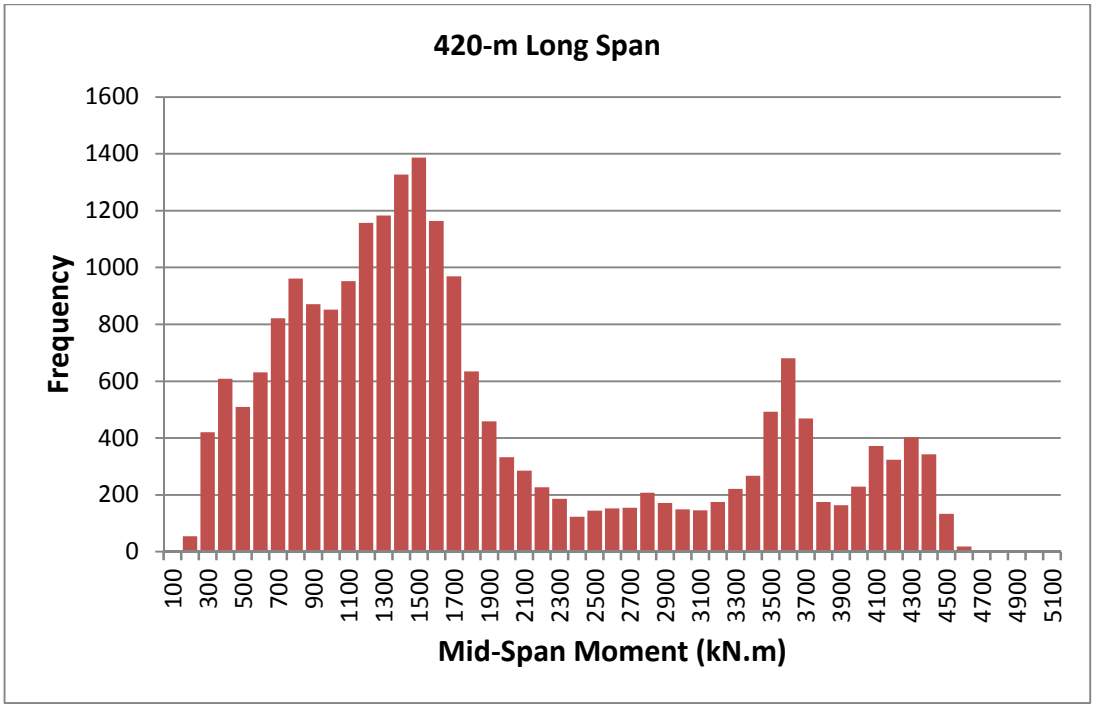

Figure 3-11 Histogram of Mid-Span Moments of Surveyed Trucks for Span Length of 420m

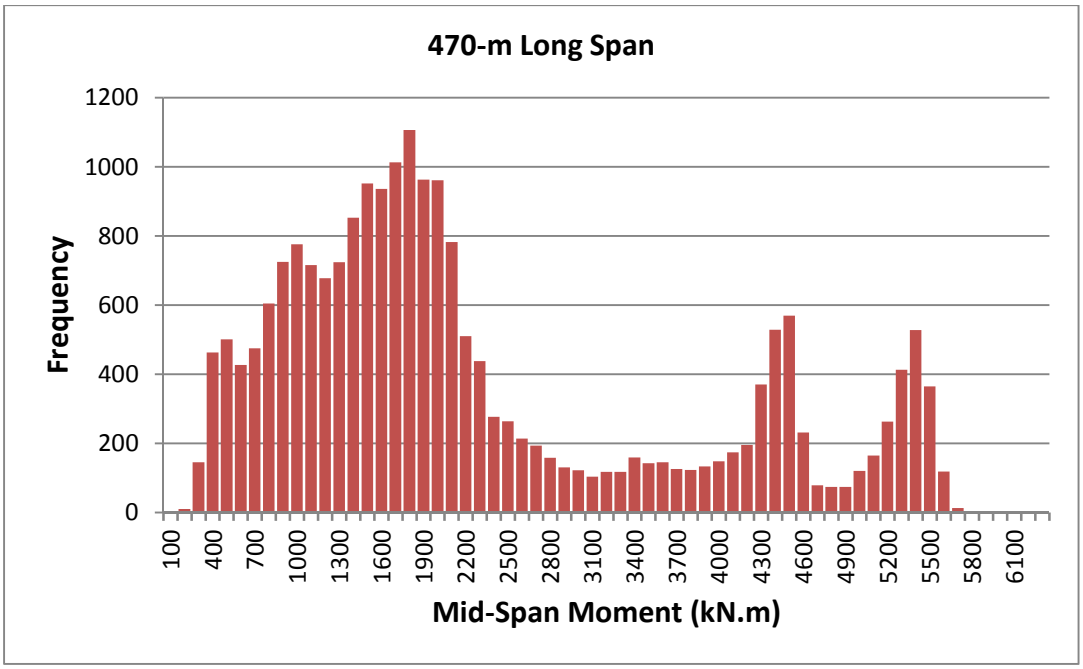

Figure 3-12 Histogram of Mid-Span Moments of Surveyed Trucks for Span Length of 470m

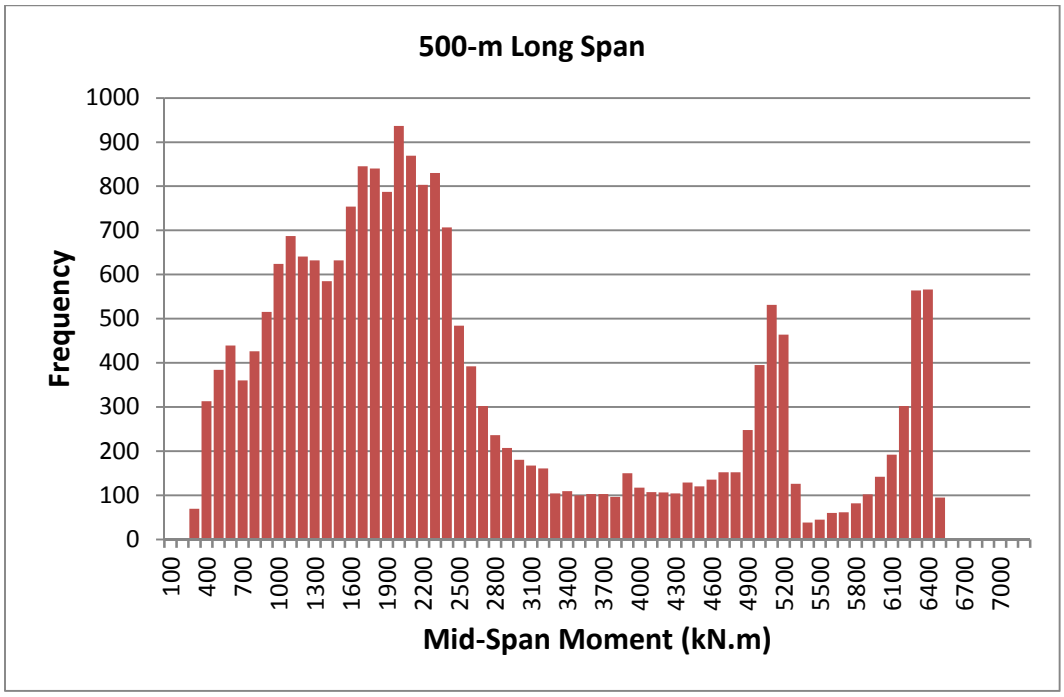

Figure 3-13 Histogram of Mid-Span Moments of Surveyed Trucks for Span Length of 500m

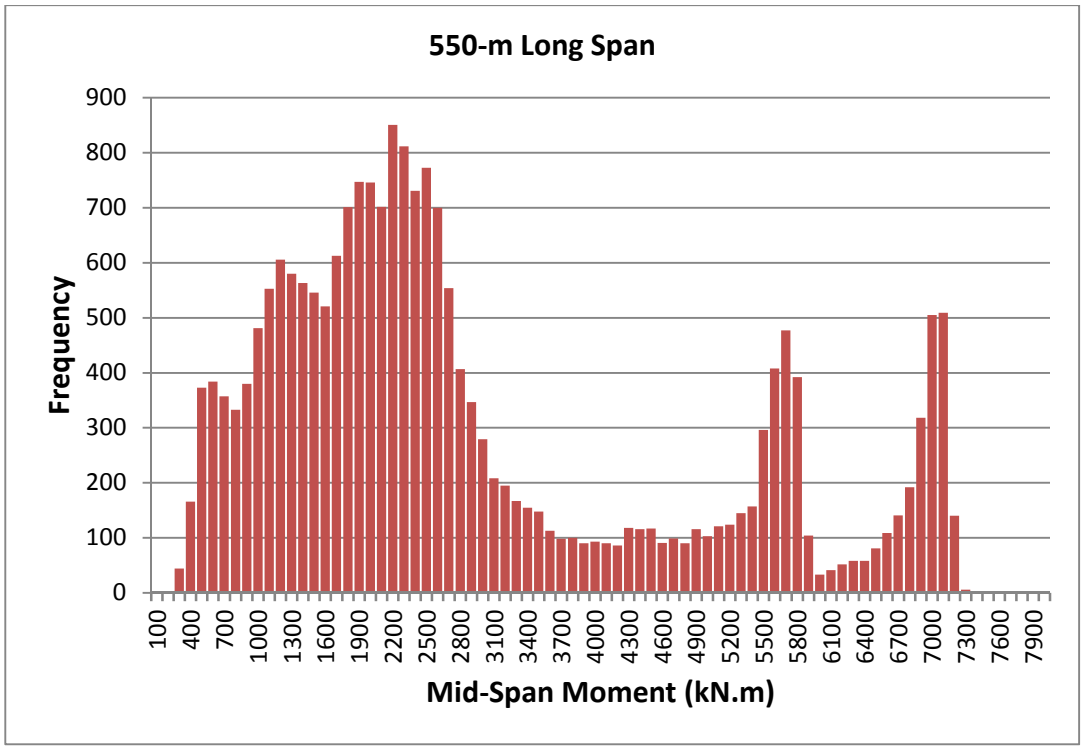

Figure 3-14 Histogram of Mid-Span Moments of Surveyed Trucks for Span Length of 550m

3.2.3 Assessment of Statistical Parameters of Live Load

The extreme value theory, which is used in calibration of AASHTO LRFD (Nowak, 1999), is applied to determine the statistical parameters regarding live load. Basically, the main idea underlying this theory is the projection of any previously observed available data to the future to obtain forthcoming data that are more extreme than available data.

The moment ratios of surveyed trucks to AYK45, HL-93, H30S24 and grouped truck loading are plotted on both normal probability papers and Gumbel probability papers for three different cases. These cases are:

- Complete data – Overall Case
- Part of exceeding 90-percentile values of complete data – Upper-tail Case
- Isolated 10-percent highest values of data – Extreme Case

3.2.3.1 Fitting Straight Lines to the CDFs of Moments of Surveyed Trucks

To determine the probability distribution type of the surveyed truck data cumulative distribution functions (CDFs) of data truck mid-span moment ratios (moment ratio of surveyed truck to design truck) are plotted on both normal and Gumbel probability papers.

Moment ratios of overall surveyed truck data are plotted on normal probability papers in Figure 3-15 to Figure 3-18 for AYK-45, HL-93, H30-S24 and grouped truck loadings. The vertical axis in these figures is the inverse of the standard normal distribution function (f), ISND, denoted by z;

$$z = \emptyset^{-1}[F(M)] \qquad (3\text{-}2)$$

where, M is the mid-span moment, F(M) is the cumulative distribution function of the mid-span moment, □$^{-1}$ is the inverse standard normal distribution function. The horizontal axis in these figures is the mid-span moment ratio.

In Figure 3-19 to Figure 3-33, for each span length and live load model overall truck survey data moment ratios were plotted on normal probability paper. However, the plots show that the data does not fit to the straight line. This indicates that the probability distribution type of the data cannot be expressed with the normal distribution. Therefore, moment ratios were plotted on the Gumbel probability paper to evaluate the acceptability of this probability distribution.

Gumbel probability method is used when limit distribution of data is not known. Moreover, to analyze the extreme value problems in practical cases Gumble probability method provides better results. In Gumbel probability paper, vertical axis is the reduced variate, η, defined as (Castillo, 1988);

$$\eta = -ln[-\ln[F(M)]] \qquad (3\text{-}3)$$

where M is mid-span moment, F(M) is the cumulative distribution function of mid-span moment. Horizontal axis is the mid-span moment ratio.

In Figure 3-19 to Figure 3-34, for each span length and live load model overall truck survey data moment ratios were plotted on Gumbel probability paper. The plots shows that the data can be expressed with Gumbel probability since a better fit to the straight line is occurred when compared with normal distribution. As a result, surveyed truck moments are assumed to follow the Gumbel probability distribution.

The Gumbel papers for upper tail of overall surveyed truck moment ratios are plotted in Figure 3-35 to Figure 3-38. The last but not least, the Gumbel papers for extreme surveyed truck moment ratios are plotted in Figure 3-39 to Figure 3-42. The equations of straight lines which are fitted to data are presented on plots. These equation will be used for today's results to extrapolate to longer time periods, the future. In accordance with the Eqn 3-3, reduced variate and the cumulative distribution function is directly related with each other. Hence, the extrapolation is performed with CDF's.

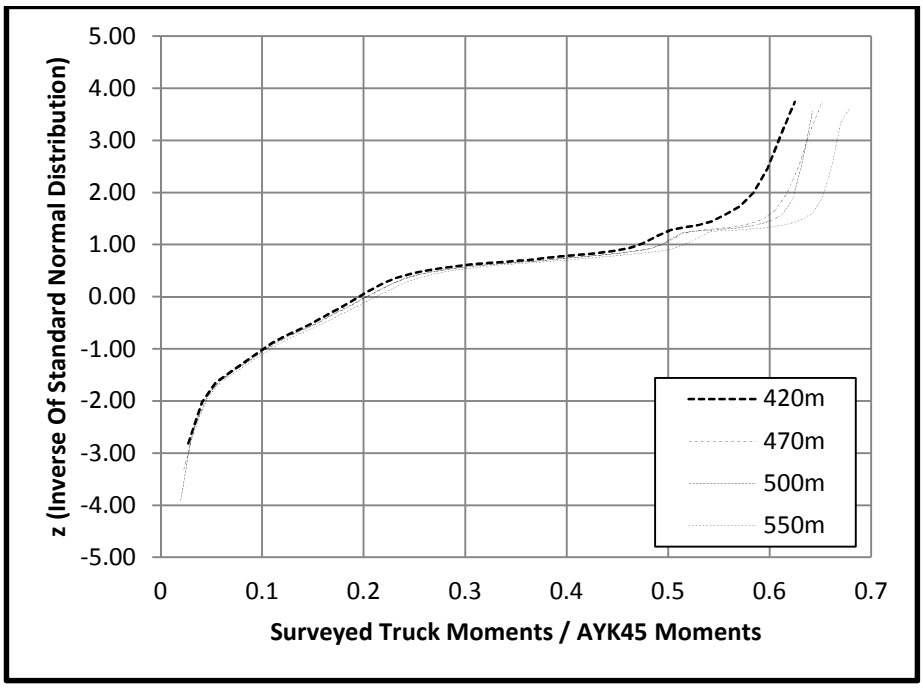

Figure 3-15 Plot of Moment Ratios Computed Based on Overall Truck Survey Data on Normal Probability Paper (AYK-45)

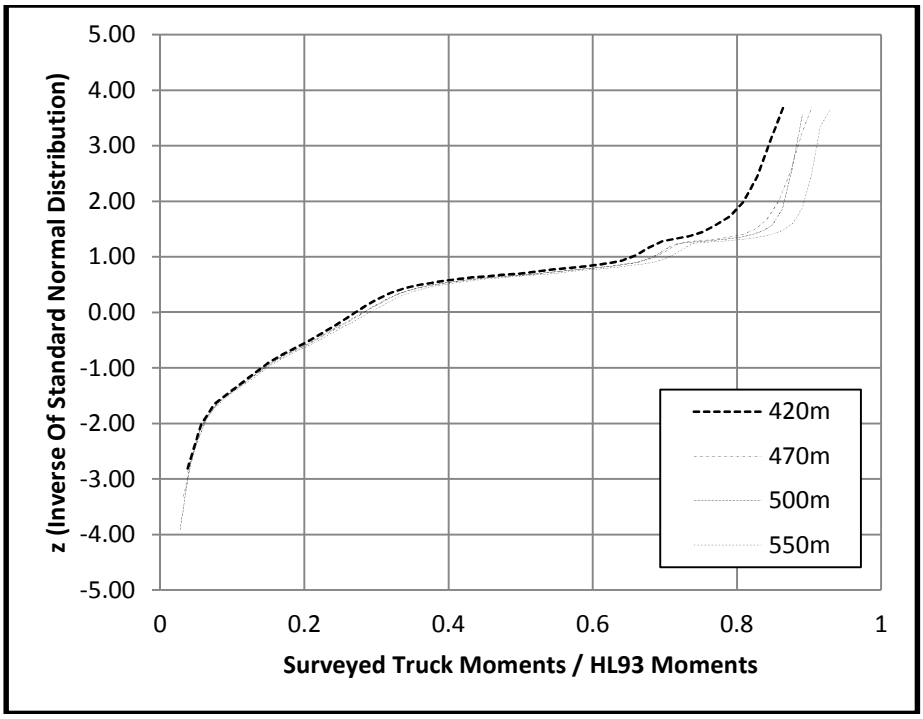

Figure 3-16 Plot of Moment Ratios Computed Based on Overall Truck Survey Data on Normal Probability Paper (HL-93)

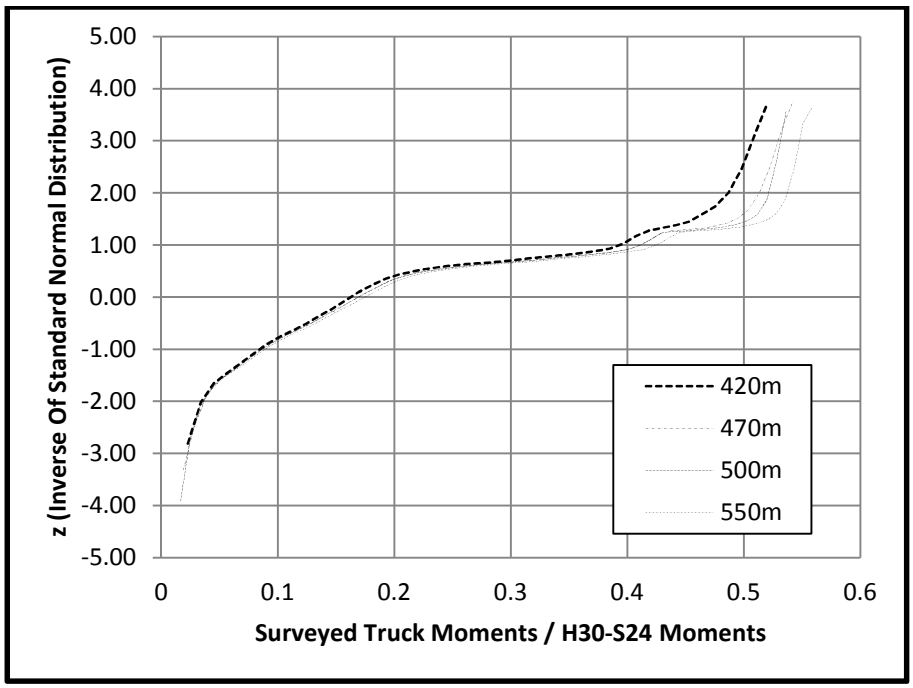

Figure 3-17 Plot of Moment Ratios Computed Based on Overall Truck Survey Data on Normal Probability Paper (H30-S24)

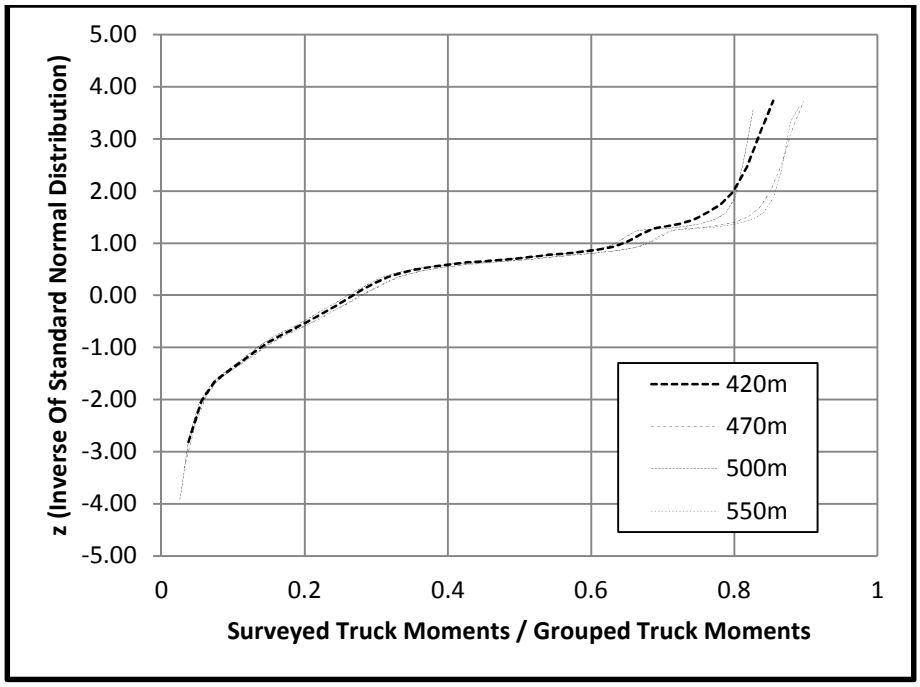

Figure 3-18 Plot of Moment Ratios Computed Based on Overall Truck Survey Data on Normal Probability Paper (Grouped Truck Loading)

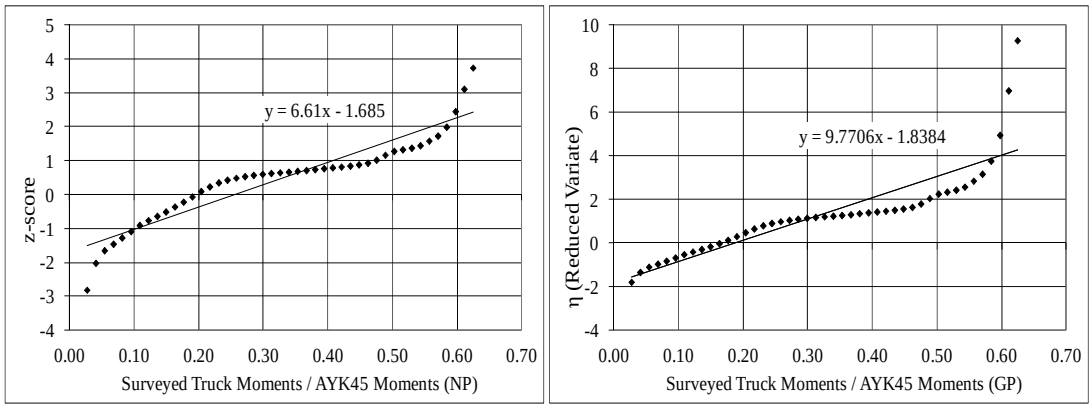

Figure 3-19 Straight Lines Fitted to Overall Moment Ratios on Normal (NP) and Gumbel (GP) Probability Papers (AYK45 - 420m span)

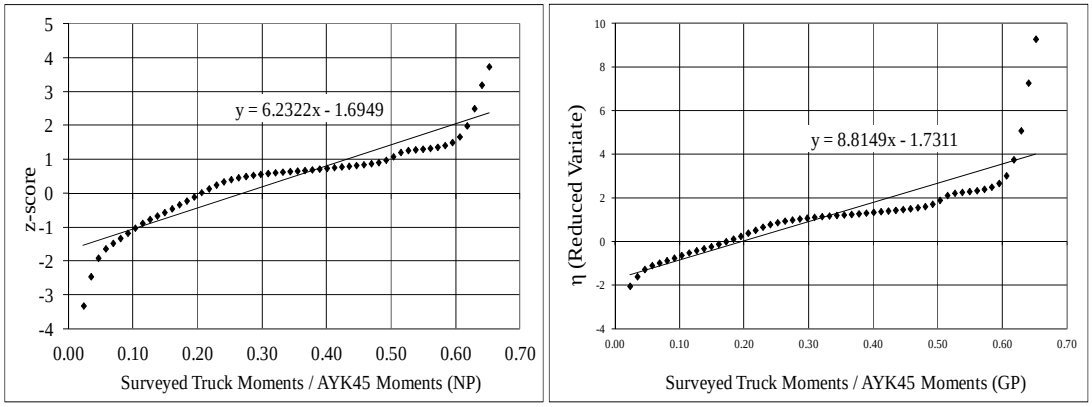

Figure 3-20 Straight Lines Fitted to Overall Moment Ratios on Normal (NP) and Gumbel (GP) Probability Papers (AYK45 - 470m span)

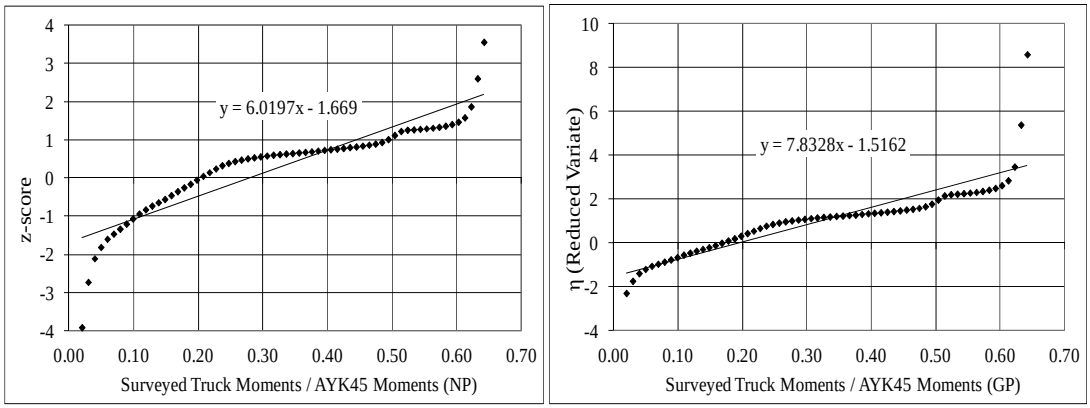

Figure 3-21 Straight Lines Fitted to Overall Moment Ratios on Normal (NP) and Gumbel (GP) Probability Papers (AYK45 - 500m span)

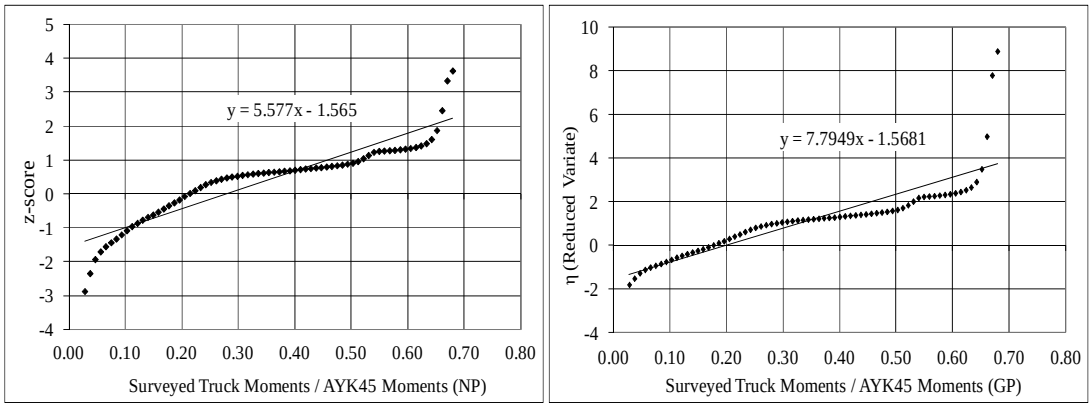

Figure 3-22 Straight Lines Fitted to Overall Moment Ratios on Normal (NP) and Gumbel (GP) Probability Papers (AYK45 - 550m span)

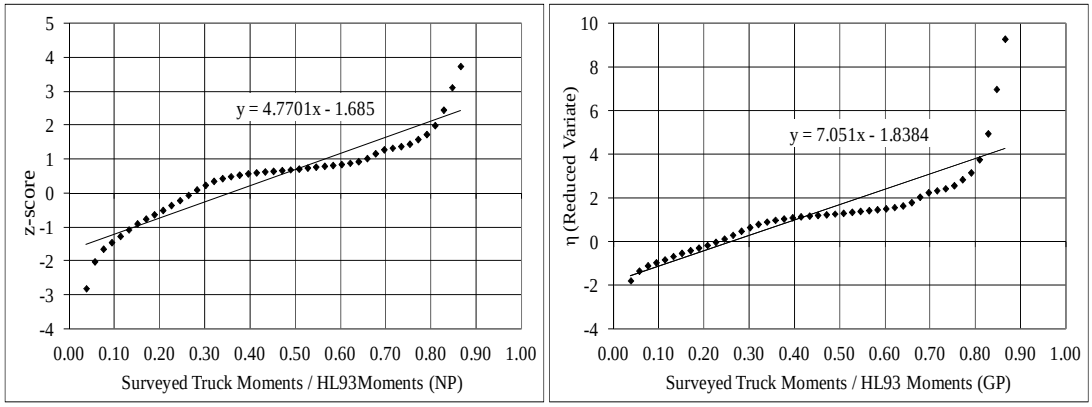

Figure 3-23 Straight Lines Fitted to Overall Moment Ratios on Normal (NP) and Gumbel (GP) Probability Papers (HL93 - 420m span)

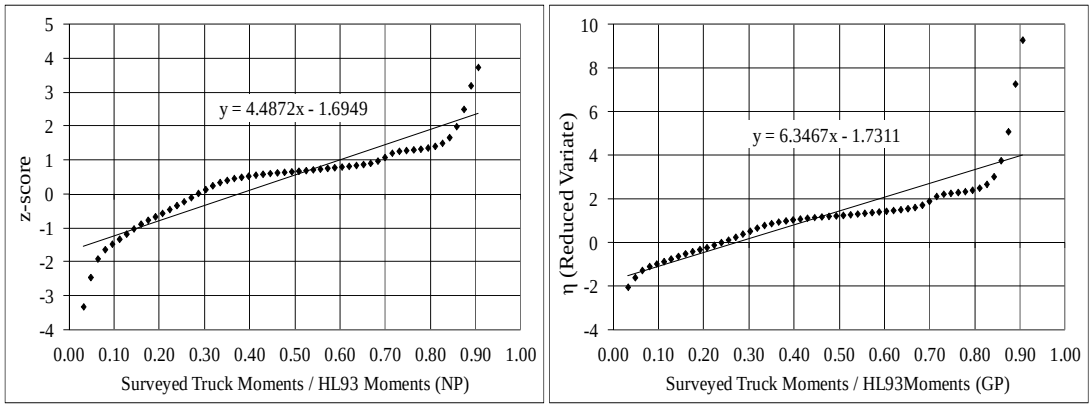

Figure 3-24 Straight Lines Fitted to Overall Moment Ratios on Normal (NP) and Gumbel (GP) Probability Papers (HL93 - 470m span)

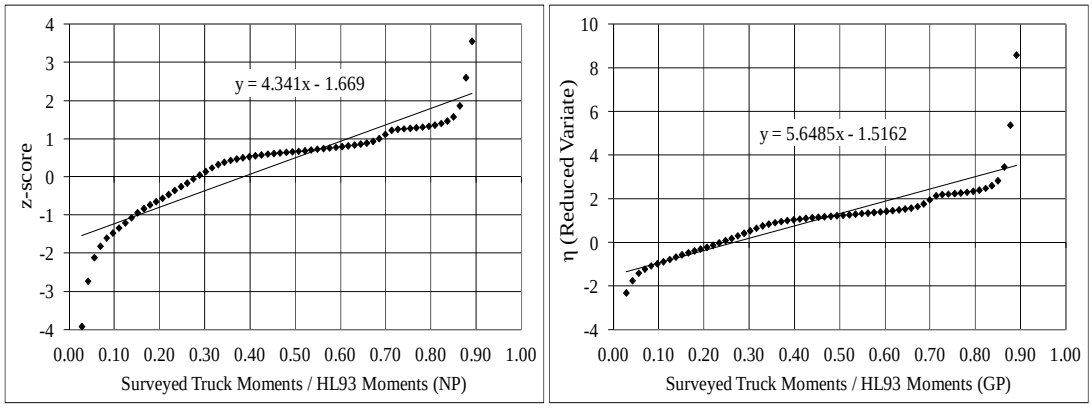

Figure 3-25 Straight Lines Fitted to Overall Moment Ratios on Normal (NP) and Gumbel (GP) Probability Papers (HL93 - 500m span)

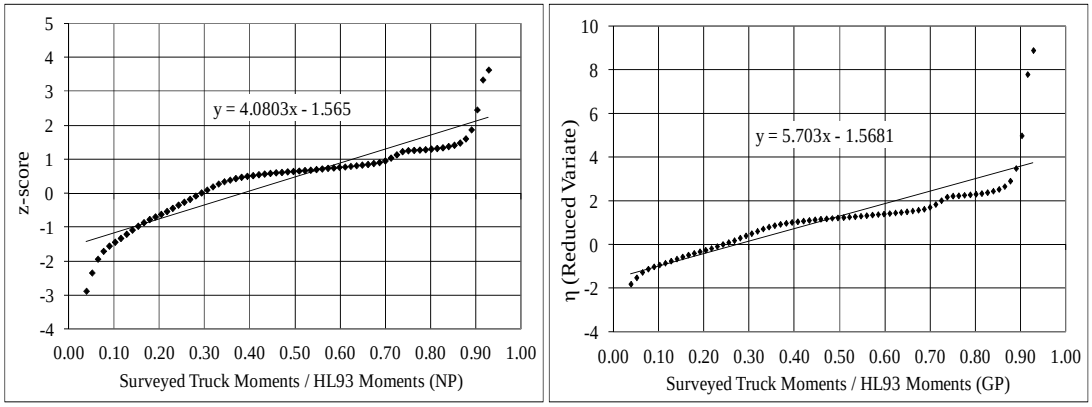

Figure 3-26 Straight Lines Fitted to Overall Moment Ratios on Normal (NP) and Gumbel (GP) Probability Papers (HL93 - 550m span)

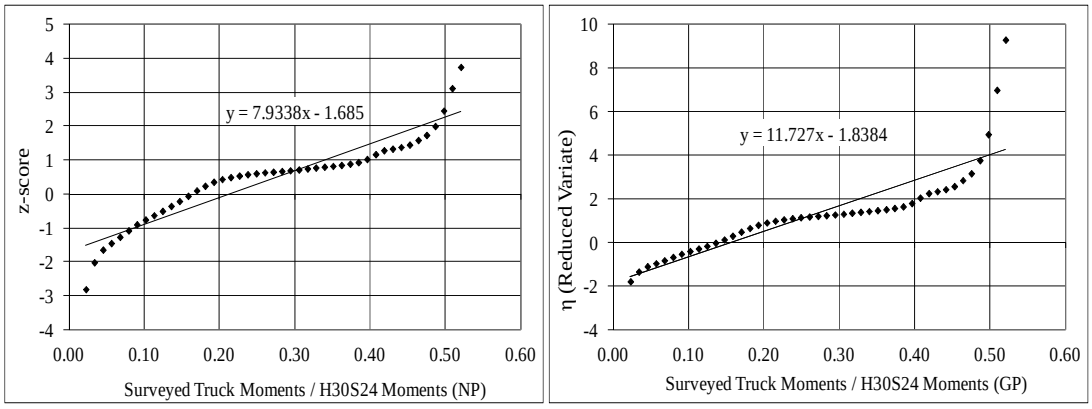

Figure 3-27 Straight Lines Fitted to Overall Moment Ratios on Normal (NP) and Gumbel (GP) Probability Papers (H30S24 - 420m span)

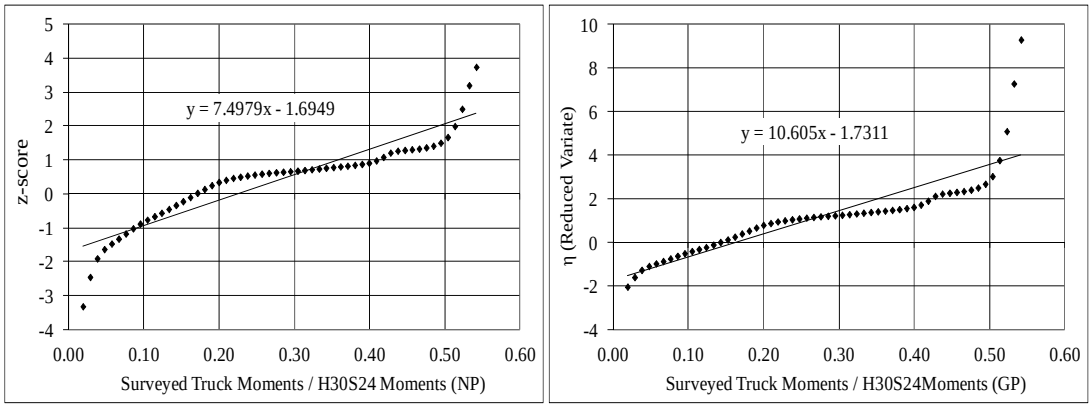

Figure 3-28 Straight Lines Fitted to Overall Moment Ratios on Normal (NP) and Gumbel (GP) Probability Papers (H30S24 - 470m span)

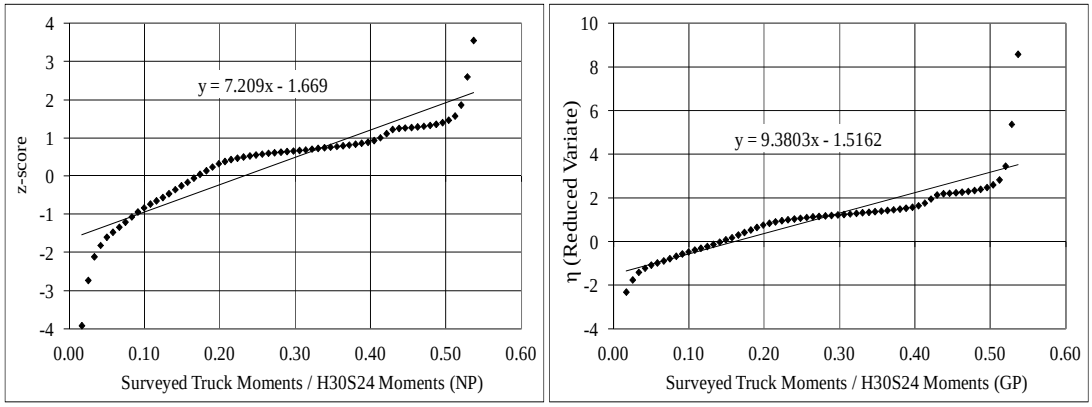

Figure 3-29 Straight Lines Fitted to Overall Moment Ratios on Normal (NP) and Gumbel (GP) Probability Papers (H30S24 - 500m span)

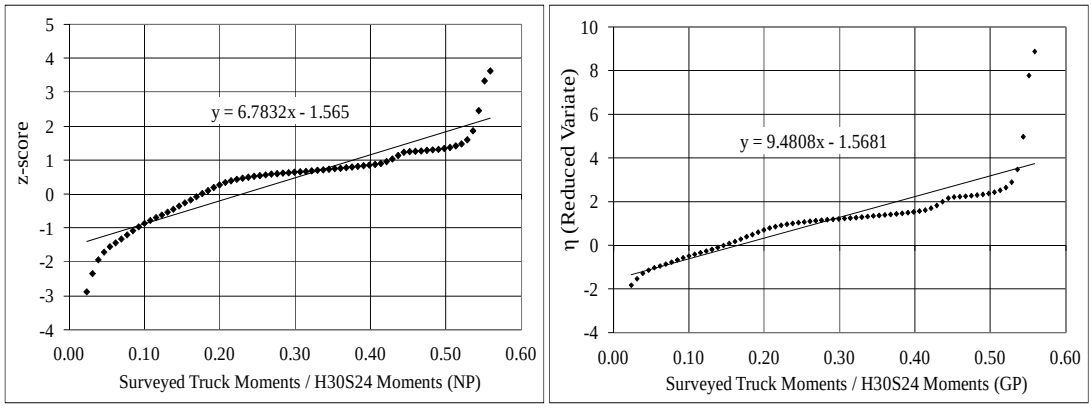

Figure 3-30 Straight Lines Fitted to Overall Moment Ratios on Normal (NP) and Gumbel (GP) Probability Papers (H30S24 - 550m span)

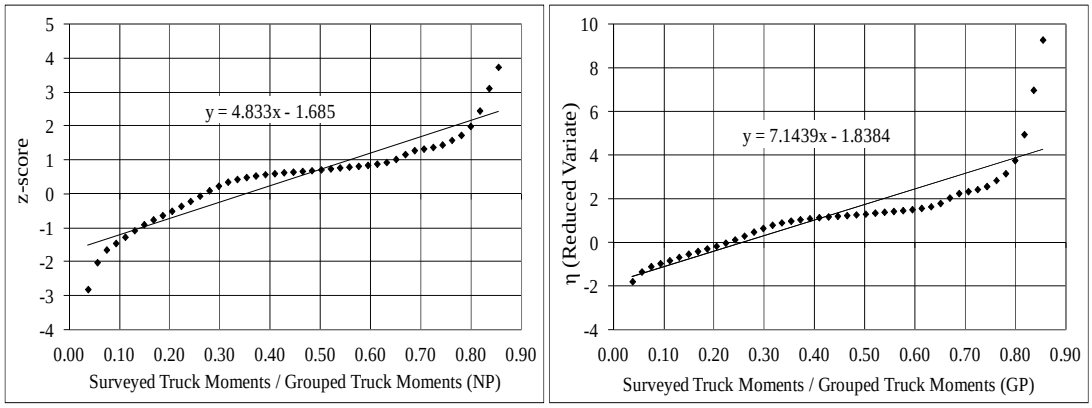

Figure 3-31 Straight Lines Fitted to Overall Moment Ratios on Normal (NP) and Gumbel (GP) Probability Papers (Grouped Truck Loading - 420m span)

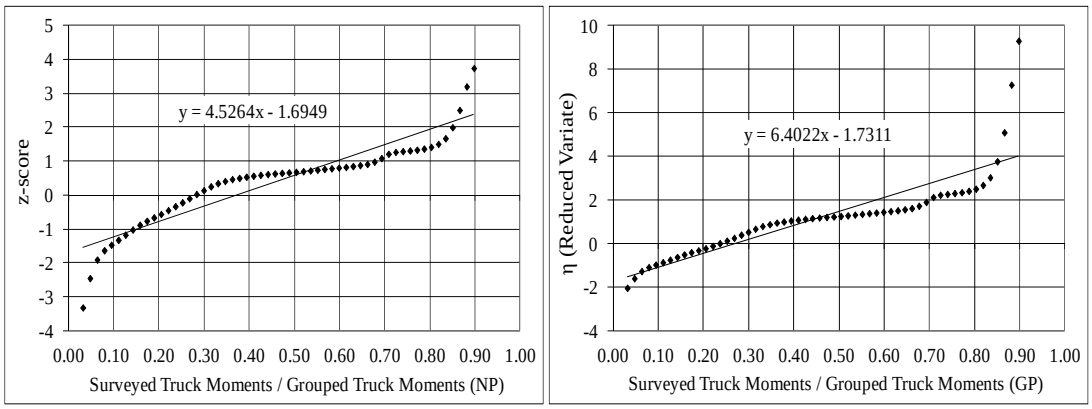

Figure 3-32 Straight Lines Fitted to Overall Moment Ratios on Normal (NP) and Gumbel (GP) Probability Papers (Grouped Truck Loading - 470m span)

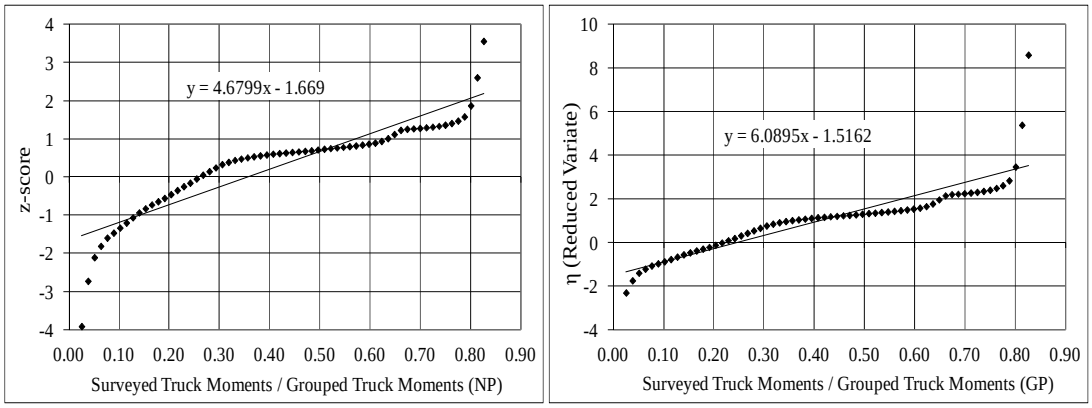

Figure 3-33 Straight Lines Fitted to Overall Moment Ratios on Normal (NP) and Gumbel (GP) Probability Papers (Grouped Truck Loading - 500m span)

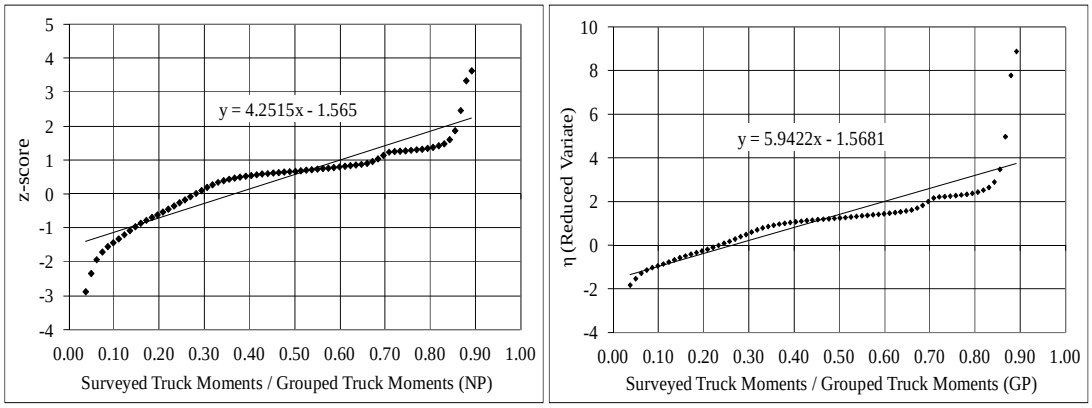

Figure 3-34 Straight Lines Fitted to Overall Moment Ratios on Normal (NP) and Gumbel (GP) Probability Papers (Grouped Truck Loading - 550m span)

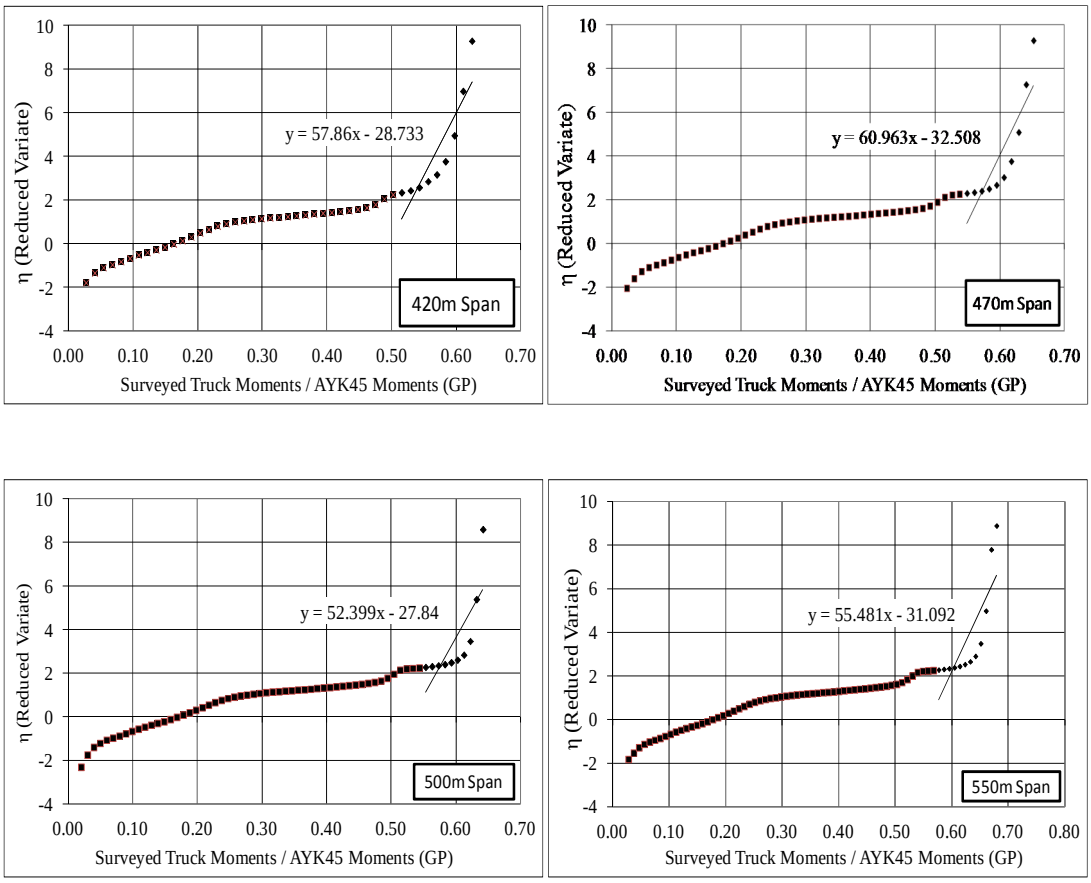

Figure 3-35 Straight Lines Fitted to the Upper Tail of Moment Ratios Plotted on Gumbel (GP) Probability Papers (AYK-45)

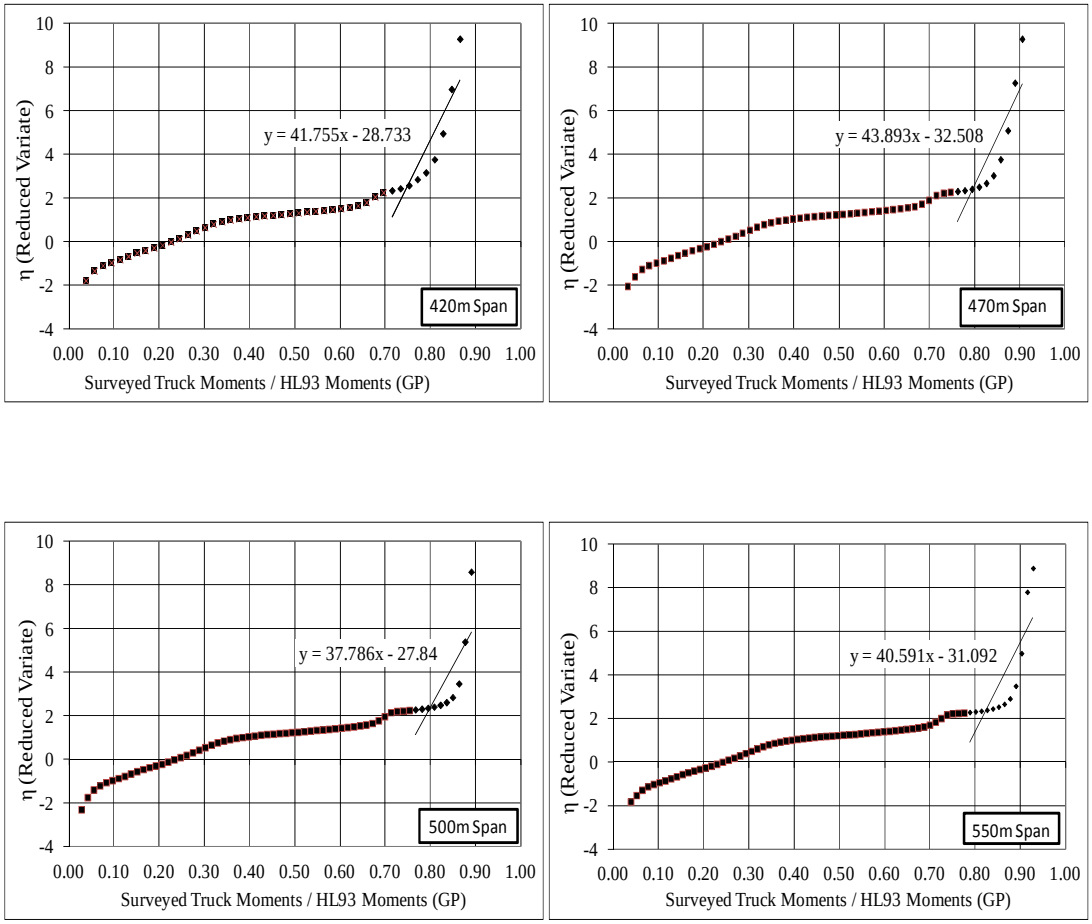

Figure 3-36 Straight Lines Fitted to the Upper Tail of Moment Ratios Plotted on Gumbel (GP) Probability Papers (HL-93)

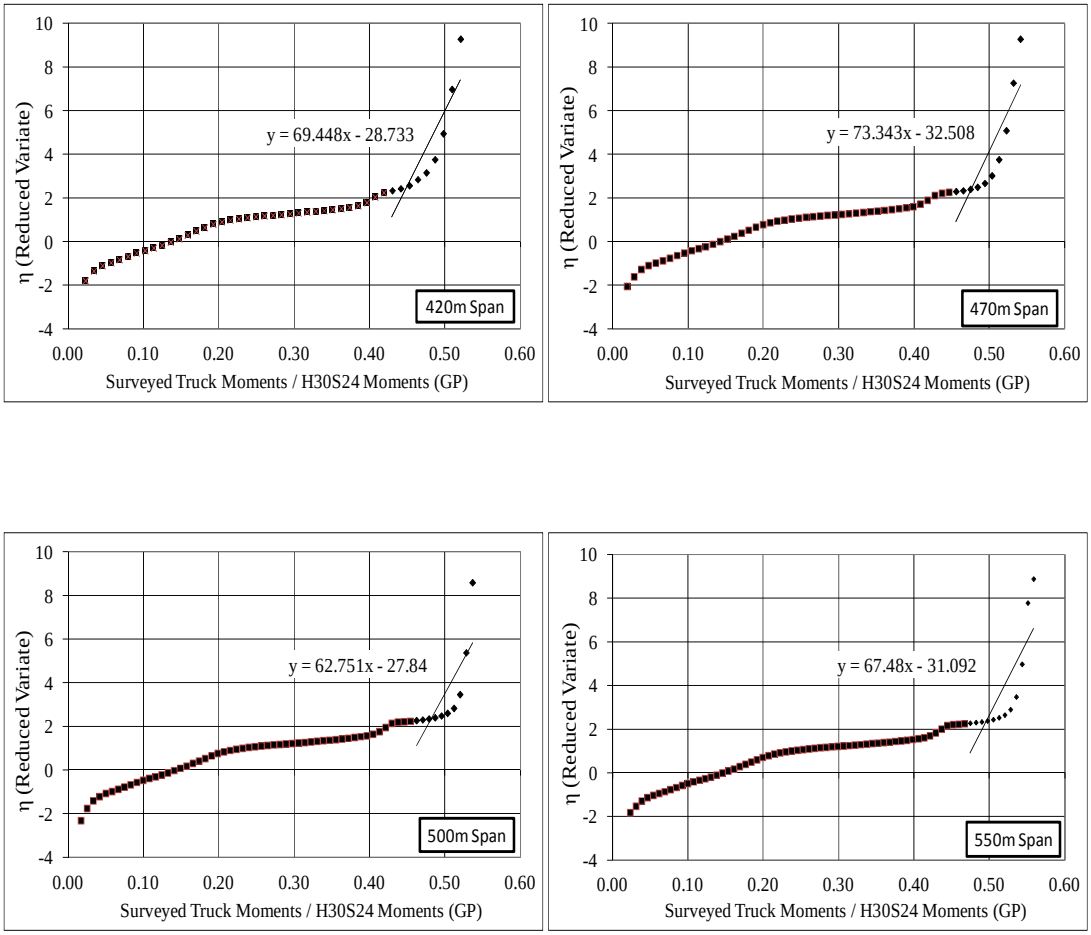

Figure 3-37 Straight Lines Fitted to the Upper Tail of Moment Ratios Plotted on Gumbel (GP) Probability Papers (H30-S24)

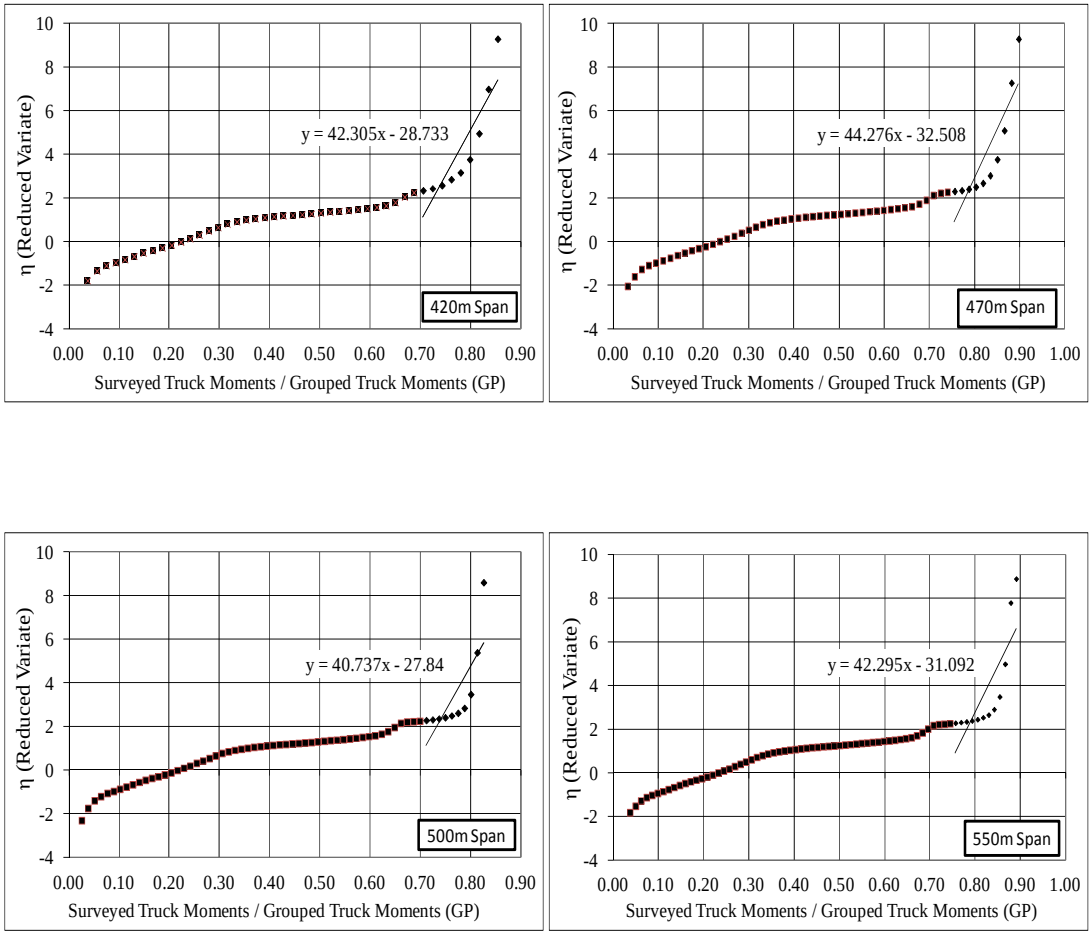

Figure 3-38 Straight Lines Fitted to the Upper Tail of Moment Ratios Plotted on Gumbel (GP) Probability Papers (Grouped Truck Loading)

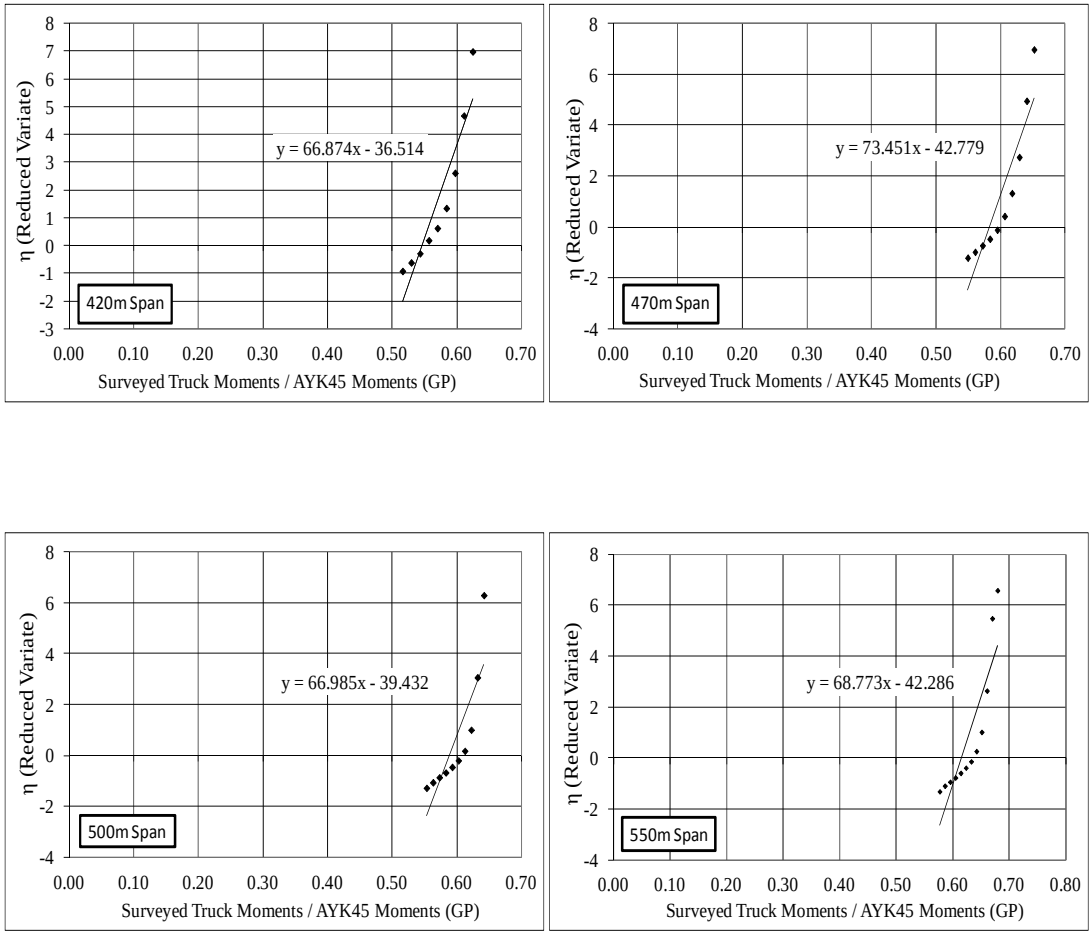

Figure 3-39 Straight Lines Fitted to the Extreme Surveyed Truck Moment Ratios Plotted on Gumbel (GP) Probability Papers (AYK-45)

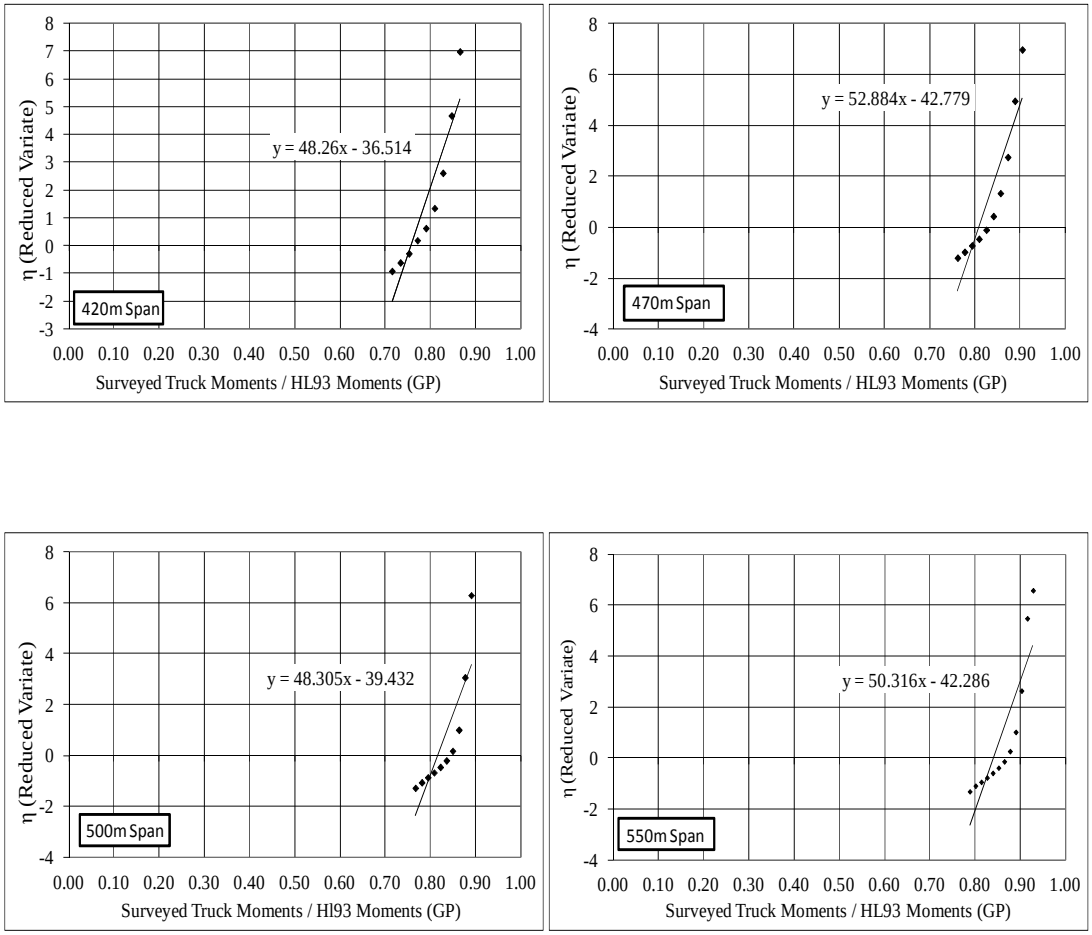

Figure 3-40 Straight Lines Fitted to the Extreme Surveyed Truck Moment Ratios Plotted on Gumbel (GP) Probability Papers (HL-93)

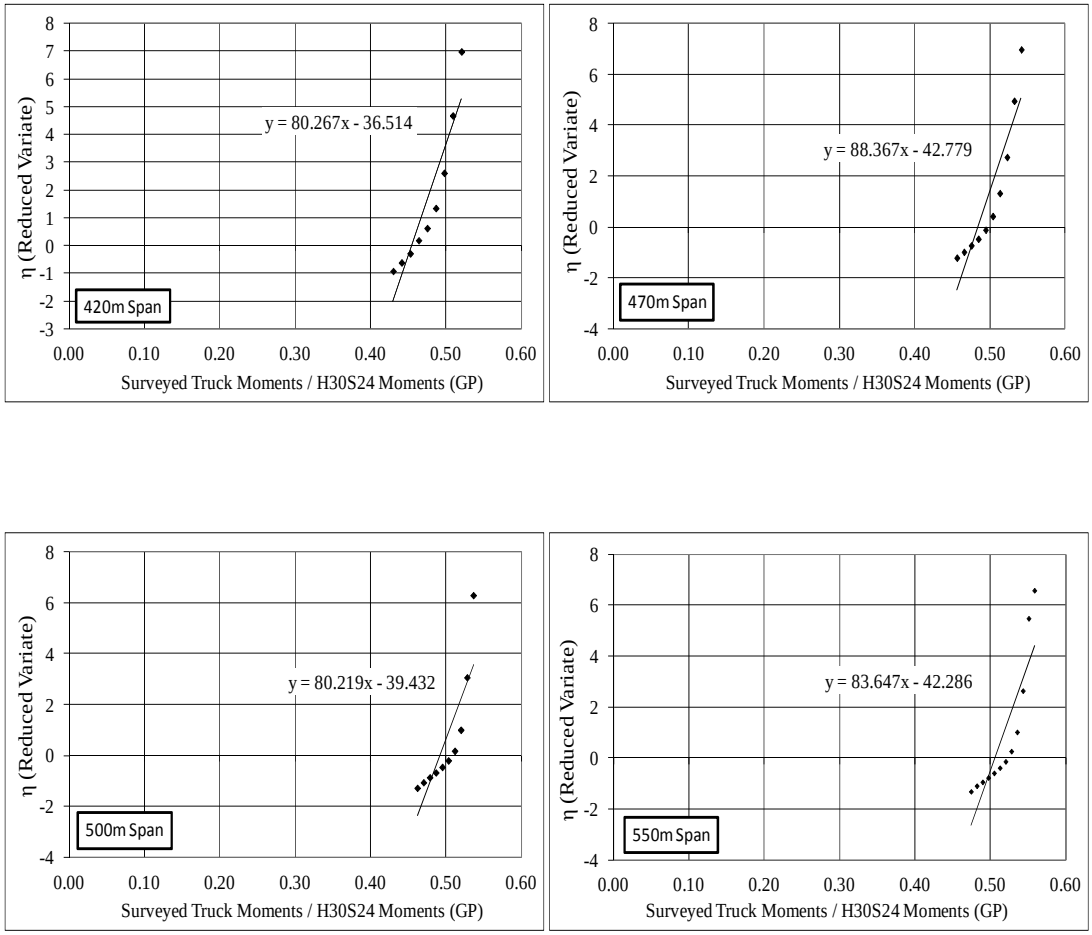

Figure 3-41 Straight Lines Fitted to the Extreme Surveyed Truck Moment Ratios Plotted on Gumbel (GP) Probability Papers (H30-S24)

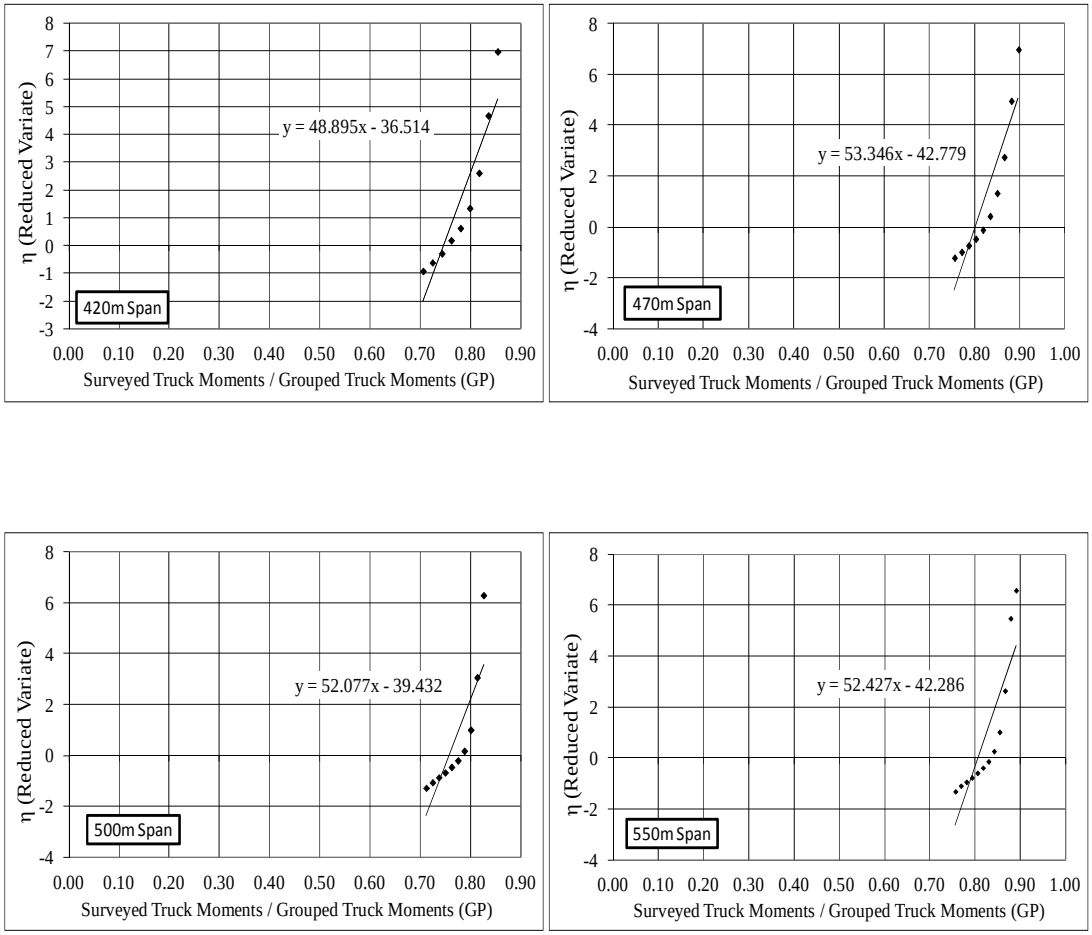

Figure 3-42 Straight Lines Fitted to the Extreme Surveyed Truck Moment Ratios Plotted on Gumbel (GP) Probability Papers (Grouped Truck Loading)

3.2.3.2 Mean Maximum Moments Predicted by Extrapolation

The life time of a bridge is considered as 75 years which is equal to the return period of maximum live load in the AASHTO LRFD specification. Therefore, it is necessary to obtain the live load effects projected to 75 years. This procedure is done by extrapolating the today's cumulative distribution functions to 75 years shown in Figures 3-19 to 3-42.

For extrapolation calculations the study of Nowak about the calibration of AASHTO LRFD (1999) is followed. It is assumed that two weeks of heavy traffic on a bridge with average daily traffic of 1000 trucks is represented by surveyed truck data. The extrapolation of the CDFs of moment ratios is performed for the longer periods of time, e.g. 2 months, a year, 10 years, 50 years or 75 years.

In Table 3-4, for each time period the number of trucks that pass through the bridge, corresponding occurrence probabilities, inverse standard normal distribution values (ISND), and reduced variates are shown.

Table 3-4 Number of Trucks vs. Time Period and Probability

Time Period T	# of Trucks N	Probability 1/N	ISND z	Reduced Variate η
75 years	20,000,000	$5x10^{-8}$	5.33	16.81
50 years	15,000,000	$7x10^{-8}$	5.27	16.52
5 years	1,500,000	$7x10^{-7}$	4.83	14.22
1 year	300,000	$3x10^{-6}$	4.50	12.61
6 months	150,000	$7x10^{-6}$	4.35	11.92
2 months	50,000	$2x10^{-5}$	4.11	10.82
1 month	30,000	$3x10^{-5}$	3.99	10.31
2 weeks	10,000	$1x10^{-4}$	3.72	9.21
1 day	1,000	$1x10^{-3}$	3.09	6.91

The equations of straight lines that presented in Figures 3-19 to 3-42 for Gumbel papers are solved to determine the extrapolated values of mean maximum moment ratios for all time periods listed in Table 3-4. The calculated mean maximum moment ratios and the extrapolation plots are shown in the following tables and figures for overall, upper-tail and extreme cases.

Table 3-5 Mean Maximum Moment Ratios for AYK-45 (*Overall*)

Span (m)	**Surveyed Truck Moment / AYK-45 Moment**								
	1 day	**2 weeks**	**1 month**	**2 months**	**6 months**	**1 year**	**5 years**	**50 years**	**75 years**
420	0.60	0.63	0.64	0.65	0.66	0.67	0.70	0.73	0.74
470	0.63	0.65	0.66	0.67	0.68	0.69	0.72	0.75	0.75
500	0.63	0.67	0.68	0.69	0.71	0.72	0.74	0.77	0.77
550	0.66	0.69	0.70	0.71	0.73	0.74	0.75	0.79	0.79

Table 3-6 Mean Maximum Moment Ratios for HL-93 (*Overall*)

Span (m)	Surveyed Truck Moment / HL-93 Moment								
	1 day	2 weeks	1 month	2 months	6 months	1 year	5 years	50 years	75 years
420	0.83	0.87	0.89	0.90	0.92	0.94	0.97	1.01	1.01
470	0.86	0.90	0.92	0.93	0.95	0.97	0.99	1.03	1.04
500	0.88	0.93	0.95	0.96	0.98	0.99	1.02	1.07	1.07
550	0.90	0.94	0.97	0.98	0.99	1.00	1.03	1.08	1.08

Table 3-7 Mean Maximum Moment Ratios for H30-S24 (*Overall*)

Span (m)	Surveyed Truck Moment / H30-S24 Moment								
	1 day	2 weeks	1 month	2 months	6 months	1 year	5 years	50 years	75 years
420	0.50	0.53	0.54	0.55	0.56	0.57	0.59	0.61	0.61
470	0.52	0.55	0.56	0.57	0.58	0.59	0.60	0.62	0.62
500	0.54	0.57	0.58	0.59	0.60	0.60	0.62	0.65	0.65
550	0.55	0.58	0.59	0.59	0.60	0.61	0.63	0.65	0.66

Table 3-8 Mean Maximum Moment Ratios for Grouped Truck Loading (*Overall*)

Span (m)	Surveyed Truck Moment / Grouped Truck Loading Moment								
	1 day	2 weeks	1 month	2 months	6 months	1 year	5 years	50 years	75 years
420	0.82	0.86	0.88	0.89	0.91	0.92	0.96	0.99	1.00
470	0.86	0.89	0.92	0.92	0.95	0.96	0.98	1.02	1.03
500	0.82	0.86	0.88	0.88	0.91	0.92	0.95	0.98	0.99
550	0.86	0.90	0.92	0.93	0.95	0.97	0.99	1.03	1.04

Table 3-9 Mean Maximum Moment Ratios for AYK-45 (*Upper-Tail*)

Span (m)	Surveyed Truck Moment / AYK-45 Moment								
	1 day	2 weeks	1 month	2 months	6 months	1 year	5 years	50 years	75 years
420	0.62	0.66	0.67	0.68	0.70	0.71	0.74	0.78	0.79
470	0.65	0.68	0.70	0.71	0.73	0.74	0.77	0.80	0.81
500	0.66	0.71	0.73	0.74	0.76	0.77	0.80	0.85	0.85
550	0.68	0.73	0.75	0.76	0.78	0.79	0.82	0.86	0.86

Table 3-10 Mean Maximum Moment Ratios for HL-93 (*Upper-Tail*)

Span (m)	Surveyed Truck Moment / HL-93 Moment								
	1 day	2 weeks	1 month	2 months	6 months	1 year	5 years	50 years	75 years
420	0.85	0.91	0.94	0.95	0.97	0.99	1.03	1.08	1.09
470	0.90	0.95	0.98	0.99	1.01	1.03	1.06	1.12	1.12
500	0.92	0.98	1.01	1.02	1.05	1.07	1.11	1.17	1.18
550	0.94	0.99	1.02	1.03	1.06	1.08	1.12	1.17	1.18

Table 3-11 Mean Maximum Moment Ratios for H30-S24 (*Upper-Tail*)

Span (m)	Surveyed Truck Moment / H30-S24 Moment								
	1 day	2 weeks	1 month	2 months	6 months	1 year	5 years	50 years	75 years
420	0.51	0.55	0.56	0.57	0.59	0.60	0.62	0.65	0.66
470	0.54	0.57	0.58	0.59	0.61	0.62	0.64	0.67	0.67
500	0.55	0.59	0.61	0.62	0.63	0.64	0.67	0.71	0.71
550	0.56	0.60	0.61	0.62	0.64	0.65	0.67	0.71	0.71

Table 3-12 Mean Maximum Moment Ratios for Grouped Truck Loading (*Upper-Tail*)

Span (m)	Surveyed Truck Moment / Grouped Truck Loading Moment								
	1 day	2 weeks	1 month	2 months	6 months	1 year	5 years	50 years	75 years
420	0.84	0.90	0.92	0.93	0.96	0.98	1.02	1.07	1.08
470	0.89	0.94	0.97	0.98	1.00	1.02	1.06	1.11	1.11
500	0.85	0.91	0.94	0.95	0.98	0.99	1.03	1.09	1.10
550	0.90	0.95	0.98	0.99	1.02	1.03	1.07	1.13	1.13

Table 3-13 Mean Maximum Moment Ratios for AYK-45 (*Extreme*)

Span (m)	Surveyed Truck Moment / AYK-45 Moment								
	1 day	2 weeks	1 month	2 months	6 months	1 year	5 years	50 years	75 years
420	0.65	0.68	0.70	0.71	0.72	0.73	0.76	0.79	0.80
470	0.68	0.71	0.72	0.73	0.74	0.75	0.78	0.81	0.81
500	0.69	0.73	0.74	0.75	0.77	0.78	0.80	0.84	0.84
550	0.72	0.75	0.76	0.77	0.79	0.80	0.82	0.86	0.86

Table 3-14 Mean Maximum Moment Ratios for HL-93 (*Extreme*)

Span (m)	Surveyed Truck Moment / HL-93 Moment								
	1 day	2 weeks	1 month	2 months	6 months	1 year	5 years	50 years	75 years
420	0.90	0.95	0.97	0.98	1.00	1.02	1.05	1.10	1.10
470	0.94	0.98	1.00	1.01	1.03	1.05	1.08	1.12	1.13
500	0.96	1.01	1.03	1.04	1.06	1.08	1.11	1.16	1.16
550	0.98	1.02	1.05	1.06	1.08	1.09	1.12	1.17	1.17

Table 3-15 Mean Maximum Moment Ratios for H30-S24 (*Extreme*)

Span (m)	Surveyed Truck Moment / H30-S24 Moment								
	1 day	2 weeks	1 month	2 months	6 months	1 year	5 years	50 years	75 years
420	0.54	0.57	0.58	0.59	0.60	0.61	0.63	0.66	0.66
470	0.56	0.59	0.60	0.61	0.62	0.63	0.65	0.67	0.67
500	0.58	0.61	0.62	0.63	0.64	0.65	0.67	0.70	0.70
550	0.59	0.62	0.63	0.63	0.65	0.66	0.68	0.70	0.71

Table 3-16 Mean Maximum Moment Ratios for Grouped Truck Loading (*Extreme*)

Span (m)	Surveyed Truck Moment / Grouped Truck Moment								
	1 day	2 weeks	1 month	2 months	6 months	1 year	5 years	50 years	75 years
420	0.89	0.94	0.96	0.97	0.99	1.00	1.04	1.08	1.09
470	0.93	0.97	1.00	1.00	1.03	1.04	1.07	1.11	1.12
500	0.89	0.93	0.96	0.96	0.99	1.00	1.03	1.07	1.08
550	0.94	0.98	1.00	1.01	1.03	1.05	1.08	1.12	1.13

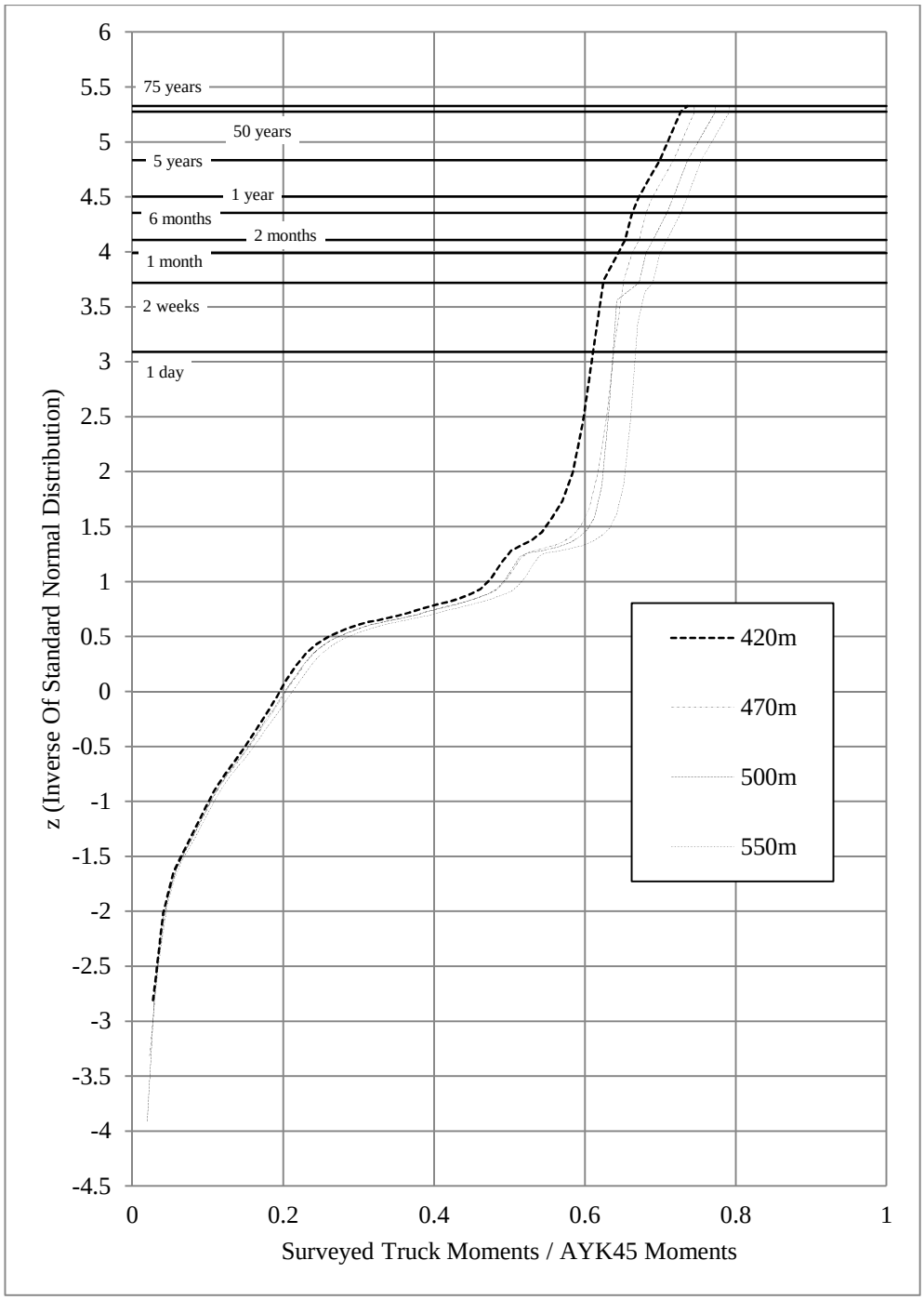

Figure 3-43 Extrapolated Moment Ratios for AYK-45 (*Overall*)

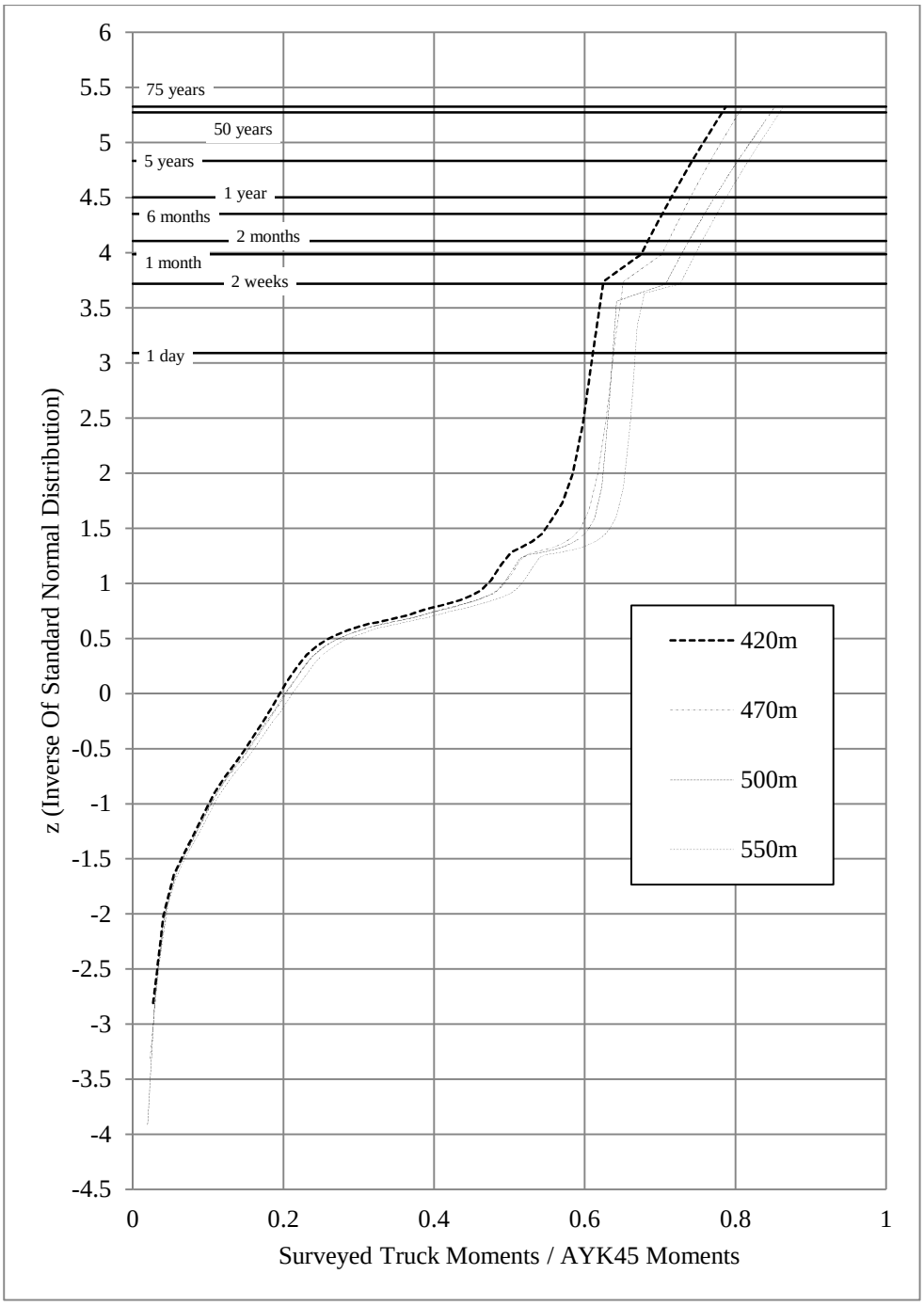

Figure 3-44 Extrapolated Moment Ratios for AYK-45 (*Upper-tail*)

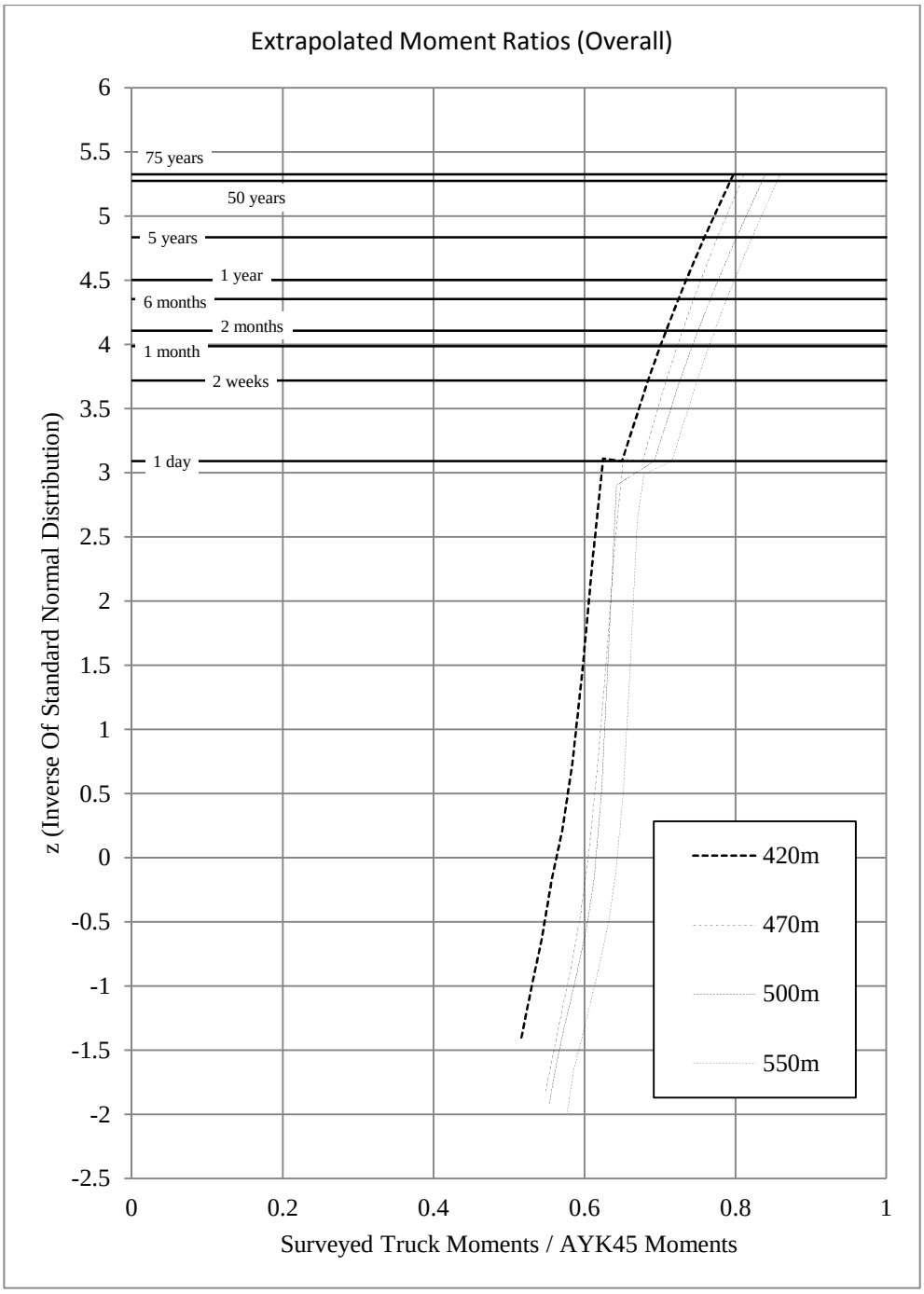

Figure 3-45 Extrapolated Moment Ratios for AYK-45 (*Extreme*)

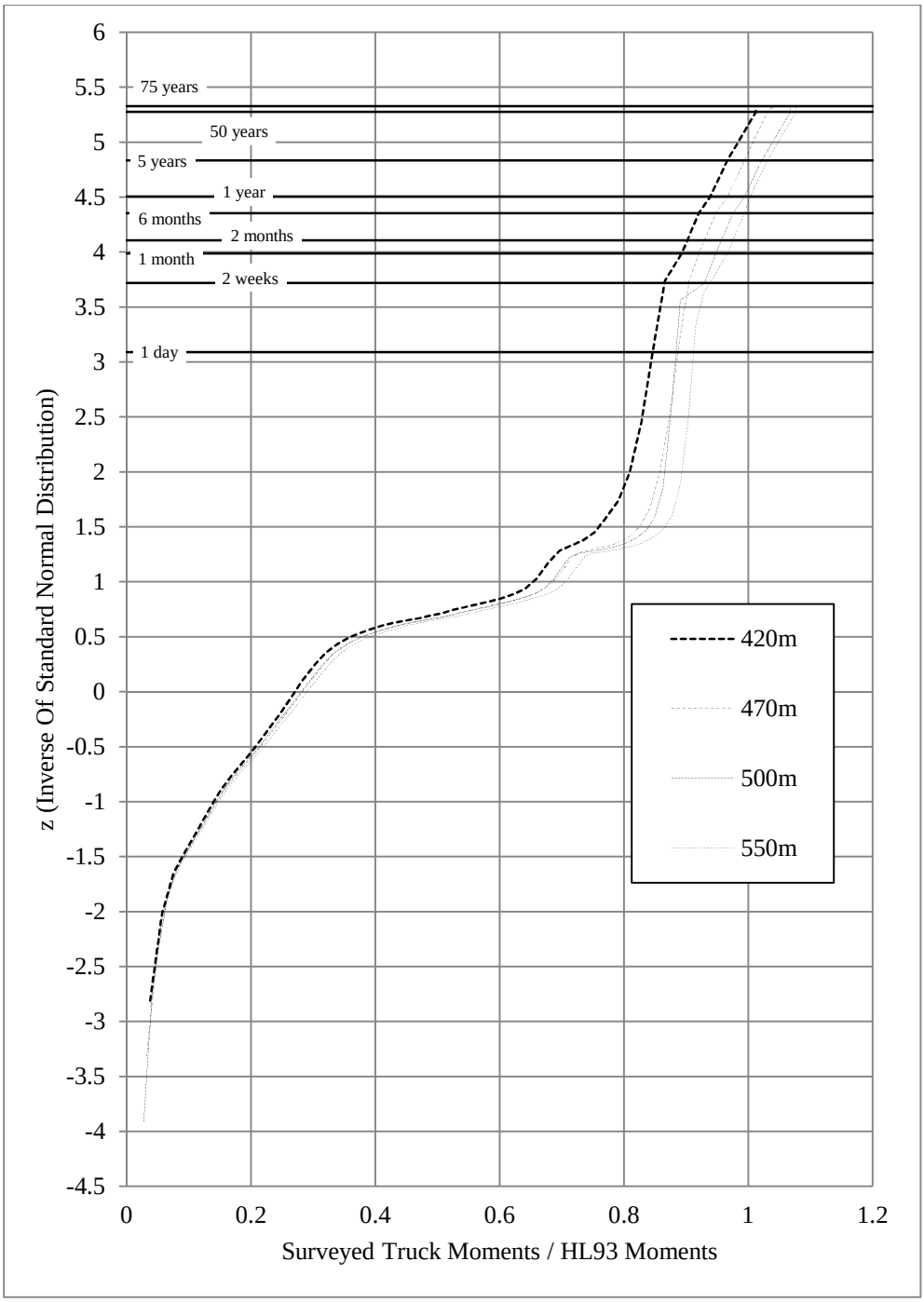

Figure 3-46 Extrapolated Moment Ratios for HL-93 (*Overall*)

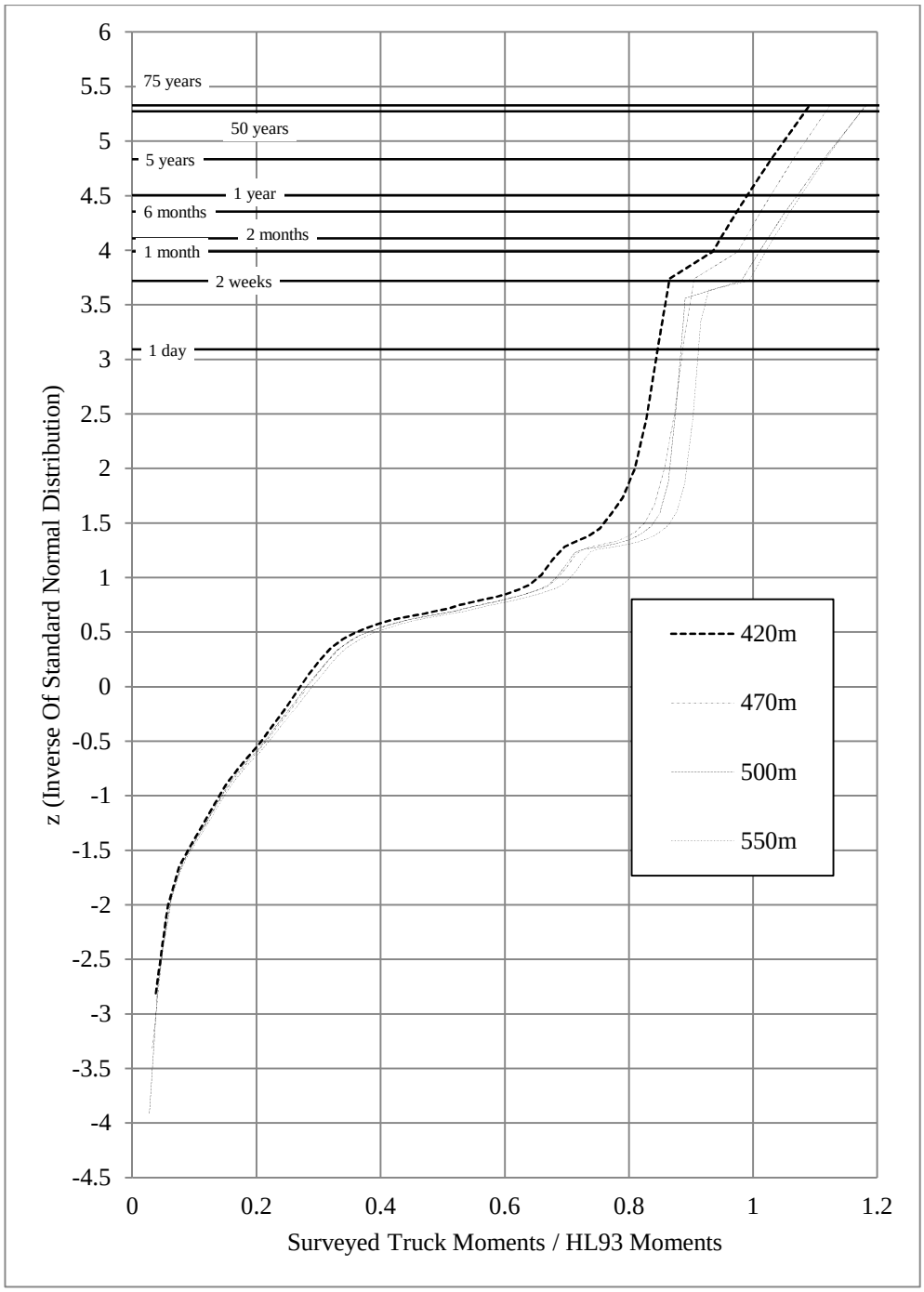

Figure 3-47 Extrapolated Moment Ratios for HL-93 (*Upper-tail*)

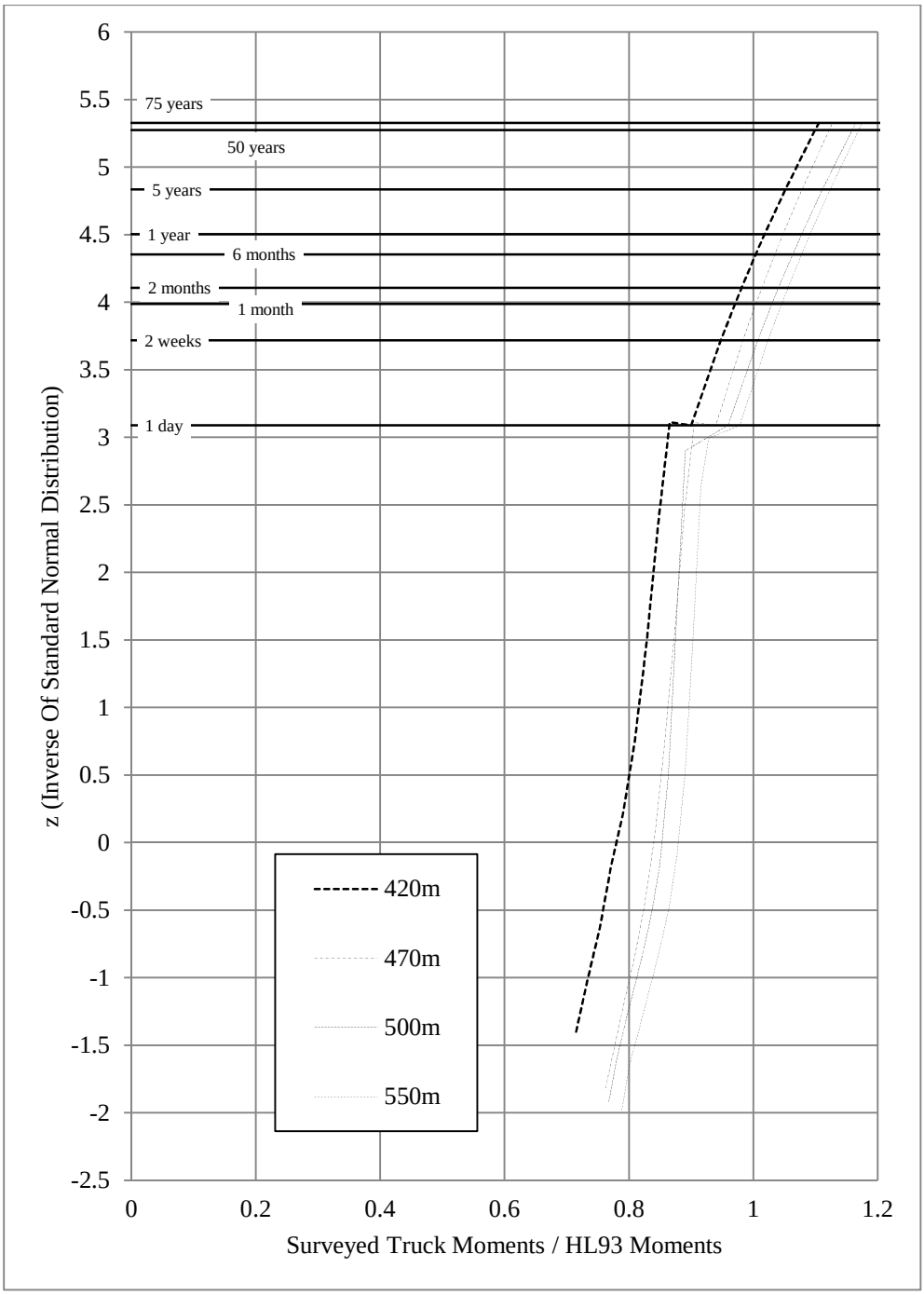

Figure 3-48 Extrapolated Moment Ratios for HL-93 (*Extreme*)

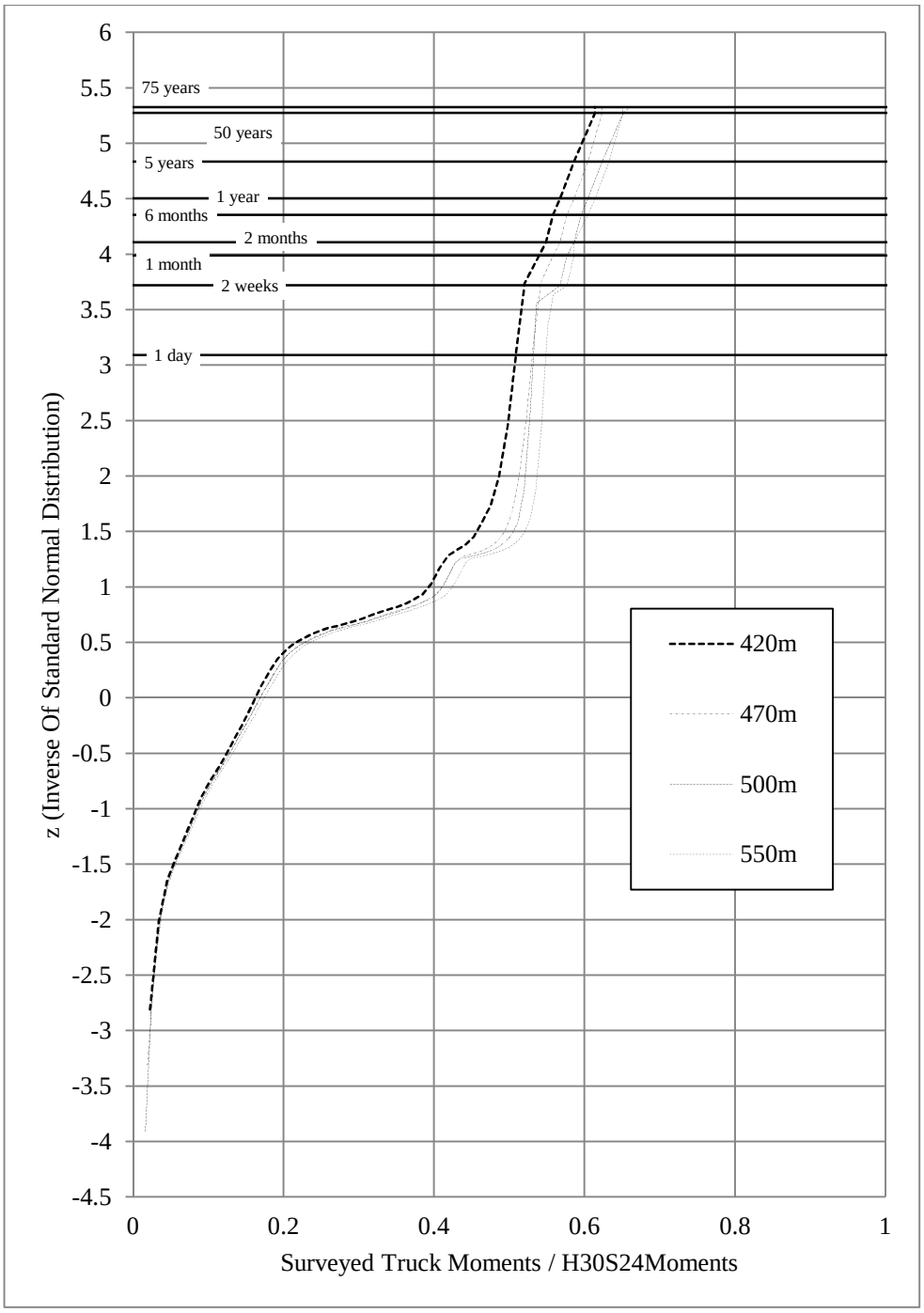

Figure 3-49 Extrapolated Moment Ratios for H30-S24 (*Overall*)

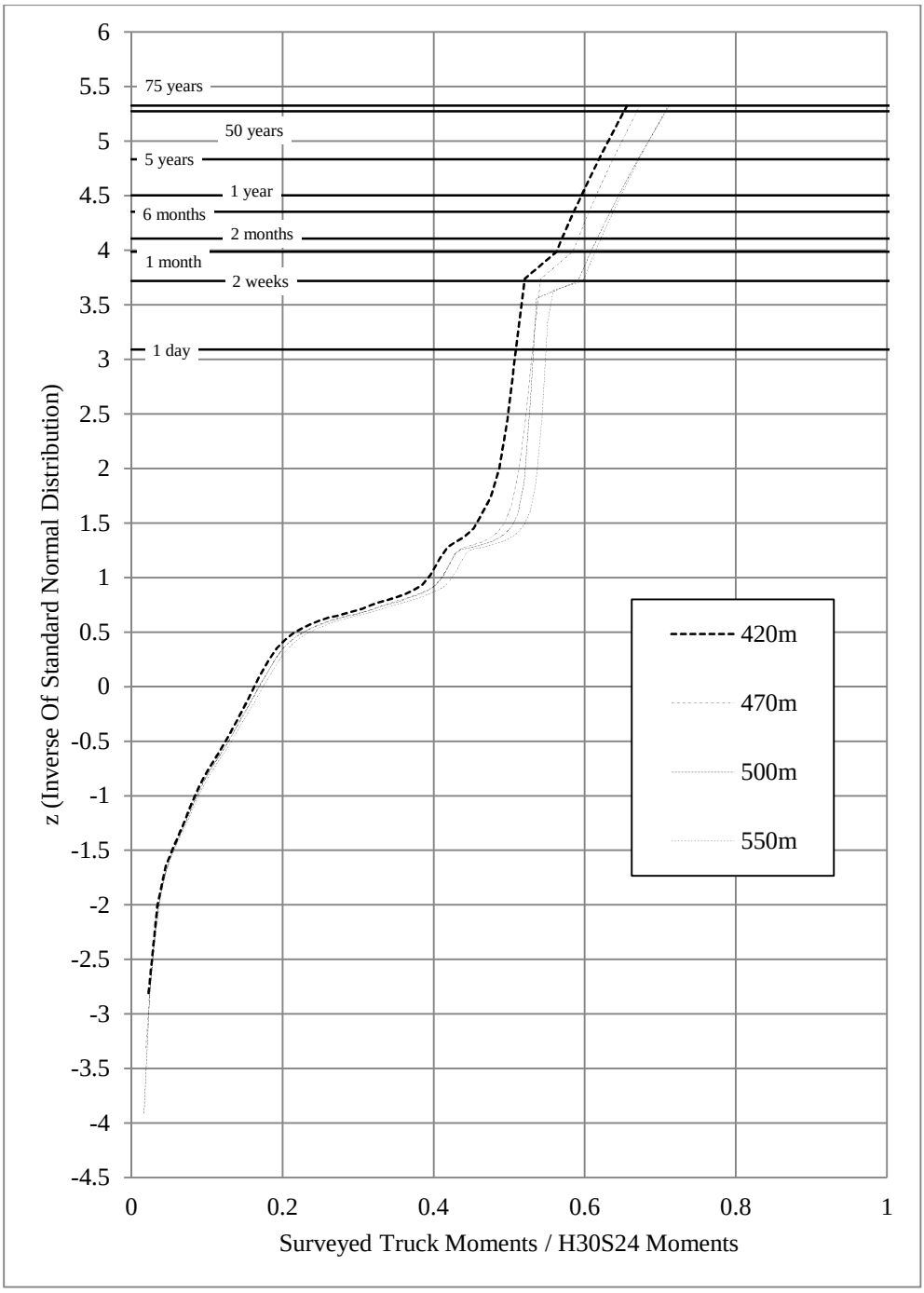

Figure 3-50 Extrapolated Moment Ratios for H30-S24 (*Upper-tail*)

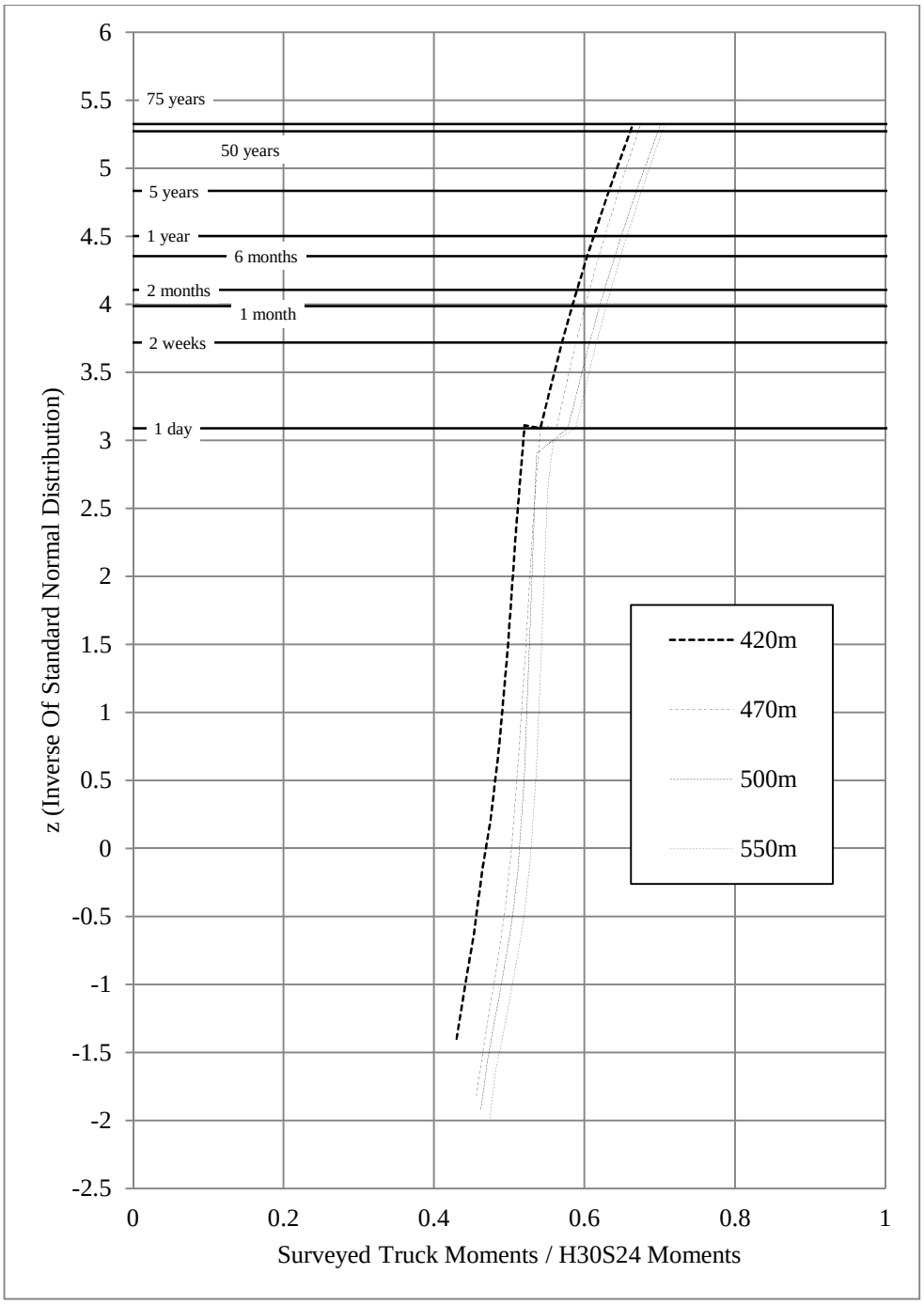

Figure 3-51 Extrapolated Moment Ratios for H30-S24 (*Extreme*)

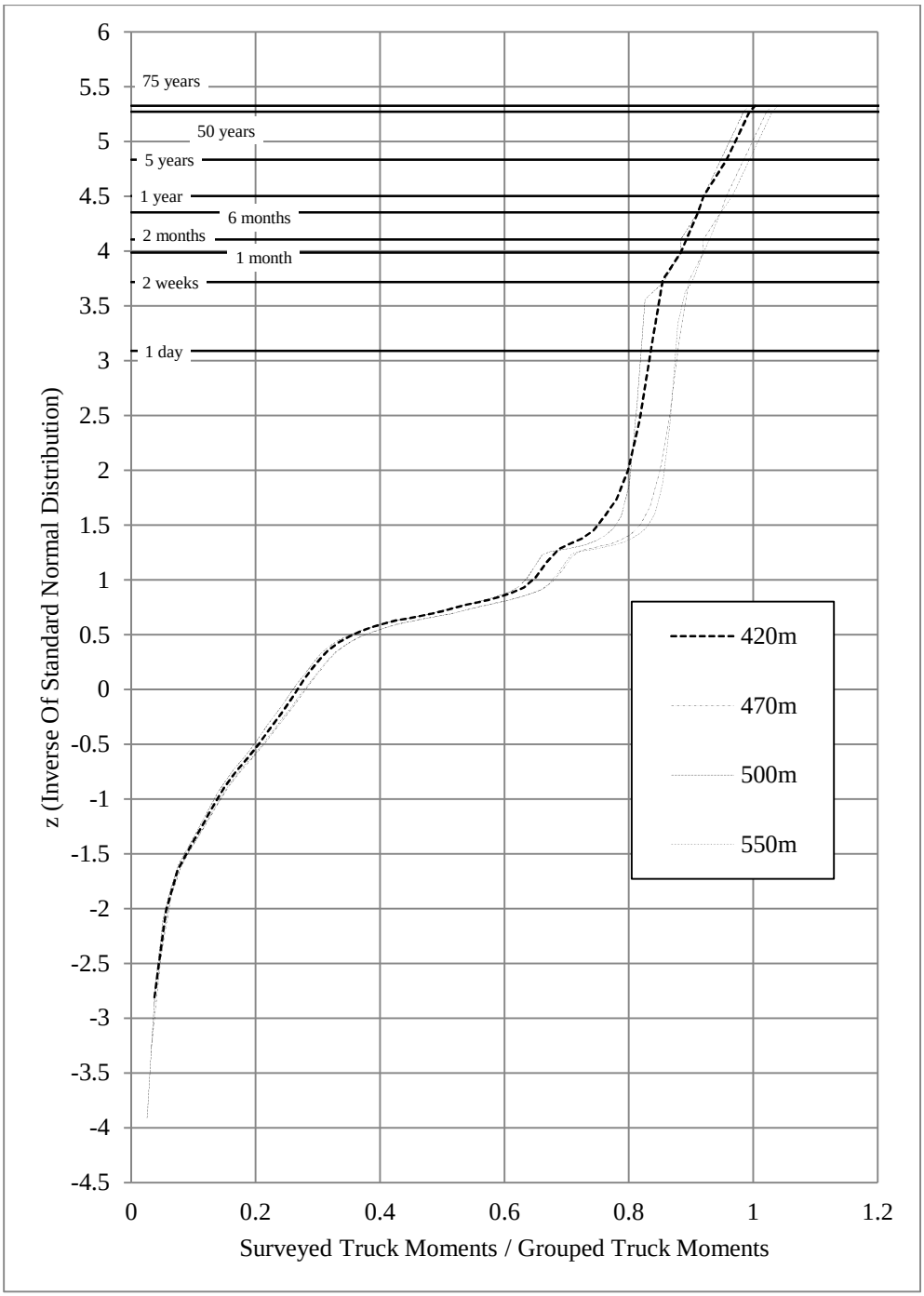

Figure 3-52 Extrapolated Moment Ratios for Grouped Truck Loading (*Overall*)

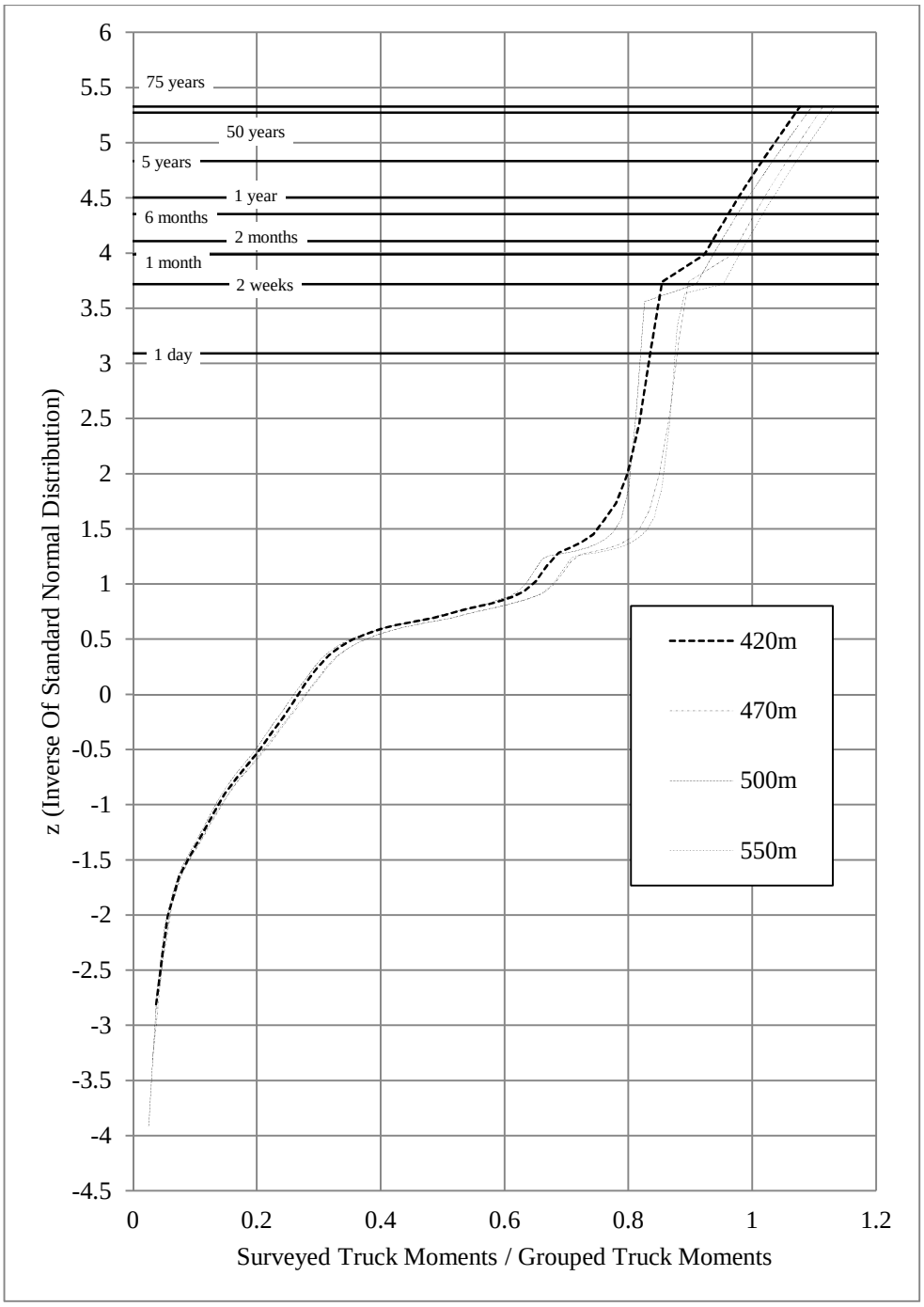

Figure 3-53 Extrapolated Moment Ratios for Grouped Truck Loading (*Upper-tail*)

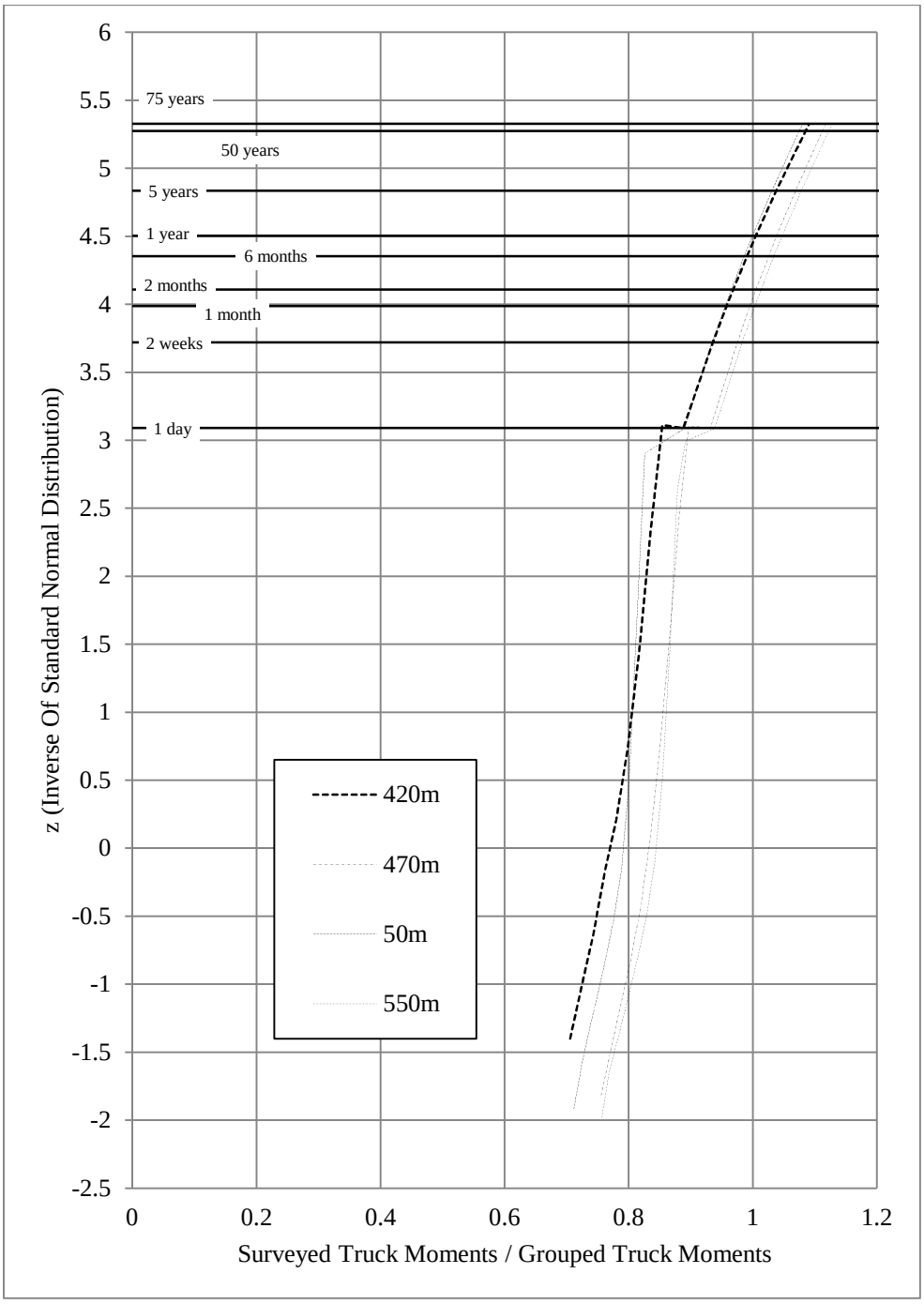

Figure 3-54 Extrapolated Moment Ratios for Grouped Truck Loading (*Extreme*)

3.2.3.3 Estimation of the Coefficient of Variation

Gumbel distribution method calculates the coefficient of variation of live load from the straight line equations fitted to the surveyed truck data points. The CDF of the Gumbel distribution for maxima is given by (Castillo, 1988);

$$y = F(x;\lambda,\delta) = \exp\left[-\exp\left[-\frac{x-\lambda}{\delta}\right]\right]; \quad -\infty < x < \infty \tag{3-4}$$

where, λ and δ are the Gumbel distribution parameters. Then, the straight line equation on Gumbel probability paper forms into (Castillo, 1988);

$$\eta = h(y) = -\log\left[\log\left(\frac{1}{y}\right)\right] \rightarrow \quad \eta = \frac{x-\lambda}{\delta} \tag{3-5}$$

The Gumbel parameters λ and δ can be determined by setting η = 0 and η = 1 (Castillo, 1988);

$$0 = x - \lambda \rightarrow x = \lambda \quad \text{and} \quad 1 = \frac{x-\lambda}{\delta} \rightarrow x = \lambda + \delta \tag{3-6}$$

After fitting the straight line on Gumbel probability paper, the abscissas associated with ordinate values 0 and λ of the reduced variate, η , give the values of λ and l +δ , respectively. After obtaining the values of λ and, the mean and variance of the Gumbel distribution can be calculated by the following expressions (Argınhan, 2010);

$$\mu = \lambda + 0.5772\delta \quad \text{and} \quad \sigma^2 = \frac{\pi^2\delta^2}{6} \tag{3-7}$$

where, μ and σ are the mean and standard variation, respectively.

From Gumbel probability papers (straight line equations) the coefficients of variation values are calculated for the three different cases that are overall, upper tail and extreme by using the procedure explained above. The results are tabulated in the Table 3-17 to Table 3-22.

Table 3-17 Parameters of Gumbel Distribution (*Overall*)

Span (m)	AYK-45		HL-93		H30-S24		Grouped Truck	
	λ	δ	λ	δ	λ	δ	λ	δ
420	0.188	0.102	0.261	0.142	0.157	0.085	0.257	0.140
470	0.196	0.113	0.273	0.158	0.163	0.094	0.270	0.156
500	0.194	0.128	0.268	0.177	0.162	0.107	0.249	0.164
550	0.201	0.128	0.275	0.175	0.165	0.105	0.264	0.168

Table 3-18 Mean, Standard Deviation and Coefficient of Variation of Moment Ratios (*Overall*) Estimated According to Gumbel Distribution

Span (m)	AYK-45			HL-93			H30-S24			Grouped Truck		
	μ	σ	COV	μ	σ	COV	μ	σ	COV	μ	σ	COV
420	0.247	0.131	0.531	0.343	0.182	0.531	0.206	0.109	0.531	0.338	0.180	0.531
470	0.262	0.145	0.556	0.364	0.202	0.556	0.218	0.121	0.556	0.361	0.200	0.556
500	0.267	0.164	0.613	0.371	0.227	0.613	0.223	0.137	0.613	0.344	0.211	0.613
550	0.275	0.165	0.598	0.376	0.225	0.598	0.226	0.135	0.598	0.361	0.216	0.598

Table 3-19 Parameters of Gumbel Distribution (*Upper-tail*)

Span (m)	AYK-45		HL-93		H30-S24		Grouped Truck	
	λ	δ	λ	δ	λ	δ	λ	δ
420	0.497	0.017	0.688	0.024	0.414	0.014	0.679	0.024
470	0.533	0.016	0.741	0.023	0.443	0.014	0.734	0.023
500	0.531	0.019	0.737	0.026	0.444	0.016	0.683	0.025
550	0.560	0.018	0.766	0.025	0.461	0.015	0.735	0.024

Table 3-20 Mean, Standard Deviation and Coefficient of Variation of Moment Ratios (*Upper-tail*) Estimated According to Gumbel Distribution

Span	AYK-45			HL-93			H30-S24			Grouped Truck		
(m)	μ	σ	COV	μ	σ	COV	μ	σ	COV	μ	σ	COV
420	0.507	0.22	0.44	0.702	0.31	0.44	0.422	0.18	0.44	0.693	0.30	0.44
470	0.543	0.21	0.39	0.754	0.29	0.39	0.451	0.17	0.39	0.747	0.29	0.39
500	0.542	0.24	0.45	0.752	0.34	0.45	0.453	0.20	0.45	0.698	0.31	0.45
550	0.571	0.23	0.40	0.780	0.32	0.40	0.469	0.19	0.40	0.749	0.30	0.40

Table 3-21 Parameters of Gumbel Distribution (*Extreme*)

Span	AYK-45		HL-93		H30-S24		Grouped Truck	
(m)	λ	δ	λ	δ	λ	δ	λ	δ
420	0.546	0.015	0.757	0.021	0.455	0.012	0.747	0.020
470	0.582	0.014	0.809	0.019	0.484	0.011	0.802	0.019
500	0.589	0.015	0.816	0.021	0.492	0.012	0.757	0.019
550	0.615	0.015	0.840	0.020	0.506	0.012	0.807	0.019

Table 3-22 Mean, Standard Deviation and Coefficient of Variation of Moment Ratios (*Extreme*) Estimated According to Gumbel Distribution

Span	AYK-45			HL-93			H30-S24			Grouped Truck		
(m)	μ	σ	COV	μ	σ	COV	μ	σ	COV	μ	σ	COV
420	0.555	0.19	0.35	0.769	0.27	0.35	0.462	0.16	0.35	0.759	0.26	0.35
470	0.590	0.17	0.30	0.820	0.24	0.30	0.491	0.15	0.30	0.813	0.24	0.30
500	0.597	0.19	0.32	0.828	0.27	0.32	0.499	0.16	0.32	0.768	0.25	0.32
550	0.623	0.19	0.30	0.852	0.25	0.30	0.512	0.15	0.30	0.818	0.24	0.30

3.2.3.4 Comparison of the Different Extrapolation Cases

In Figure 3-43 to Figure 3-54, 75-year maximum moment ratios vs. span lengths are presented for all three cases investigated, and coefficients of variation are plotted in Figure 3-59. As expected, extrapolated maximum moment ratios of extreme and upper-tail cases are higher than the overall case. Nevertheless, coefficients of variation values are significantly higher for the overall case, which is also expected because of having a heterogeneous data set (heavy and light trucks). For reliability

analyses that will be discussed in the forthcoming chapters, statistical parameters of overall case will be considered because of the following two reasons.

- Using higher coefficient of variation of live load results in less (critical) reliability index.
- Overall data set represents the real-life traffic better than extreme and upper-tail cases since those two cases consider only the heaviest trucks of the surveyed data. An isolated data set may give more conservative results (over-design), however; they cannot represent the real life simulation.

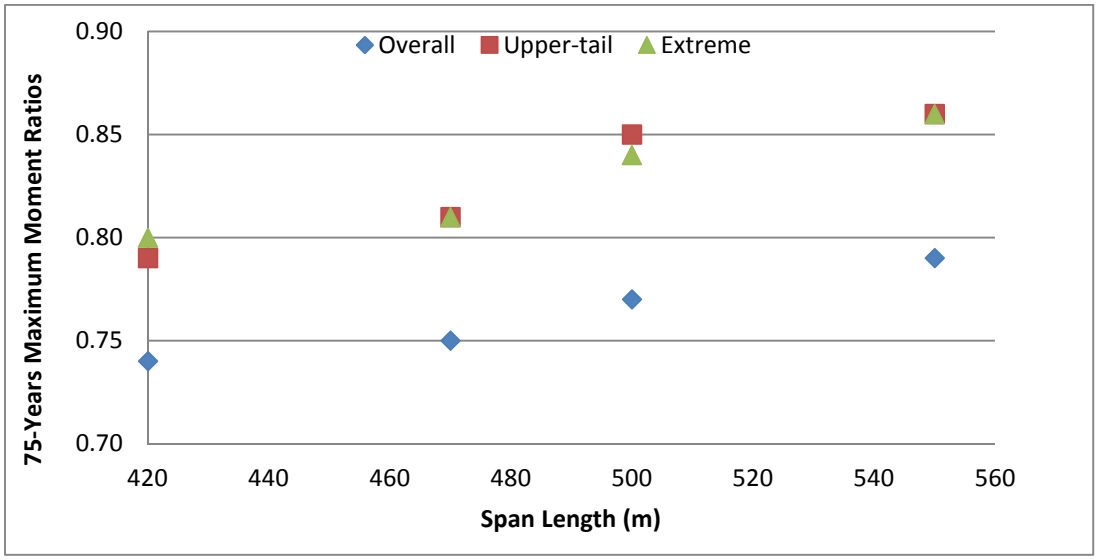

Figure 3-55 Variation of 75 year Mean Maximum Moment Ratio with Span Lengths for AYK-45

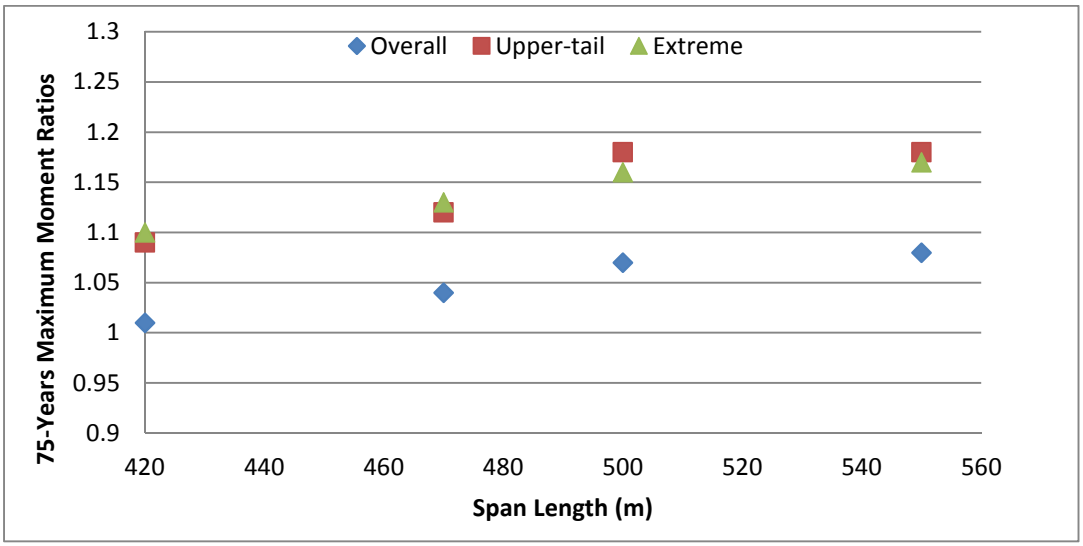

Figure 3-56 Variation of 75 year Mean Maximum Moment Ratio with Span Lengths for HL-93

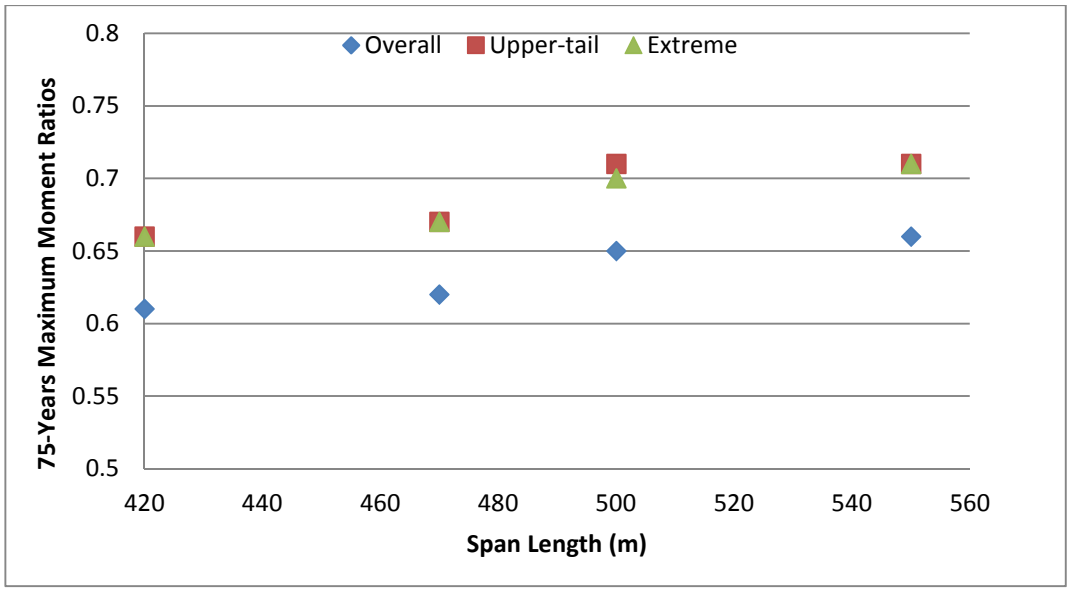

Figure 3-57 Variation of 75 year Mean Maximum Moment Ratio with Span Lengths for H30-S24

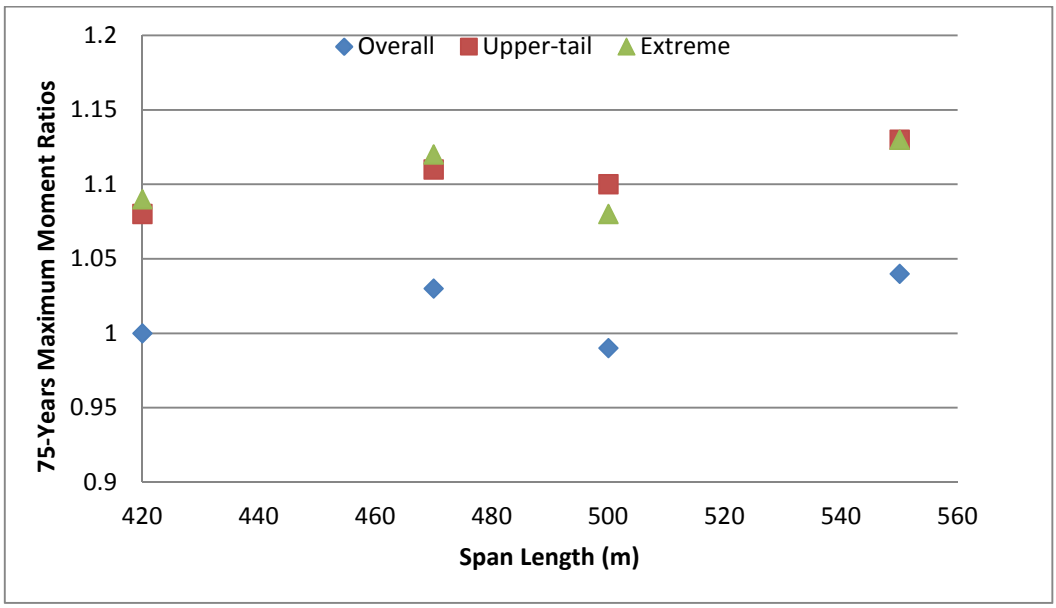

Figure 3-58 Variation of 75 year Mean Maximum Moment Ratio with Span Lengths for Grouped Truck Loading

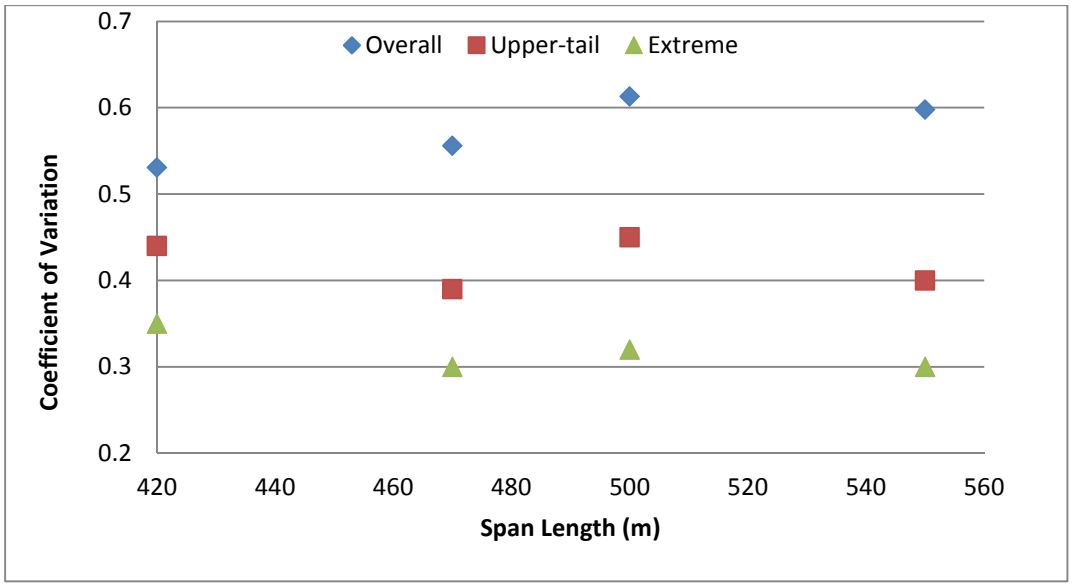

Figure 3-59 Comparison of the Coefficients of Variation

3.3 Dynamic Load

The dynamic load depends on the vehicle weight, vehicle type, axle configuration, road roughness, bridge span length, and transverse position of truck on the bridge. Moreover, dynamic load is a random load and it is variable in time. An equivalent static live load is described to define the dynamic load and a dynamic load factor (DLF) is used for that purpose. One of the definition for DLF is the ratio of dynamic response and static response. In this definition, dynamic response stands for the absolute maximum dynamic response at any point (e.g. stress, strain or deflection) measured from the test data and static response stands for the maximum static response from the filtered dynamic response (Nassif and Nowak, 1995). The dynamic and static behavior of a bridge under a live load of 5-axle truck traveling at a speed of 104 km/h is presented in Figure 3-60.

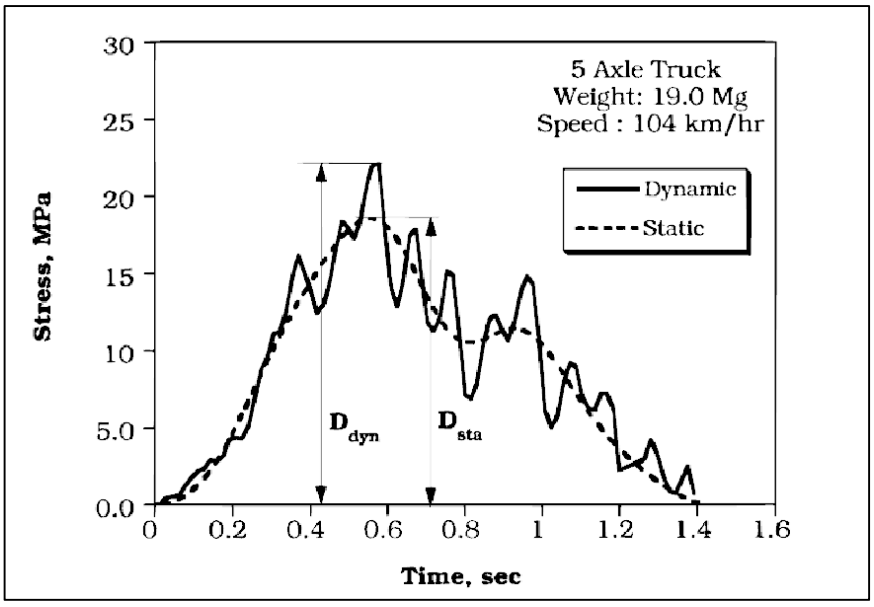

Figure 3-60 Static and Dynamic Response of a Bridge Due to a Truck (Nassif and Nowak, 1995)

The static response of the design truck is increased by 33% in order to take into account the dynamic load effect in Strength I limit state in AASHTO LRFD Bridge Design Specification. In calibration report (Nowak, 1999), statistical parameters of dynamic load are reported as 0.15 for mean value and 0.80 for the coefficient of variation. In this study, these values are used.

3.4 Multiple Presence Factor

The investigated bridges in this study have six lanes. The design of the bridge girders is performed with considering all the six-lanes are loaded with design live load models at the same time. Although the probability of having multiple heavy trucks traveling at the same speed of a multi-lane bridge is rare event, this case has to be handled. For this reason, in AASHTO LRFD Bridge Design Specification, the following multiple presence factors are offered;

Table 3-23 Multiple Presence Factors in AASHTO LRFD

Number of Design Lanes	Multiple Presence Factor
1	1.2
2	1
3	0.85
More Than 3	0.65

According to table presented above, multiple presence factor is selected as 0.65 in this study.

3.5 Chapter Summary

In this chapter, statistical parameters of loads, i.e. bias factors and COVs, are gathered and calculated. Moreover, live load models are introduced. Statistics of dead load are obtained from Nowak's Calibration Report (1999). Dead load is composed of four components, D_1 is weight of factory made elements, D_2 is weight of cast-in place concrete, D_3 is weight of wearing surface and D_4 is weight of miscellaneous. In this study, four different live load models are used. These are AYK-45, H30-S24, HL-93 and grouped truck loading (created from Turkish truck survey data). After performing necessary structural analyses with all live load models and all bridge models, statistics of live loads are calculated by applying extreme value theory (75-years projection process) and Gumbel distribution formulation. In Table 3-24, statistical parameters for dead loads, live loads and impact factor are summarized. In the following chapter, statistics of resistance are determined.

Table 3-24 Summary of Statistical Parameters of Loads

Parameter	Description	Probability Distribution	Bias Factor	Coefficient of Variation
D1	Dead Load – Factory Made Members	Normal	1.03	0.08
D2	Dead Load – Cast in Place Members	Normal	1.05	0.10
D3	Dead Load – Wearing Surface	Normal	1.00	0.25
D4	Dead Load - Miscellaneous	Normal	1.05	0.10
LL	Live Load – AYK45	Gumbel	0.263	0.574
	Live Load – HL93	Gumbel	0.363	0.574
	Live Load – H30S24	Gumbel	0.218	0.574
	Live Load – Grouped Truck Loading	Gumbel	0.351	0.574
IM	Impact Factor	Normal	0.15	0.8

CHAPTER 4

STATISTICS OF RESISTANCE

In positive moment region, flexural resistance capacity for slab on steel plate bridge girders determined with respect to nominal resistance values. In this chapter, statistical parameters for resistance (i.e. material properties; steel and concrete) are stated. Both international and local research databases are used to obtain these parameters.

4.1 Material Properties

As mentioned before composite steel girders are used in this study. Since these girders are composed of steel and concrete, the statistics of concrete and steel will be assessed as material properties since materials give the strength to the structure.

4.1.1 Concrete

Concrete is a composite material composed of water, aggregate and cement, basically. Construction industry in Turkey uses concrete as main construction material very widely. According to European Ready Mixed Concrete Organization (ERMCO), Among the European countries Turkey is one of the leader country in RMC manufacturing (RMC Industry Statistics Report, 2014). In Figure 4-1, country RMC production per capita in Europe is presented and Turkey is shown as “TK”.

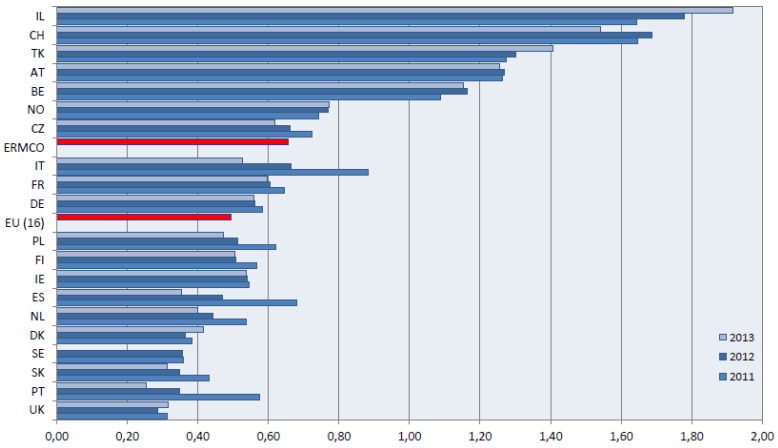

Figure 4-1 RMC Production per Capita in Europe (ERMCO, 2014)

Prior to 1999, the most widely produced concrete classes were C14, C16 and C18 in Turkey. However, after the year 2000, high strength concrete production has been increased. Turkish Ready Mixed Concrete Association (THBB), published a graph (2013) for concrete production percentages with grades versus years in Turkey. In Figure 4-2, these values are presented. According to graph, in years, production of higher strength concrete is preferred which shows the development in construction industry of Turkey. Moreover, another result can be interpreted from the graph that is in recent years about 50% of the produced concrete has a compressive strength of 30 MPa or more.

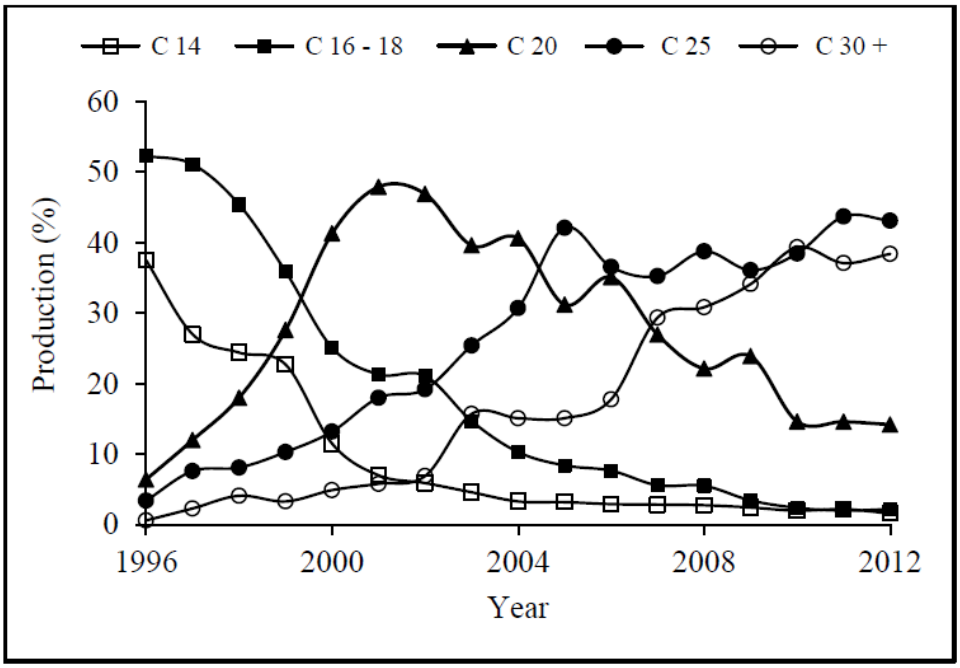

Figure 4-2 Concrete Production (in percentages) with respect to Years

Compressive strength is the most important characteristic property of concrete. In many structural designs, concrete is assigned to overcome the compressive stresses. Even the other stresses (shear or tension) occur in concrete, measures and defining characteristics of those are made in terms of compressive strength of concrete (Kesler, 1966). Therefore, statistics of compressive strength of concrete is assessed.

The minimum allowable concrete compressive strength for decks is 4.0 ksi (27.6 MPa) according to AASHTO LRFD 2010 5.4.2.1. As mentioned, in Turkey C30 grade of concrete is used frequently. Therefore, as concrete class for bridge decks of this study C30 class concrete is selected.

Fırat (2006) conducted a study to determine the concrete quality produced in Turkey. The 28-day compressive strength results were collected for 150x150x150 mm cubic test specimens from many different test laboratories in Turkey by Fırat. Collected test results belonged to the years between 2000 and 2005. However, Fırat also made a comparison between the collected results and the available previous test results. In Table 4-1 and Table 4-2, Fırat's study results are shown.

Table 4-1 Statistics of 28-Day Cubic Compressive Strength of Concrete (Fırat, 2006)

Year	Number of Samples	Mean (MPa)	COV	Number of Values Under Limit	Percentage of Values Under Limit (%)
94/95	417	20.60	-	58	13
2000	732	26.97	0.142	40	5.46
2001	535	30.97	0.107	23	4.30
2002	465	31.21	0.104	10	2.15
2003	644	30.78	0.131	36	5.59
2004	1283	28.87	0.123	30	2.34
2005	615	29.97	0.120	24	3.90

Table 4-2 Statistics of 28-Day Cubic Compressive Strength of Different Concrete Grades (Fırat, 2006)

Grade of Concrete	Number of Samples	$f'_{c,cube}$ (MPa)	Mean (MPa)	COV	Number of Values Under Limit	Percentage of Values Under Limit (%)
C14	137	18	20.04	0.143	1	0.83
C16	755	20	25.11	0.144	13	1.73
C18	739	22	25.82	0.120	23	3.11
C20	5817	25	28.46	0.104	118	2.70
C25	2767	30	32.48	0.100	53	2.81
C30	870	37	40.07	0.079	14	2.47

Since C30 grade of concrete was selected for bridge deck, statistics of this grade will be investigated. According to Table 4-2, C30 concrete grade has mean value for 28-day cubic compressive strength 40.07 MPa and coefficient of variation 0.079 (Fırat, 2006). However, in these statistics epistemic uncertainties are not considered.

Epistemic uncertainties that affect the strength of concrete are listed below.

- Human errors
- Rate of loading
- Discrepancies between in-situ conditions and laboratory test conditions
- Difference of test batches and site batches

*N*1 is a correlation factor is introduced to take into account the difference between actual strength at site and test specimen strength at laboratory. Bloem (1968, as cited in Ang and Tang, 1984) stated that strength of site concrete is lower up to 10% to 21% than the strength of laboratory concrete. Fırat (2007) cited that Mirza et al. (1979) reported the range of strength difference between cores and test specimens as 0.74 – 0.96 with and overall average value of 0.87. Correspondingly, Ellingwood and Ang (1972) stated this ratio range as 0.83 - 0.92. In Fırat's study (2006) the mean correction factor was taken as 0.86 (the average value of the ranges). Moreover, since the quality control rules in bridge construction is obeyed more strictly when

compared with in a regular construction, Argınhan (2010) made an upper triangular distribution assumption between lower limit and upper limit of ranges. Argınhan (2010) concluded the mean correction factor, $N1$, as 0.89. Coefficient of variation, $\Delta 1$, is suggested as 0.1 by Mirza et al. (1979, as cited in Fırat, 2006). Finally, in this study, mean correction factor, $N1$ is taken as 0.89 and COV, $\Delta 1$, is taken as 0.1.

Another epistemic uncertainty that affect the strength of concrete is rate of loading. In order to take into account this uncertainty type, $N2$ which is a correlation factor, was introduced by Mirza et al. (1979, as cited in Fırat, 2006). An empirical formula was used to define the value of $N2$ stated below:

$$N_2 = 0.89x(1 + 0.08log_{10}(R)) \quad (4\text{-}1)$$

where R is the rate of loading in unit of psi/sec. When R is taken as 1 psi per second, $N2$ is calculated as 0.89. Kömürcü (1995, as cited in Fırat, 2006) stated that mean correction factor, $N2$, can be taken as 0.88 and corresponding COV, $\Delta 2$ can be taken as zero i.e. with no prediction uncertainty. For the rate of loading statistics the same suggested values are used in this study.

Human error is the last epistemic uncertainty that has to be considered while determining the statistics of concrete strength. Some actions and mistakes may be made by technical person like selecting specimens from a special batch instead of randomly taken from actual mix or not applying standard testing procedures, properly. To take into account this uncertainty type, Kömürcü (1995, as cited in Fırat, 2006) introduced a mean correction factor, $N3$, as 0.95 and a prediction uncertainty, $\Delta 3$, as 0.05. Due to high attention to quality control in bridge construction Argınhan (2010) used this correction factor as 1.0. In this study, mean correction factor, $N3$ is taken as 1.00 and COV, $\Delta 3$, is taken as 0.05.

All epistemic uncertainties are combined as following:

$$\overline{N_{f_c'}} = \overline{N_1} \times \overline{N_2} \times \overline{N_3} = 0.89 \times 0.88 \times 1.0 \cong 0.8 \qquad (4\text{-}2)$$

$$\Delta_{f_c'} = \sqrt{\Delta_1^2 + \Delta_2^2 + \Delta_3^2} = \sqrt{0.1^2 + 0^2 + 0.05^2} = 0.11 \qquad (4\text{-}3)$$

Compressive strength (true strength) of C30 grade of concrete is re-calculated as 0.8×40.07 = 32.1 MPa (for cubic specimen). C30 grade of concrete has a cubic compressive strength of 37 MPa. Bias factor for compressive strength of C30 grade of concrete is 32.1/37 = 0.87.

Total coefficient of variation is combined as following:

$$\Omega_{f_c'} = \sqrt{\delta_{f_c'}^2 + \Delta_{f_c'}^2} = \sqrt{0.079^2 + 0.11^2} = 0.135 \qquad (4\text{-}4)$$

where $\delta fc'$ is inherent uncertainty and $\Delta fc'$ is the total epistemic uncertainty. In Table 4-3, statistical parameters of C30 grade of concrete is summed up.

Table 4-3 Summary of Statistics of C30 Grade of Concrete

Statistical Parameters (Cubic)	Values
Laboratory Measured Mean (MPa)	40.07
In-situ Mean (MPa)	32.06
Nominal (MPa)	37
Bias Factor (Mean/Nominal)	0.87
Coefficient of Variation	0.135
Standard Deviation (MPa)	4.32

4.1.2 Steel

In steel production process, as raw materials iron ore, coke, limestone, and chemical additives are used. Iron ore, coke and limestone are typical raw materials to produce steel; however, chemical admixtures are used for providing custom-designed products for special applications, just similar to chemical admixtures used for producing concrete having some special properties. To be able to reduce the non-uniformity in steel production, better controlled process has to be applied. This results with more reliable final product (Barker and Puckett, 2007).

Güreş (2013) stated that in year 2012 Turkey is the 8th largest steel producer of the world according to international production values. In Turkey, nearly 60% of the steel structures have been built for industrial purposes. Only 3% of the steel structures are bridges (Altay and Güneyisi, 2008). Distribution of steel structure percentages in Turkey in terms of their types is presented in Figure 4-3.

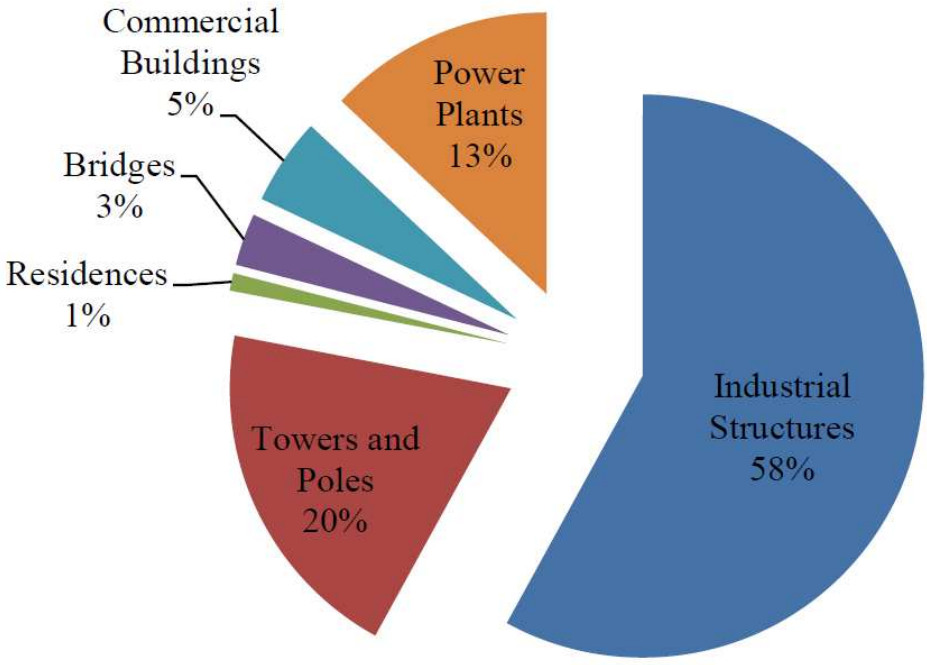

Figure 4-3 Distribution of Steel Structures (Altay and Güneyisi, 2008)

While considering the properties of steel related with strength yield strength, tensile strength, ductility, hardness, and toughness are evaluated. The definitions of those (Koç, 2013):

• *"Yield strength is the stress at which an increase in strain occurs without an increase in stress."*
• *"Tensile strength is the maximum stress reached in a tensile test."*
• *"Ductility is an index of the ability of the material to withstand inelastic deformations without fracture and can be expressed as a ratio of elongation at fracture to the elongation at first yield."*
• *"Hardness refers to the resistance to surface indentation from a standard indenter."*
• *"Toughness is the ability of a material to absorb energy without fracture."*

In Turkey, S235, S275 and S355 grade of steel are used, commonly. The most important properties of steel which are yield and tensile strength are tabulated in Table 4-4 for mentioned grades.

Table 4-4 Strength Values of Different Steel Grades

Grade	Yield Strength (MPa)	Tensile Strength (MPa)
S235	235	360-510
S275	275	430-580
S355	355	510-680

Statistical parameters for steel are taken from an international paper of Liu (2002) because there is no research for mechanical properties of steel in Turkey. Bias factor for yield strength is taken as 1.12 and coefficient of variation of that is taken as 0.0866.

4.2 Dimensions and Theoretical Behavior

Steel section dimensions involve uncertainties due to manufacturing errors. The dimensions of steel sections are assumed to be distributed normally. Dimensions can be classified as thickness and width. Bias factor and coefficient of variation of thickness are 1 and 0.0350, respectively, and 1 and 0.0135 for width (Li, 2007).

As cited in Koç (2013) *"Theoretical behavior is another variable that influences resistance. It involves uncertainties due to assumptions or approximations in analysis. Therefore, that should be taken into consideration in reliability analysis. Nowak (1999) describes a multiplier named professional factor to consider this uncertainty. For composite steel girders, bias factor and coefficient of variation of professional factor can be taken as 1.05 and 0.06, respectively. Nominal value of professional factor is taken 1.0 in reliability analysis."*

4.3 Chapter Summary

In chapter 4, statistical parameters, bias factors and COVs, are gathered and calculated for composite edge girder resistance components. Resistance is composed of concrete (deck – C30) and steel (steel plate girder – S355) materials. However, other than materials used in edge girder cross-section there are also two points affecting the resistance which are dimensions and theoretical behavior. In Table 4-5, statistical parameters for resistance components are summarized. In chapter 5, bridge girder nominal capacity calculation, structural analysis and design results are expressed and presented.

Table 4-5 Summary of Statistical Parameters of Resistance

Parameter	Bias Factor	COV	Distribution Type
Compressive Strength of Concrete	0.87	0.135	Normal
Yield Strength of Steel	1.12	0.0866	Log-normal
Thickness	1.00	0.0350	Normal
Width	1.00	0.0135	Normal
Professional Factor	1.05	0.06	Normal

CHAPTER 5

DESIGN OF BRIDGE GIRDERS

Demand and capacity are the two essential parts of engineering designs. As in engineering disciplines, in structural engineering demand and capacity are computed in design process. In this chapter, the design process of the main girders of cable stayed bridges is described. Computing nominal flexural resistance capacities of composite girders (i.e. obtaining M_n), obtaining demand forces from structural analysis (i.e. obtaining M_u) and evaluating design results of the girders are explained.

In this study, a real life cable-stayed bridge which is Cooper River Bridge in South Carolina is selected as reference bridge design. Original bridge has a main span length (L1) of 470 meters and 195 meters edge spans (L2). From original bridge type by modifying the span dimensions other three bridges are obtained to increase the span length range of the study. Furthermore, tower stiffness values are modified to keep the Kl/r values constant for all bridges considered in this study. Cables are re-designed based on AASHTO LRFD Table 3.4.1-1. The bridge dimensions and some properties are tabulated in Table 5-1 for all four different studied bridges. Moreover, in Figure 5-1 typical cable stayed bridge side view and span length abbreviations are presented.

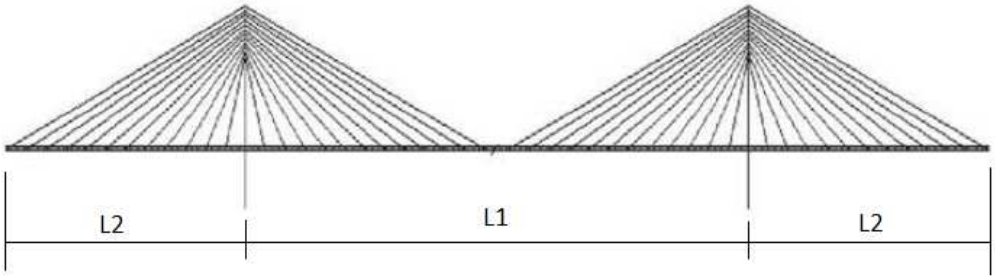

Figure 5-1 Typical Side View of a Cable Stayed Bridge

Table 5-1 Some Important Bridge Dimensions and Properties

Bridge Number	Main Span Length-L1 (m)	Edge Span Length-L2 (m)	Width (m)	Lane Number	Cable Spacing (m)
Bridge #1	420	195	39	6	14.65
Bridge #2 (Original)	470	195	39	6	14.65
Bridge #3	500	205	39	6	14.65
Bridge #4	550	210	39	6	14.65

The load carrying system of a cable stayed bridge is as follows. Structural components of the cable stayed bridge is presented in Figure 5-2.

- The dead and live loads are transferred to edge girders by floor beams.
- The loads on edge girders are taken by cables as tension forces.
- Cable tension forces are transferred to pylons as compression and bending forces.
- Finally, pylon forces are transferred to foundation system.

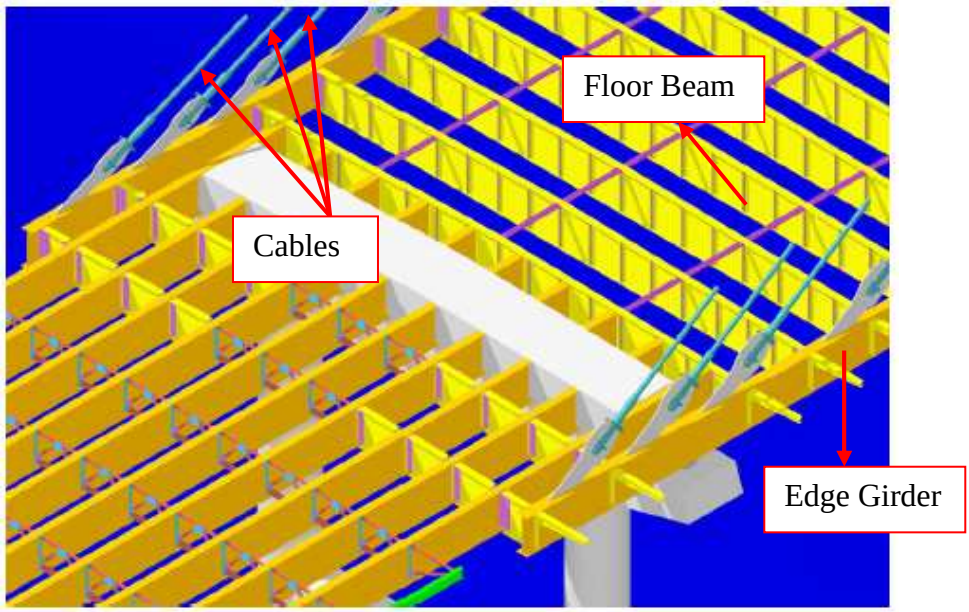

Figure 5-2 Structural System of Cable Stayed Bridge (Abrahams et al.)

As mentioned in chapter 3, in this study as live load model four different design truck models are used (AYK-45, H30-S24, HL-93 and Grouped Truck Loading). However, bridge girders are designed with respect to AYK-45 loading, only because AYK-45 truck live load model is a new loading prepared for new Turkish LRFD specifications and it is a good method to compare this new loading type with other existing live load models. By doing this design procedure (selecting girder cross-section dimensions w.r.t. AYK-45 and just analyzing for the other loadings) it is possible to see whether AYK-45 loading is reliable or not for long-span bridges. Furthermore, designs are carried out to obtain a minimum reliability index of 4.30.

5.1 Effect of Axial Load

In this study, composite edge girder flexural capacity is calculated with pure-bending beam formulation rather than beam-column formulation. In other words, axial load on the girder is ignored because axial stress on steel-plate I girder is very low at area of interest which is mid-span region. In addition, along the edge girder of the bridge the maximum ratio of axial stress to yield stress of steel is around 0.10. This means that edge girders can be designed as beam elements under bending action, only. In the following, axial stress calculations, necessary diagrams, figures and comparisons are presented.

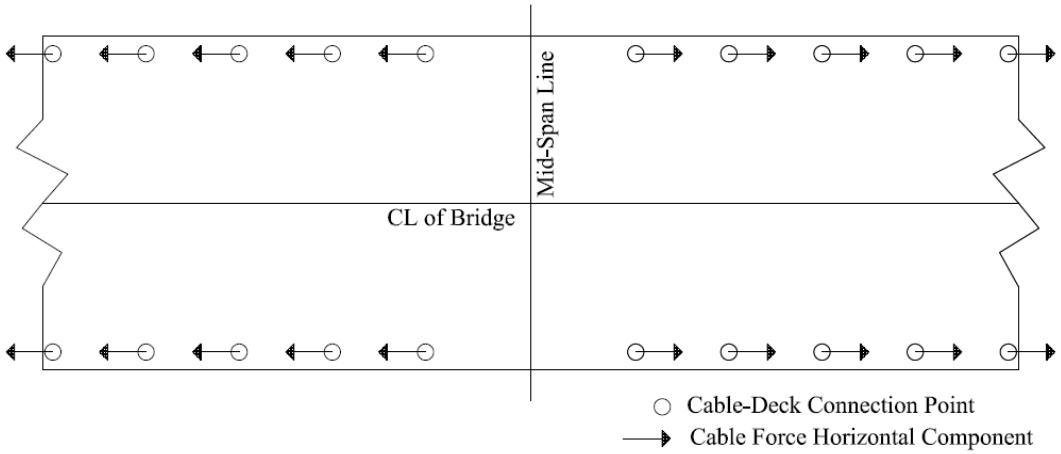

Figure 5-3 Bridge Deck Plan View Sketch

In Figure 5-3, plan view of bridge deck is shown as a sketch. Axial stress on the edge girder develops as follows;

- Horizontal force component of cable is transferred to the deck from cable-deck connection points.
- Axial force distribution occurs to whole deck section and an axial stress occurs on the deck.
- This axial stress creates axial strain on the deck. Since steel plate I girder and concrete deck show a composite characteristic, steel plate I girder has the same strain with the deck.
- Axial stress on the edge girder can be find multiplying this axial strain with modulus of elasticity of steel.

In Figure 5-4, typical axial force diagram of a cable-stayed bridge is presented.

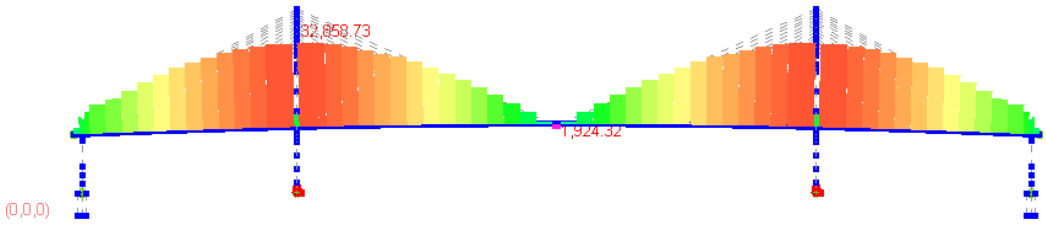

Figure 5-4 Typical Axial Force Diagram

According to diagram shown above, at area of interest axial force is very low. Moreover, axial force is increasing while moving towards to pylons due to cumulative effect of cable forces. In Table 5-2, axial stress calculations on edge girders are tabulated for axial forces at pylons (max. axial force values). In Table 5-3, axial stress calculations on edge girders are tabulated for axial forces at area of interest, mid-span region, (min. axial force values). Please note that total deck cross-section area is 39m x 0.25m = 9.75m^2 and steel yield strength is σ_y=355MPa.

Table 5-2 Axial Stress Values on Steel Edge Girders at Pylons

Main Span Length (m)	Axial Force, P (kN)	Deck Area, A (m^2)	Stress on Deck σ_d= P/A (Mpa)	$r=E_{steel}/E_{concrete}$ (200GPa/32GPa)	Stress on Girder $\sigma_g=r \times \sigma_d$ (Mpa)	Stress Ratio (σ_g/σ_{yield})
420	54,070	9.75	5.55	6.25	34.66	0.10
470	65,718	9.75	6.74	6.25	42.13	0.12
500	72,880	9.75	7.47	6.25	46.72	0.13
550	76,990	9.75	7.90	6.25	49.35	0.14

Table 5-3 Axial Stress Values on Steel Edge Girders at Mid-Span Region

Main Span Length (m)	Axial Force, P (kN)	Deck Area, A (m^2)	Stress on Deck σ_d= P/A (Mpa)	$r=E_{steel}/E_{concrete}$ (200GPa/32GPa)	Stress on Girder $\sigma_g=r \times \sigma_d$ (Mpa)	Stress Ratio (σ_g/σ_{yield})
420	2,332	9.75	0.24	6.25	1.50	0.004
470	3,850	9.75	0.40	6.25	2.50	0.008
500	6,550	9.75	0.68	6.25	4.26	0.012
550	7,560	9.75	0.80	6.25	4.90	0.014

According to Table 5-2, the ratios of axial stress to yield stress of steel at pylons is changing between 0.10 and 0.14. These values are very close to 10% limit to name a structural element as beam. In addition, in Table 5-3 the stress ratios of axial stress to yield stress of steel at mid-span region is very low. Therefore, in this study axial force effects on edge girders are neglected.

5.2 Nominal Flexural Resistance Capacity of Composite Steel Girder Based On AASHTO LRFD Design Specifications

For positive moment region flexural capacity of slab on steel plate bridge girder has been calculated with respect to AASHTO LRFD with nominal resistance values. In AASHTO LRFD Bridge Design Specifications flexural capacity and some design limits that have to be considered are stated.

The steel bridge girders that have slab on them can be expressed as in a simple manner for design purposes. In Figure 5-5, this simplified composite cross-section is presented.

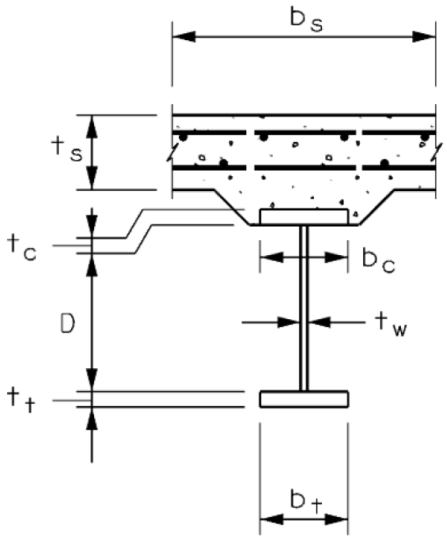

Figure 5-5 Typical Cross-Section of Isolated Composite Steel Girder (AASHTO LRFD 2010)

where b_s is concrete deck effective width, t_s is thickness of the concrete deck, D is depth of web, t_w is web thickness, b_c and b_t are flange widths of top and bottom flanges, respectively, and t_c and t_t are flange thicknesses of top and bottom flanges, respectively.

According to AASHTO LRFD 2010, effective width b_s may be taken as one-half the distance to the adjacent girder from each side. Moreover, according to the Report 543 - Effective Slab Width for Composite Steel Bridge Members belonging to National Cooperative Highway Research Program (NCHRP, 2005), effective slab width at positive moment region, bs, for Cooper River Bridge is the half of the distance between two main girders of bridge. In Figure 5-6, b_{eff}/b ratio equals to 0.99 at the middle of the bridge, where $b_{eff}(b_s)$ is the effective width of slab and b is the half of the distance between the main girders of the bridge.

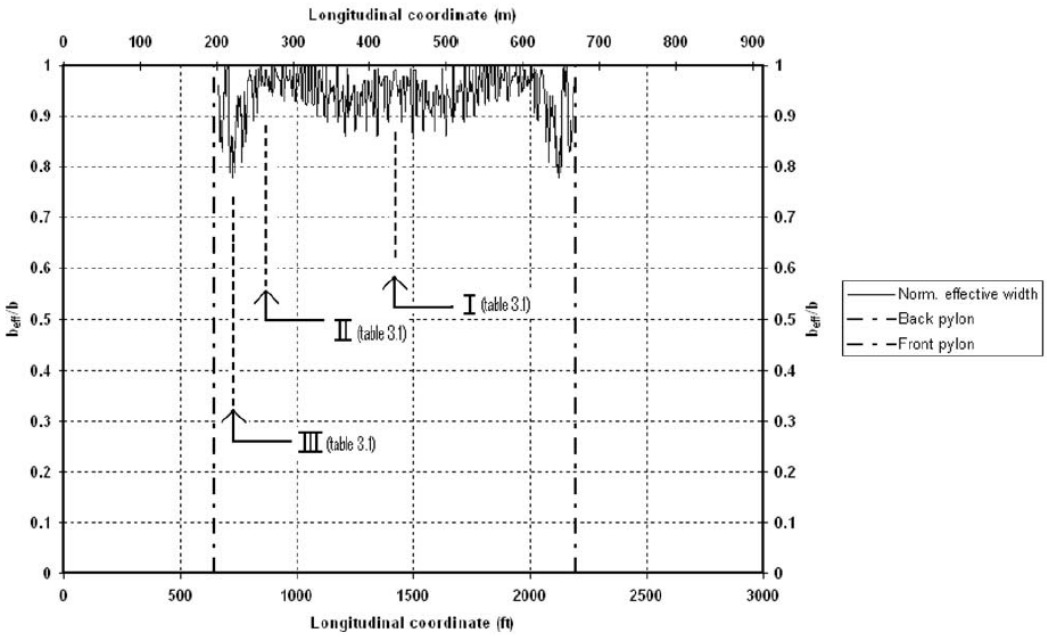

Figure 5-6 Longitudinal distribution of the normalized effective width for the main span of the Cooper River Bridge (NCHRP, 2005)

In this study, effective slab width is chosen as the half of transverse distance of bridge which is 39m / 2=19.5m, as stated in NCHRP report and AASHTO LRFD.

In AASHTO LRFD Bridge Design Specifications (2010), cross-section proportion limitations are stated in the part the 6.10.2. The limits are as the following:

$$\frac{D}{t_w} \leq 150 \tag{4-1a}$$

$$\frac{b_f}{2t_f} \leq 12 \tag{4-1b}$$

$$b_f \geq D/6 \tag{4-1c}$$

$$t_f \geq 1.1t_w \tag{4-1d}$$

The nominal flexural resistance capacity in positive moment region is calculated with following the procedure which is stated in AASHTO LRFD part 6.10.7.1.2.

If $D_p \leq 0.1D_t$;

$$M_n = M_p \tag{4-2a}$$

Otherwise;

$$M_n = M_p(1.07 - 0.7\frac{D_p}{D_t}) \tag{4-2b}$$

in which M_p is plastic moment of the composite section, D_p is the distance between the top of the concrete deck and the composite section's neutral axis for the plastic moment, and D_t is total depth of the composite section.
M_p, plastic moment of composite section, is calculated in accordance with Article D6.1 of AASHTO LRFD. There are seven different possibilities for the location of plastic neutral axis (PNA). M_p is calculated with different a formula for every seven different case. These locations are stated below;

- PNA is in web
- PNA is in top flange
- PNA is in concrete deck below bottom reinforcement
- PNA is in concrete deck at bottom reinforcement
- PNA is in concrete deck above bottom reinforcement and below top reinforcement
- PNA is in concrete deck at top reinforcement
- PNA is in concrete deck above top reinforcement

In Table 5-4 by AASHTO LRFD (2010, as cited in Caner, 2011), Mp, plastic moment of composite section, and PNA location formulas are tabulated for all seven cases. In Figure 5-7, location of PNA for seven cases are illustrated.

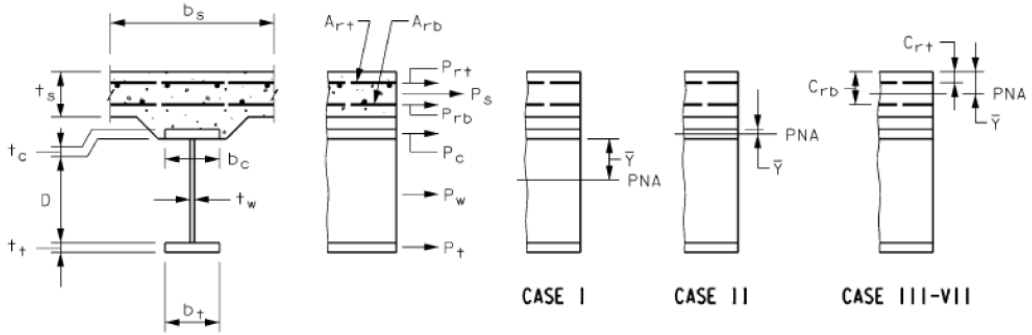

Figure 5-7 Location of PNA: in Web (CASE I), in Flange (CASE II), and in Deck (CASE III-VII) (AASHTO LRFD 2010)

Table 5-4 Plastic Moment and PNA Formulas (AASHTO LRFD, 2010)

Case	PNA	Condition	$\overline{Y}$ and M_p
I	In Web	$P_t+P_w \geq P_c+P_s+P_{rb}+P_{rt}$	$\overline{Y}=\left(\frac{D}{2}\right)\left[\frac{P_t-P_c-P_s-P_{rt}-P_{rb}}{P_w}+1\right]$ $M_p=\frac{P_w}{2D}\left[\overline{Y}^2+(D-\overline{Y})^2\right]+[P_s d_s+P_{rt}d_{rt}+P_{rb}d_{rb}+P_c d_c+P_t d_t]$
II	In Top Flange	$P_t+P_w+P_c \geq P_s+P_{rb}+P_{rt}$	$\overline{Y}=\left(\frac{t_c}{2}\right)\left[\frac{P_w+P_t-P_s-P_{rt}-P_{rb}}{P_c}+1\right]$ $M_p=\frac{P_c}{2t_c}\left[\overline{Y}^2+(t_c-\overline{Y})^2\right]+[P_s d_s+P_{rt}d_{rt}+P_{rb}d_{rb}+P_w d_w+P_t d_t]$
III	Concrete Deck, Below P_{rb}	$P_t+P_w+P_c \geq \left(\frac{C_{rb}}{t_s}\right)P_s+P_{rb}+P_{rt}$	$\overline{Y}=(t_s)\left[\frac{P_c+P_w+P_t-P_{rt}-P_{rb}}{P_s}\right]$ $M_p=\left(\frac{\overline{Y}^2P_s}{2t_s}\right)+[P_{rt}d_{rt}+P_{rb}d_{rb}+P_c d_c+P_w d_w+P_t d_t]$
IV	Concrete Deck, at P_{rb}	$P_t+P_w+P_c+P_{rb} \geq \left(\frac{C_{rb}}{t_s}\right)P_s+P_{rt}$	$\overline{Y}=C_{rb}$ $M_p=\left(\frac{\overline{Y}^2P_s}{2t_s}\right)+[P_{rt}d_{rt}+P_c d_c+P_w d_w+P_t d_t]$
V	Concrete Deck, Above P_{rb} Below P_{rt}	$P_t+P_w+P_c+P_{rb} \geq \left(\frac{C_{rt}}{t_s}\right)P_s+P_{rt}$	$\overline{Y}=(t_s)\left[\frac{P_{rb}+P_c+P_w+P_t-P_{rt}}{P_s}\right]$ $M_p=\left(\frac{\overline{Y}^2P_s}{2t_s}\right)+[P_{rt}d_{rt}+P_{rb}d_{rb}+P_c d_c+P_w d_w+P_t d_t]$
VI	Concrete Deck, at P_{rt}	$P_t+P_w+P_c+P_{rb}+P_{rt} \geq \left(\frac{C_{rt}}{t_s}\right)P_s$	$\overline{Y}=C_{rt}$ $M_p=\left(\frac{\overline{Y}^2P_s}{2t_s}\right)+[P_{rb}d_{rb}+P_c d_c+P_w d_w+P_t d_t]$
VII	Concrete Deck, Above P_{rt}	$P_t+P_w+P_c+P_{rb}+P_{rt} < \left(\frac{C_{rt}}{t_s}\right)P_s$	$\overline{Y}=(t_s)\left[\frac{P_{rb}+P_c+P_w+P_t+P_{rt}}{P_s}\right]$ $M_p=\left(\frac{\overline{Y}^2P_s}{2t_s}\right)+[P_{rt}d_{rt}+P_{rb}d_{rb}+P_c d_c+P_w d_w+P_t d_t]$

As cited in Koç (2013) "P_w is plastic force in the web ($D\times t_w\times F_y$), P_s is plastic compressive force in the concrete deck ($0.85f_c'\times t_s\times b_e$), P_c is plastic force in the compression flange ($t_c\times b_c\times F_y$), P_t is plastic force in the tension flange ($t_t\times b_t\times F_y$), P_{rb} is plastic force in the bottom reinforcement ($F_{yrb}\times A_{rb}$), P_{rt} is plastic force in

the top reinforcement ($F_{yrt} \times A_{rt}$), Y is distance from the plastic neutral axis to the top of the web, d_s is distance from the plastic neutral axis to the mid-thickness of the concrete deck, d_c is distance from the plastic neutral axis to the mid-thickness of the compression flange, d_t is distance from the plastic neutral axis to the mid-thickness of the tension flange, d_w is distance from the plastic neutral axis to the mid-thickness of the web, t_h is average thickness of haunch, b_e is effective width of the concrete deck, F_y is specified minimum yield strength of steel, and f_c' is minimum specified 28-day compressive strength of concrete."

5.3 Flexural Demands of Steel Composite Girders

To obtain the flexural demands at positive moment region of bridges structural analyses are done with using a package program which is Larsa 4D. Structural models of bridges are composed of all frame elements. Girders are defined as having a cross-section of composite beam. Four different structural model was created in accordance with the specified properties and dimensions in the beginning of this chapter. Some illustrations of structural bridge models are presented in the following figures.

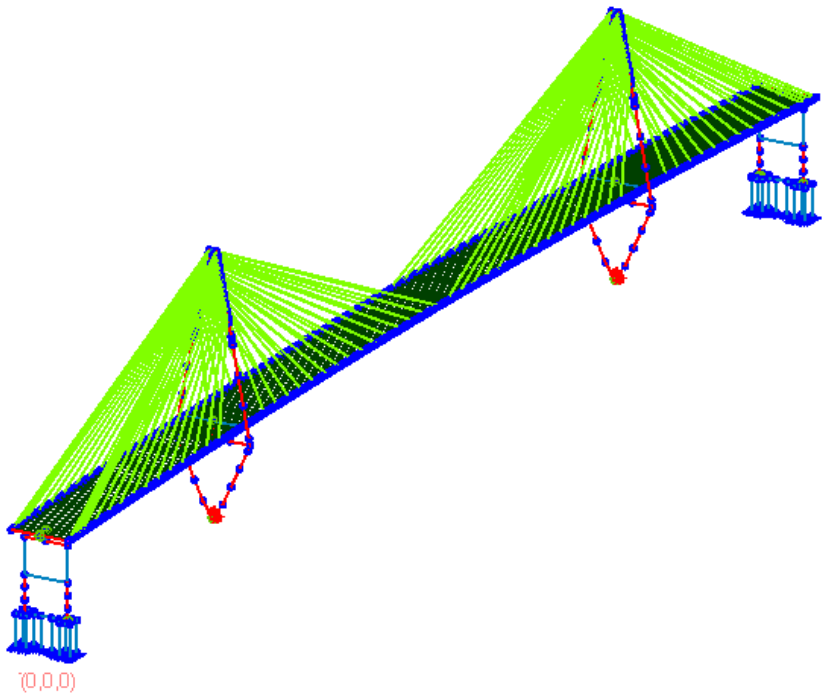

Figure 5-8 Example 3D View of Structural Model created with Larsa 4D

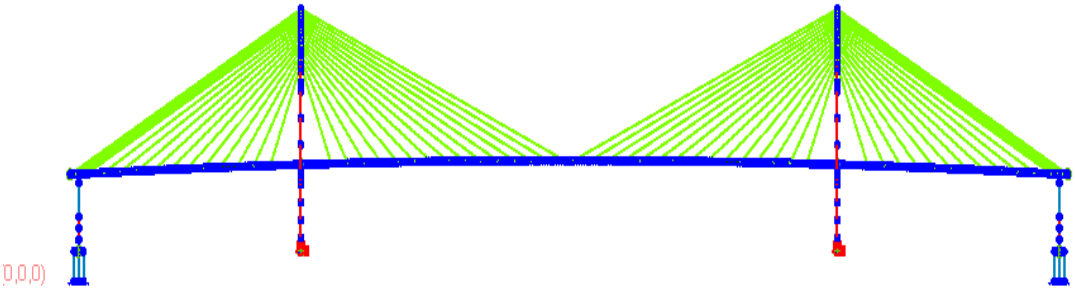

Figure 5-9 Example Side View of Structural Model created with Larsa 4D

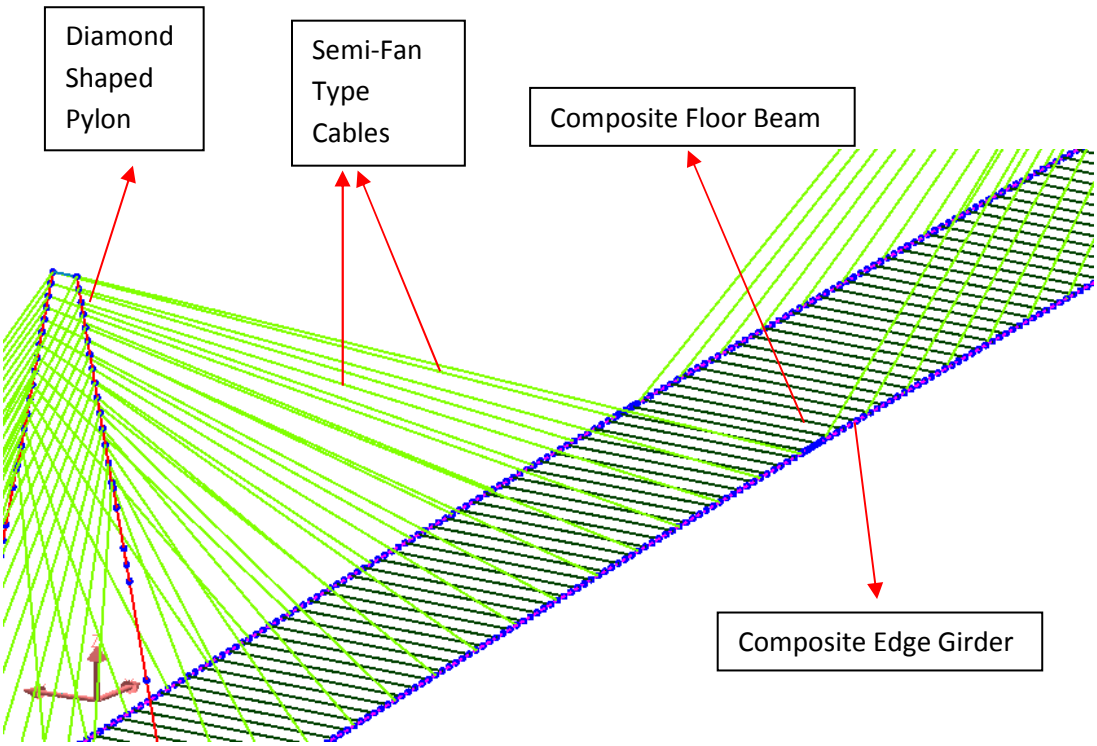

Figure 5-10 Example Close-up View of Structural Model created with Larsa 4D

While obtaining the internal forces of the frame elements two different structural analysis methods are used. These methods are non-linear static analysis and moving load analysis. The basic design philosophy for cable stayed bridges is to carry the dead load of bridge with post-tension forces on cables. In other words, the deflection under dead load should be equal to zero theoretically. Therefore, firstly non-linear static analyses are performed to adjust the deflection of bridge under dead load by

post-tension forces. After adjusting the deflections to the desired values moving load analyses are performed to be able to determine the live load model demands.

5.4 Analysis and Design Results

Four steel girders have been designed according to AASHTO LRFD specifications for span lengths of 420 to 550 m for positive moment region. Designs have been carried out according to Strength I limit state. Selected cross-section dimensions are tabulated in Table 5-5. Moreover, every cross section has a common 25 cm thick concrete slab over the steel girder.

Table 5-5 Designed Section Dimensions w.r.t. AYK-45 Loading

Span (m)	D_t (mm)	D (mm)	t_w (mm)	b_{ft} (mm)	t_{ft} (mm)	b_{fb} (mm)	t_{fb} (mm)
420	1915	1600	15	500	30	600	35
470	1950	1635	15	500	30	600	35
500	1990	1675	15	500	30	600	35
550	2015	1700	15	500	30	600	35

where D_t is total depth of section including concrete slab, D is depth of the web, t_w is thickness of the web, b_{ft} is width of the top flange, t_{ft} is thickness of the top flange, b_{fb} is width of the bottom flange and t_{fb} is thickness of the bottom flange.

In the following tables, ultimate moment values obtained with using Strength I limit state (M_u) and nominal flexural resistance capacities (M_n) are presented for all span lengths and live load models.

According to results tabulated below, M_u values are very close for HL-93 truck loading and grouped truck loading. Moreover, M_u values of H30-S24 truck loading are little bit greater than those of AYK-45 truck loading. M_n values are same for the same span lengths because designs are performed for only AYK-45 loading in order to evaluate the performance of AYK-45 truck loading.

Table 5-6 M_u and M_n values for AYK-45 Loading

Moments (kN.m)	Span Length (m)			
	420	**470**	**500**	**550**
M_{DC}	1865	1870	2100	2002
M_{DW}	1829	1687	1395	1745
M_{LL+IM}	12018	11618	12821	12397
M_{Lane}	2291	2715	2700	2724
M_U (Strength I Limit State)	21351	21171	22373	22320
M_N	27060	27719	28480	28960

Table 5-7 M_u and M_n values for HL-93 Loading

Moments (kN.m)	Span Length (m)			
	420	**470**	**500**	**550**
M_{DC}	1865	1870	2100	2002
M_{DW}	1830	1687	1395	1745
M_{LL+IM}	8669	8352	9111	8911
M_{Lane}	2130	2523	2512	2554
M_U (Strength I Limit State)	17360	17239	17938	18161
M_N	27060	27719	28480	28960

Table 5-8 M_u and M_n values for H30-S24 Loading

Moments (kN.m)	Span Length (m)			
	420	**470**	**500**	**550**
M_{DC}	1865	1870	2100	2002
M_{DW}	1830	1687	1395	1745
M_{LL+IM}	14424	13899	15151	14647
M_{Lane}	2291	2713	2701	2724
M_U (Strength I Limit State)	24089	23764	25025	24880
M_N	27060	27719	28480	28960

Table 5-9 M_u and M_n values for Grouped Truck Loading

Moments (kN.m)	Span Length (m)			
	420	**470**	**500**	**550**
M_{DC}	1865	1870	2100	2002
M_{DW}	1829	1687	1395	1745
M_{LL+IM}	8783	8425	9822	9285
M_{Lane}	2291	2715	2700	2724
M_U (Strength I Limit State)	17672	17540	18961	18780
M_N	27060	27719	28480	28960

5.5 Chapter Summary

In this chapter, nominal resistance capacity of composite edge girder is expressed. Capacity is calculated by using Table 5.2 in AASHTO LRFD (2010) specifications. Furthermore, structural analysis and design results are presented in this chapter. Structural analysis is performed with a package program which is Larsa 4D. Structural bridge models (main span lengths 420m, 470m, 500m and 550m) are created with frame elements. Edge girder design at positive moment region is carried out for AYK-45 loading only and same cross-section is used for other live load model analysis to be able to evaluate the performance of AYK-45 truck loading. According to structural analysis and design results, M_u values are very close for HL-93 truck loading and grouped truck loading. Moreover, M_u values of H30-S24 truck loading are little bit greater than those of AYK-45 truck loading. M_n values are same for the same span lengths because designs are performed for only AYK-45 loading. In chapter 6, reliability analysis and results are presented.

CHAPTER 6

RELIABILITY EVALUATION

6.1 Reliability Model

Engineering design parameters (loads and resistance) include uncertainties, generally. These uncertainties lead to not satisfy the design requirements. In Figure 6-1, fundamentals of the reliability analysis is shown. Two main random variables of the engineering design, load (S) and resistance (R), are presented on figure with their randomness expressing in terms of their means μ_S and μ_R, standard deviations σ_S and σ_R, and corresponding density functions $f_S(s)$ and $f_R(r)$, respectively.

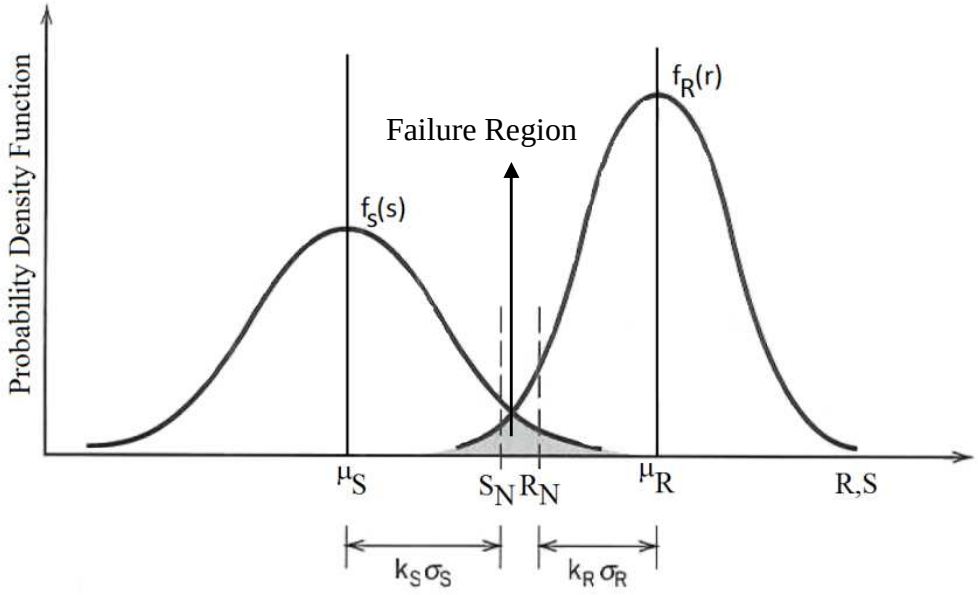

Figure 6-1 Fundamentals of Reliability Analysis

The expression of reliability can be made with probability of survival as well as probability of failure,

$$\begin{aligned} p_f &= P(failure) = P(R < S) \\ &= \int_0^\infty \left[\int_0^s f_R(r)dr\right] f_S(s)ds \\ &= \int_0^\infty F_R(s) f_S(s)ds \end{aligned} \tag{6-1}$$

in which $F_R(s)$ is the cumulative distribution function of resistance R determined at s. Equation 6-1 is considered the primary equation in reliability-based design concept.

Practically load and resistance terms are not independent variables. They depend on various basic random variables like load effects, material properties, etc. The specific design performance criterion, which is called limit state function (performance function or failure function), is defined in terms of these basic random variables as the following:

$$M = R - S = g(\boldsymbol{X}) = g(X_1, X_2, \ldots, X_n) \tag{6-2}$$

in which M is the safety margin and $\boldsymbol{X}$ is the random variable vector. M is a performance indicator for the design. The failure boundary or limit state is the case where $(\boldsymbol{X})=M=0$. Failure surface creates a boundary between survival and failure zones. Figure 6-2 shows this phenomena on a graph for two dimensional state space.

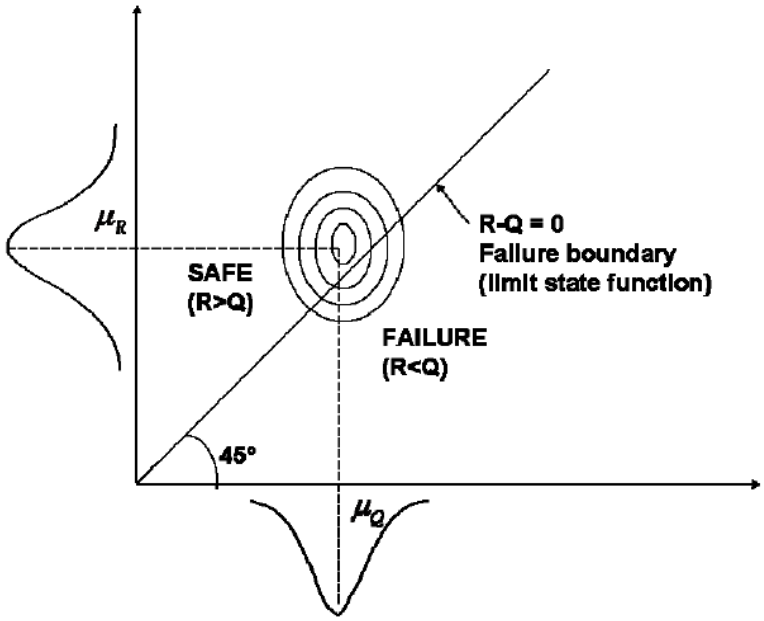

Figure 6-2 Safe Domain and Failure Domain in 2-D State Space

Probability of failure is calculated by solving the following integration,

$$p_f = \int \dots \int_{g(\cdot)<0} f_X(x_1, x_2, \dots, x_n) dx_1 dx_2 \dots dx_n \quad (6\text{-}3)$$

where $fX(x1,x2,\dots,xn)$ is the joint probability density function for the basic random variables. The integral is taken over the failure region. However, there are two main problems with calculation of probability of failure:

- lack of data for obtaining joint probability density function
- difficulty of evaluation of multiple integrals

To overcome these difficulties approximate methods are introduced. In this study, MVFOSM (Mean Value First Order Second Moment) has been introduced and used for reliability analyses.

6.1.1 Mean Value First Order Second Moment Method

The MVFOSM is stated for the first time in the study of Cornell (1969, as cited in Haldar and Mahadevan, 2000). This method depends on Taylor series approximation from the first order. Approximation is carried out around the center of the mean values of random variables for failure function. Therefore, the mean and standard deviation of the failure function, i.e., μ_g and σ_g are used to compute the reliability index term. The reliability index is an indicator of probability of failure as well as probability of survival. In Figure 6-3, the physical meaning of the reliability index is shown, it is the shortest distance in the space of reduced variables. Reliability index is commonly denoted by the Greek letter β, and is formulated as the following:

$$\beta = \frac{\mu_g}{\sigma_g} \quad (6\text{-}4)$$

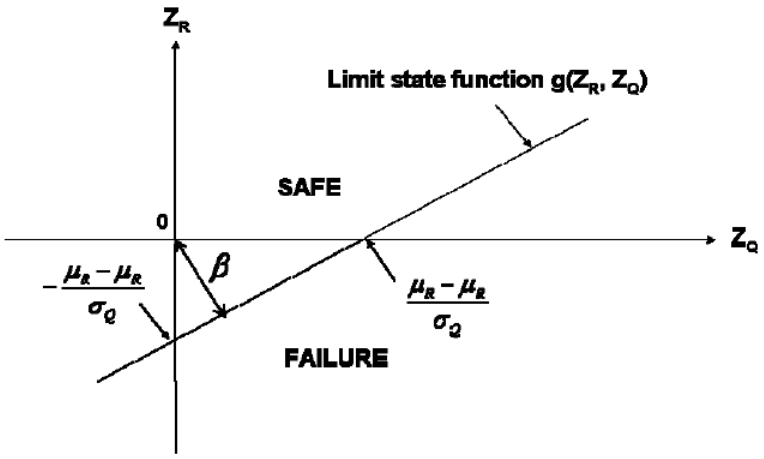

Figure 6-3 Reliability Index Defined as the Shortest Distance in the Space of Reduced Variables

Probability of failure can be defined with using reliability index as the following manner if random variables are normally distributed.

$$P_f = \Phi(-\beta) = 1 - \Phi(\beta) \tag{6-5}$$

in which Φ is standard normal cumulative distribution function. In Table 6-1, reliability indices from 0 to 6 and their corresponding probability of failures are tabulated.

Table 6-1 Reliability Index and the Corresponding Probability of Failure

Reliability Index, β	Probability of Failure, P_f
0	0.5
1	0.159
2	0.0228
3	0.00135
4	0.0000317
5	0.000000287
6	0.000000000987

If failure function is considered as linear, it will be expressed in terms of basic variables $X1,2,\ldots,Xn$ as the following;

$$g(\boldsymbol{X}) = a_0 + a_1 X_1 + \cdots + a_n X_n \tag{6-6}$$

Mean value of failure function can be expressed as;

$$\mu_g = g(\mu_{\boldsymbol{X}}) = a_0 + a_1 \mu_{X_1} + \cdots + a_n \mu_{X_n} \tag{6-7}$$

and variance of the function is expressed as;

$$\sigma_g^2 = a_1^2 \sigma_{X_1}^2 + \cdots + a_n^2 \sigma_{X_n}^2 + \sum_{i=1}^{n} \sum_{j=1, j\neq i}^{n} \frac{\partial g}{\partial X_i} \frac{\partial g}{\partial X_j} Cov(X_i, X_j) \tag{6-8}$$

where $Cov(X_i,X_j)$ is covariance of X_i and X_j, and is equal to $\rho_{XiXj}\sigma X_i \sigma X_j$, in which $\rho XiXj$ is correlation coefficient between X_i and X_j.

"In case $g(\boldsymbol{X})$ is nonlinear, the result of the mean and standard deviation would not be exact, and approximate values of those can be obtained by using a linearized function, which is constructed by expanding failure function in Taylor series centered at the mean values and keeping only the linear terms (Koç,2013)." Therefore, linearized function will be expressed with the following formula;

$$g(\boldsymbol{X}) = g(\mu_{\boldsymbol{X}}) + \sum_{i=1}^{n} \frac{\partial g}{\partial X_i} \left(X_i - \mu_{X_i}\right) \tag{6-9}$$

where $\partial g/\partial X_i$ is evaluated at mean values. Approximate values of μ_g and σ_g are obtained with

$$\mu_g \cong g\left(\mu_{X_1}, \ldots, \mu_{X_n}\right) \tag{6-10}$$

$$\sigma_g^2 \cong \sum_{i=1}^{n}\sum_{j=1}^{n} \frac{\partial g}{\partial X_i}\frac{\partial g}{\partial X_j} Cov\left(X_i, X_j\right) \tag{6-11}$$

6.2 Failure Function

The most basic form of the failure function of structural design can be defined with g = R – Q, where R is flexural resistance capacity and Q is load effect. If g is less than zero, then structure will fail. In that case, the probability of failure is expressed as PF = P(R – Q < 0) = P(g < 0).

Load effect Q is expressed as the following:

$$Q = D_1 + D_2 + D_3 + D_4 + LL\ (1+IM)\ GDF \tag{6-12}$$

in which D1, D2, D3 and D4 are dead load components, LL is live load, IM is impact factor (dynamic load factor) and GDF is girder distribution factor. For detailed information about load components, please refer to Chapter 3.

For the nominal flexural resistance capacity R at positive moment region, please refer to Chapter 5.

6.3 Target Reliability Index

After determining all needed values like demands, resistances, statistical parameters and choosing reliability index calculation method, a target reliability index, β_T should be chosen calibrate the load and resistance factors. The main aim of the calibration of load and resistance factors is to provide a uniform reliability indices in order to calculate β as close as possible to that β_T. Hence, calibration of LRFD provides an advantage of obtaining uniform reliability indices for different spans, and load effects (Moses, 2001).

When the total expected cost of a structure is minimized, then optimum target reliability is determined. The total expected cost involves the cost of project design and construction, and also the expected cost of failure. The cost of failure involves both the cost of replacement or repair and the cost of shortage of use. Moreover, legal costs (liability in case of injuries) are included in the cost of failure. In bridges, there are several different components. For example, cables, girders, pylons, pavement and expansion joints are some of the components of a cable-stayed bridge. It is obvious that failure of a cable or a girder will not have the same consequences with failure of pavement or an expansion joint. Therefore, considering the economy, it is reasonable to separate the bridge components into two as primary and secondary elements. Target reliability index for primary components is higher than that for secondary components. As the main consideration of this study, girders are the primary and repairable components of cable-stayed bridges (Nowak and Szerszen, 2000).

According to Table 6-2, repairable components of bridge have target reliability index equal to 4.32 for 50-years life time and 4.16 for 100-years life time (Inyeol and et. al, 2013). Since life-time of bridges is taken as 75-years in this study, β_T is selected as 4.30 by considering the descending trend of the target reliability indices in Table 6-2 between 20-years and 200-years life times.

In Turkish LRFD method, target reliability index is mentioned as 4.20 for gravity loads and 75-years life time period.

Table 6-2 Target Reliability for Design Life by Classification of Structural Components (Inyeol and et. al, 2013)

Class	Structural Component	Based on 1-year Time Period		Target Reliability Based on Design Life				
		Target Reliability	Probability of Failure	20 year	30 year	50 year	100 year	200 year
(Ref.)	Ordinary Bridge (100 year)	4.75	1.00×10^{-6}	4.11	4.01	3.89	3.72	3.54
1	Replaceable Components (20 year)	4.66	1.58×10^{-6}	4.00	3.90	3.78	3.60	3.42
	Replaceable Components (30 year)	4.74	1.05×10^{-6}	4.10	4.00	3.88	3.71	3.53
	Replaceable Components (50 year)	4.85	6.32×10^{-7}	4.21	4.12	4.00	3.83	3.66
2	Repairable Components Permanent Components	5.11	1.58×10^{-7}	4.52	4.43	4.32	4.16	4.00

6.4 Load and Resistance Factors

In this study, only resistance factor is calibrated. Load factors are used as similar with AASHTO LRFD Specifications. Strength I limit state load factors are summarized in Table 6-3. Resistance factor for flexural design in AASHTO LRFD Specifications is 0.90. In this thesis study, different calibrated resistance factors are introduced for different span lengths for AYK-45, H30-S24, HL-93 and grouped truck loadings. Furthermore, comparison of AYK-45 loading resistance factors with other live load models' resistance factors is investigated.

Table 6-3 Summary of Load Factors (AASHTO LRFD, Strength I Limit)

Load Type	Load Factor
DC	1.25
DW	1.50
LL	1.75
IM	33%

Applied resistance factor calibration procedure for the cross-section dependent method is stated step by step in following:

- All necessary statistical parameters and information for loads and resistance are calculated and gathered.
- AYK-45 live load model flexural demands at mid-span are determined by structural analyses for four different span lengths (iterative procedure).
- For each span length, composite girders are designed until reaching the target reliability index which is 4.30. ($M_n > M_u$) (iterative procedure)
- HL-93, H30-S24 and grouped truck live load models' flexural demands at mid-span are determined by structural analyses for four different span lengths with the same cross-sections designed for AYK-45 loading. (M_n ? M_u)
- Reliability indices are calculated for HL-93, H30-S24 and grouped truck live load models. (β ? 4.30)
- Resistance factor calibration is performed for all live load models and span lengths with satisfying the following limit equation for design.

$$\emptyset M_n = M_u \tag{6-13}$$

This procedure provides to evaluate the performance of new Turkish live load model AYK-45 among the well-known and real life live models for cable-stayed bridges.

Another applied resistance factor calibration procedure for the cross-section independent method is stated step by step in following:

- All necessary statistical parameters and information for loads and resistance are calculated and gathered.
- For each span length and live load model flexural demands at mid-span are determined by structural analyses.
- Directly β's are calculated for different □ values from 0.60 to 0.95 with using equation 6-16. To eliminate the cross-section's effect on the results the following formulae are applied.

Original formula of reliability index is;

$$\beta = \frac{M_n - M_u}{\sqrt{{\sigma_n}^2 + {\sigma_u}^2}} \quad (6\text{-}14)$$

By obtaining M_n from equation 6-13;

$$M_n = \frac{M_u}{\emptyset} \quad (6\text{-}15)$$

By putting Eqn. 6-15 into Eqn. 6-14, reliability index formula is eliminated from the cross-section effect. Note that the components related with cross-section in the σ_n are also eliminated.

$$\beta = \frac{\frac{M_u}{\emptyset} - M_u}{\sqrt{{\sigma_n}^2 + {\sigma_u}^2}} \quad (6\text{-}16)$$

This procedure provides to introduce different calibrated resistance factors for different span lengths for AYK-45, H30-S24, HL-93 and grouped truck loadings.

Reliability analyses and calibration results are presented on the following figures and tables for the constant cross-section which was designed for AYK-45.

Table 6-4 Reliability Index and Calibrated Resistance Factor Values for AYK-45

Span Length (m)	Reliability Index (β)	Calibrated Resistance Factor (□)
420	4.30	0.79
470	4.30	0.77
500	4.30	0.79
550	4.30	0.78

Table 6-5 Reliability Index and Calibrated Resistance Factor Values for H30-S24

Span Length (m)	Reliability Index (β)	Calibrated Resistance Factor (□)
420	4.15	0.9
470	4.18	0.86
500	4.2	0.88
550	4.21	0.86

Table 6-6 Reliability Index and Calibrated Resistance Factor Values for HL-93

Span Length (m)	Reliability Index (β)	Calibrated Resistance Factor (□)
420	4.5	0.65
470	4.46	0.63
500	4.46	0.63
550	4.42	0.63

Table 6-7 Reliability Index and Calibrated Resistance Factor Values for Grouped Truck Loading

Span Length (m)	Reliability Index (β)	Calibrated Resistance Factor (□)
420	4.48	0.66
470	4.44	0.64
500	4.38	0.67
550	4.37	0.65

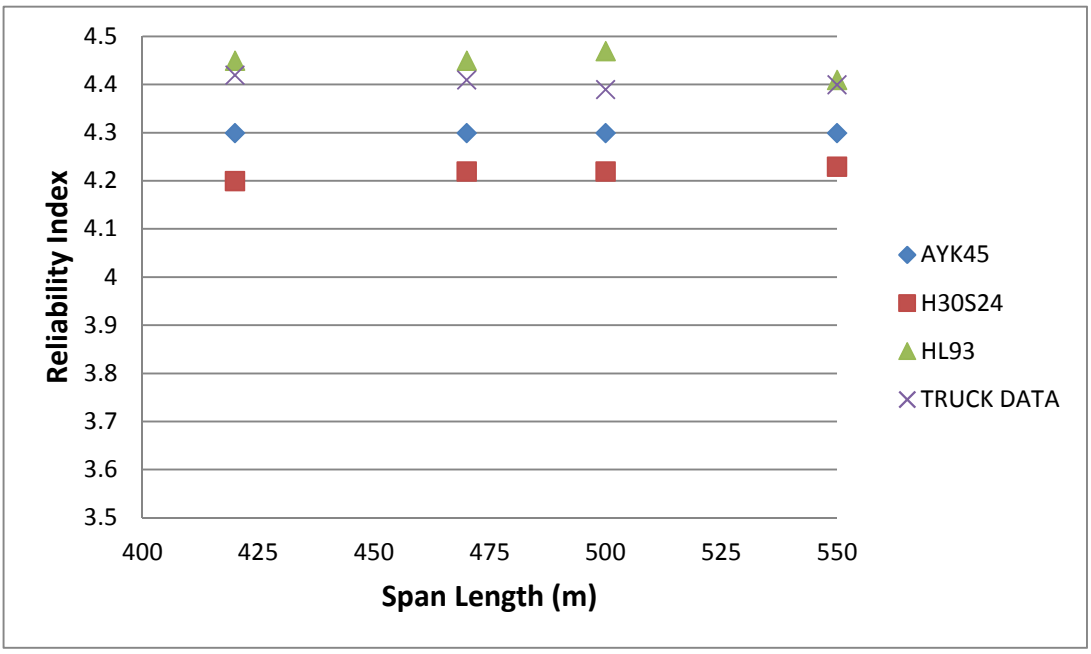

Figure 6-4 Reliability Index versus Span Length for all Live Load Models

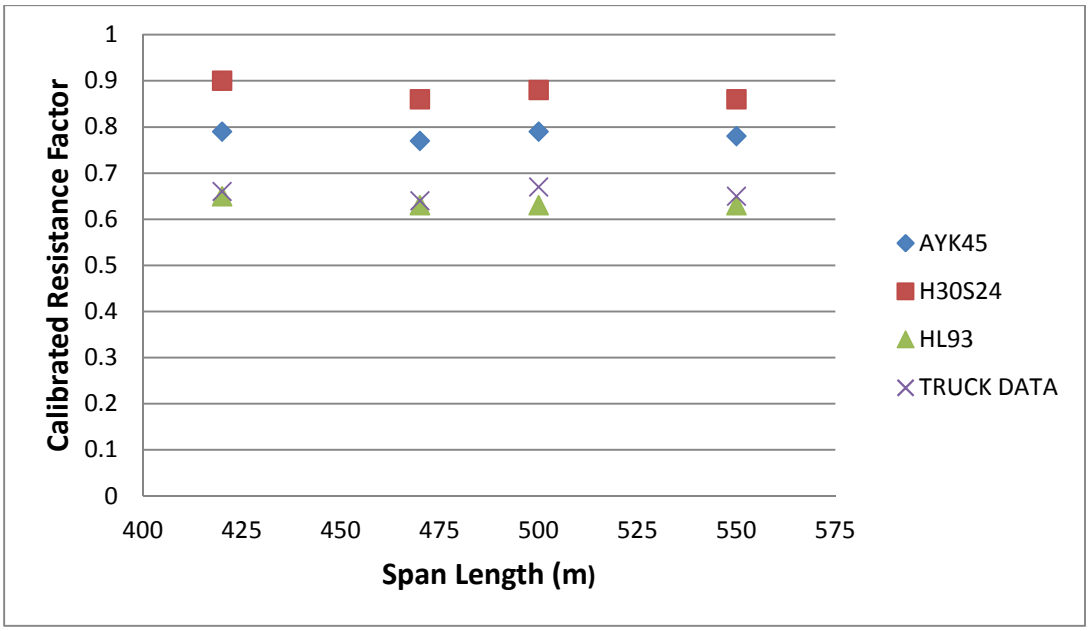

Figure 6-5 Resistance Factor versus Span Length for all Live Load Models

According to tables and figures presented above, AYK-45 truck load is more reliable than the HL-93 and grouped truck load. However, it is not conservative than H30-S24 truck load. Another interpretation is that HL-93 truck load and real life truck traffic load in Turkey give very similar results.

The results on the following tables and figures belong to cross-section independent analyses and studies. Reliability analyses are performed for a different sets of resistance factors i.e. from R=0.60 to R=0.95.

Table 6-8 Reliability Indices for Different Sets of Resistance Factors (AYK-45)

Live Load (LL) & Resistance (R) Factors	Span Length (m)				Average β
	420	470	500	550	
LL: 1.75; R:0.60	4.76	4.7	4.77	4.73	4.74
LL: 1.75; R:0.65	4.63	4.56	4.63	4.59	4.60
LL: 1.75; R:0.70	4.49	4.42	4.5	4.45	4.47
LL: 1.75; R:0.75	4.36	4.29	4.36	4.31	4.33
LL: 1.75; R:0.80	4.22	4.15	4.22	4.18	4.19
LL: 1.75; R:0.85	4.09	4.01	4.09	4.04	4.06
LL: 1.75; R:0.90	3.95	3.87	3.96	3.9	3.92
LL: 1.75; R:0.95	3.82	3.73	3.82	3.77	3.79

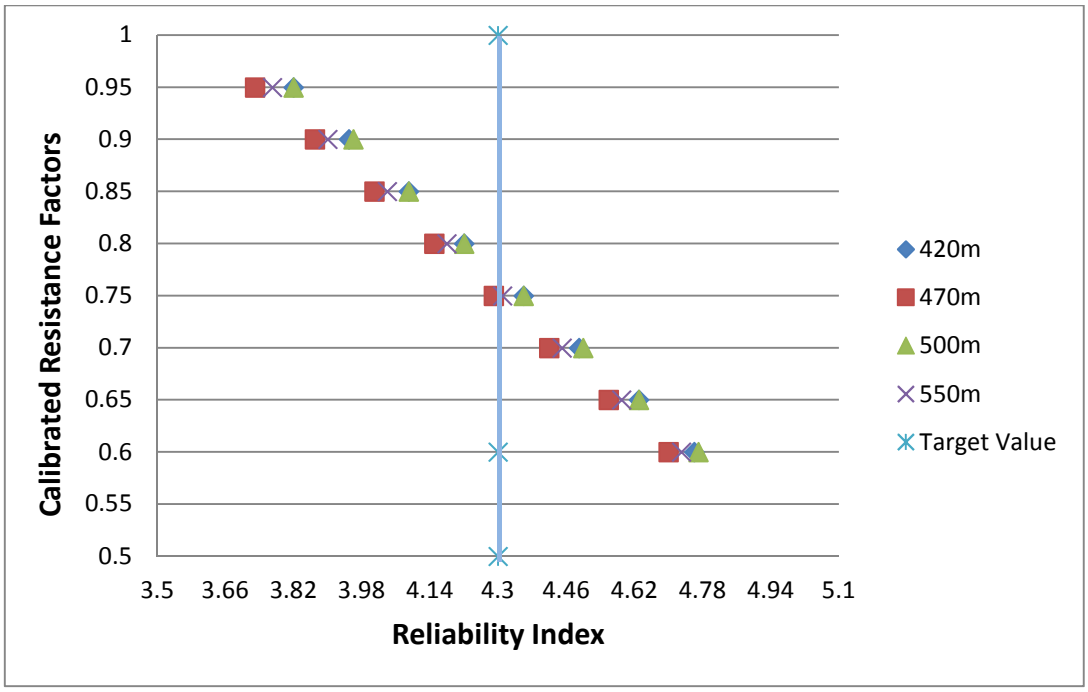

Figure 6-6 Resistance Factor versus Reliability Index (AYK-45)

Table 6-9 Reliability Indices for Different Sets of Resistance Factors (H30-S24)

Live Load (LL) & Resistance (R) Factors	Span Length (m)				Average β
	420	470	500	550	
LL: 1.75; R:0.60	4.88	4.83	4.88	4.85	4.86
LL: 1.75; R:0.65	4.76	4.7	4.76	4.72	4.74
LL: 1.75; R:0.70	4.63	4.57	4.63	4.59	4.61
LL: 1.75; R:0.75	4.5	4.44	4.5	4.46	4.48
LL: 1.75; R:0.80	4.37	4.31	4.37	4.33	4.35
LL: 1.75; R:0.85	4.25	4.18	4.25	4.2	4.22
LL: 1.75; R:0.90	4.12	4.05	4.12	4.07	4.09
LL: 1.75; R:0.95	3.99	3.92	3.99	3.94	3.96

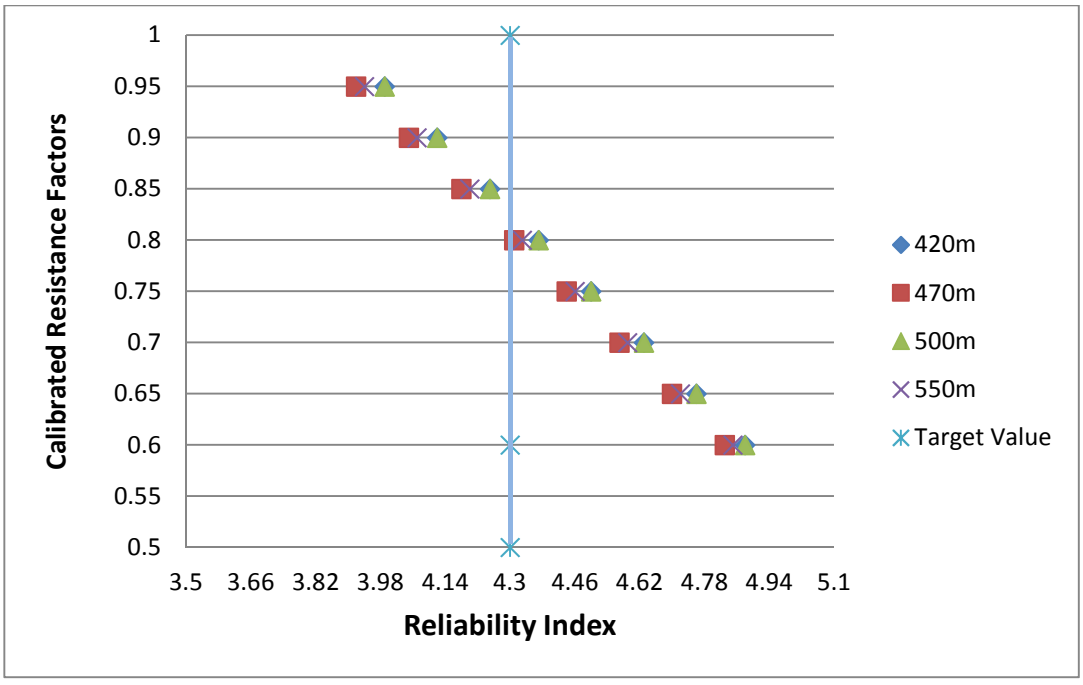

Figure 6-7 Resistance Factor versus Reliability Index (H30-S24)

Table 6-10 Reliability Indices for Different Sets of Resistance Factors (HL-93)

Live Load (LL) & Resistance (R) Factors	Span Length (m)				Average β
	420	470	500	550	
LL: 1.75; R:0.60	4.54	4.47	4.53	4.44	4.50
LL: 1.75; R:0.65	4.39	4.32	4.38	4.29	4.35
LL: 1.75; R:0.70	4.24	4.16	4.23	4.13	4.19
LL: 1.75; R:0.75	4.09	4.01	4.08	3.97	4.04
LL: 1.75; R:0.80	3.94	3.85	3.93	3.82	3.89
LL: 1.75; R:0.85	3.79	3.7	3.78	3.66	3.73
LL: 1.75; R:0.90	3.64	3.55	3.63	3.51	3.58
LL: 1.75; R:0.95	3.49	3.4	3.48	3.35	3.43

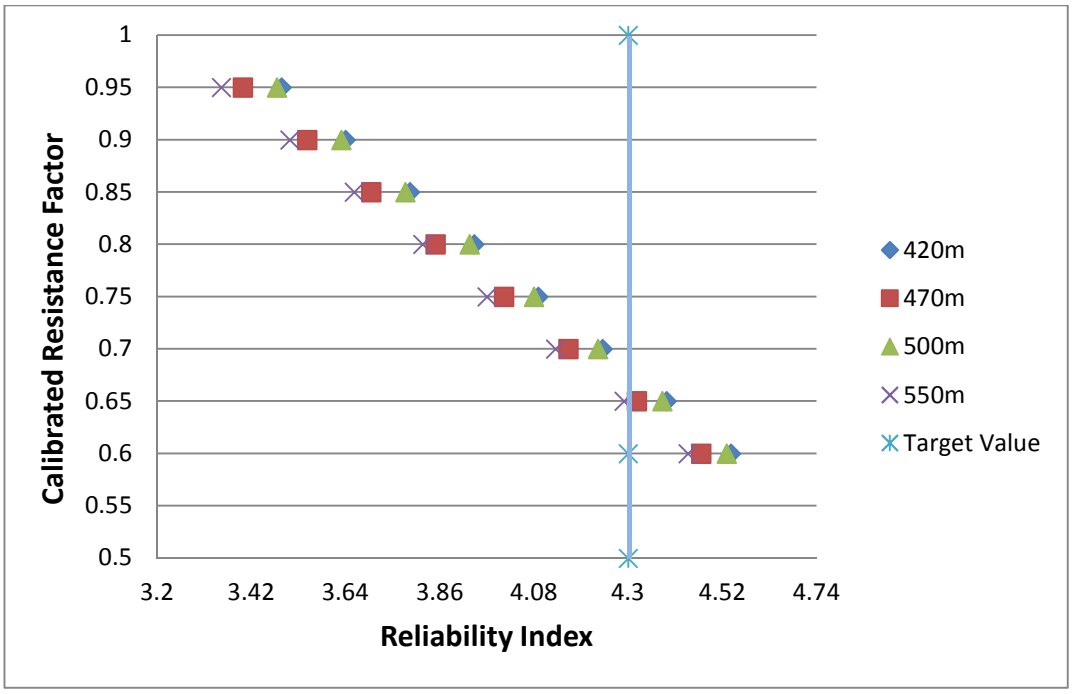

Figure 6-8 Resistance Factor versus Reliability Index (HL-93)

Table 6-11 Reliability Indices for Different Sets of Resistance Factors (Grouped Truck Load)

Live Load (LL) & Resistance (R) Factors	Span Length (m)				Average β
	420	470	500	550	
LL: 1.75; R:0.60	4.53	4.46	4.55	4.5	4.51
LL: 1.75; R:0.65	4.38	4.3	4.4	4.35	4.36
LL: 1.75; R:0.70	4.23	4.15	4.25	4.2	4.21
LL: 1.75; R:0.75	4.08	3.99	4.1	4.04	4.05
LL: 1.75; R:0.80	3.93	3.84	3.96	3.89	3.91
LL: 1.75; R:0.85	3.78	3.68	3.81	3.74	3.75
LL: 1.75; R:0.90	3.63	3.53	3.66	3.59	3.60
LL: 1.75; R:0.95	3.48	3.38	3.51	3.44	3.45

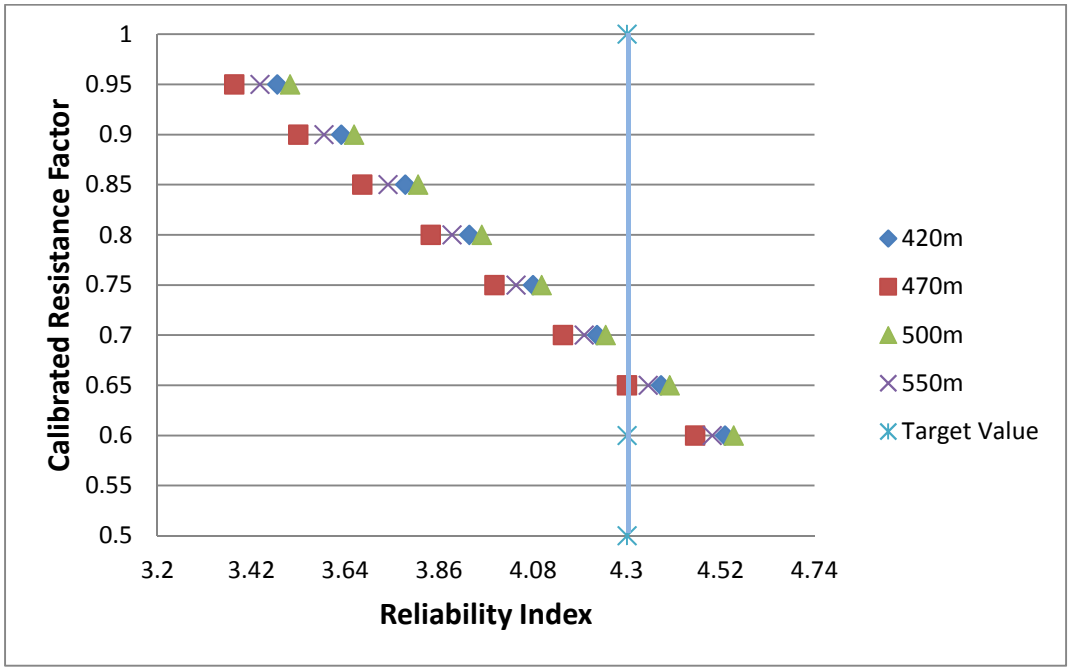

Figure 6-9 Resistance Factor versus Reliability Index (Grouped Truck Load)

According to tables and graphs presented above, the average calibrated resistance factors for the target reliability index that is 4.30 may be considered as;

- AYK-45; R=0.76
- H30-S24; R=0.82
- HL-93; R=0.66
- Grouped Truck Load; R=0.67

6.5 Chapter Summary

In this chapter, reliability concept basics are explained. Moreover, reliability analysis and design results are shown. In reliability analysis Mean Value First Order Second Moment (MVFOSM) method is used. This method depends on Taylor series approximation from the first order. For reliability calculations failure function is determined as g=R-Q where R is flexural resistance capacity and Q is load effect. If g<0, then failure will occur. For this system, target reliability index is selected as 4.30 and as load factors AASHTO LRFD (2010) Strength I Limit state load factors are used. The two different reliability analysis procedures are applied. The first one is cross-section dependent method to investigate the performance of AYK-45 truck loading and the second one is cross-section independent method to introduce different calibrated resistance factors for different span lengths for AYK-45, H30-S24, HL-93 and grouped truck loadings. According to reliability analysis results for cross section dependent method AYK-45 is more reliable than HL-93 and grouped truck live load model which represents an extreme situation in real life traffic. HL-93 truck load and Turkish truck survey data give very close results. It may be concluded that HL-93 truck load is not conservative enough to design special type of bridge like cable-stayed bridges. It may be suitable for only ordinary highway bridges. According to reliability analysis results for cross section independent method the average calibrated resistance factors for the target reliability index that is 4.30 may be considered as;

- AYK-45; R=0.76
- H30-S24; R=0.82
- HL-93; R=0.66
- Grouped Truck Load; R=0.67

In chapter 7, a summary of whole study and concluding comments are presented. Moreover, some recommendations are made for future studies.

CHAPTER 7

CONCLUSION

7.1 Summary and Concluding Comments

Highway bridges were usually designed according to LFD method in Turkey. However, as design method many countries in the world use LRFD. Therefore, Turkish General Directorate of Highways started a study with METU to prepare a design guide based on load and resistance factor design method. In this guide, load and resistance factors are calibrated considering the conditions of Turkey. Moreover, a new live load model is suggested in this guide by Koç (2013) which is AYK-45.

The bridge span lengths, in this study, are 420 m, 470 m, 500 m and 550 m. Four cable-stayed steel composite bridge girders are designed and analyzed at positive moment region with respect to different four live load models, namely AYK-45, H30-S34, HL-93 and grouped truck load. AASHTO LRFD design requirements are used to design the girders. Different than AASHTO LRFD, resistance factors are selected as 0.60, 0.65, 0.70, 0.75, 0.80, 0.85, 0.90 and 0.95. Live load factor is fixed at 1.75. Dead load factors are fixed at 1.25 for structural and nonstructural elements (DC) and 1.50 for wearing surface (DW). Designs are performed for only AYK-45 loading to compare this new loading model with well-known live load models and real traffic load. Moreover, seven different resistance factor is used to determine the calibrated factor that provides the target reliability index (4.30) for all live load models considered in this study with a cross-section independent method.

Load and resistance statistical parameters, namely bias factor and coefficient of variation are determined for the reliability analyses. Mean Value First Order Second Moment Method (MVFOSM) is used to compute the reliability indices. Moreover, probability distribution types of those are determined. To determine the statistical characteristics and values, available local database and international database where local one is not available is used. For example, dead load statistical parameters are obtained from an international study which is Nowak's (1999) study.

Live load statistical parameters are determined with using a truck survey data conducted in Turkey in years 2005, 2006 and 2013 which contains axle distance and weight information of about 28,000 trucks. 2005 and 2006 truck survey data used by Argınhan's study (2010) and Koç's study (2013). In this study, the survey results of the year 2013 are added to the database used by Argınhan and Koç. For the future projection purposes three different cases; overall, upper-tail and extreme are evaluated. However, overall case is investigated because overall case reduces the reliability index and overall case covers the whole survey data. This means that results are more realistic for overall case than the extreme case.

In new design guide for highway bridges of Turkey, target reliability index is selected as 4.30 for calibration of load and resistance factors. However, reliability index is targeted as 3.50 in the USA for the same purpose. In Figure 7-1, the calibrated resistance factors are shown for all live models of this study. These results corresponding to β_T=4.30 are obtained from "overall" case. According to this graph, resistance factor of AYK45 live load model is changing between 0.75 and 0.77. However, resistance factor of H30-S24 live load model is changing between 0.80 and 0.83. As a result, the average calibrated resistance factor based on local parameters may be taken as 0.75 and 0.80 for AYK-45 and H30-S24, respectively. Moreover, HL-93 and grouped survey truck load model show very similar behavior. The calibrated resistance factor is changing between 0.65 and 0.68 for them with a suggested average value of 0.65. If two bridges which have main span lengths of 450m and 550 is designed with AYK-45 loading and the mentioned load and resistance factors are used in design, then a uniform safety level that has a reliability index of 4.30 is provided for both of them. Please note that calibrated resistance factors seem that there is a little fluctuation from bridge to bridge. The main reason of this is not to design the bridge completely. If bridges designed completely, then these fluctuations had disappeared. Since the major aim of this study is not to design a cable stayed bridge, these little fluctuations are allowed.

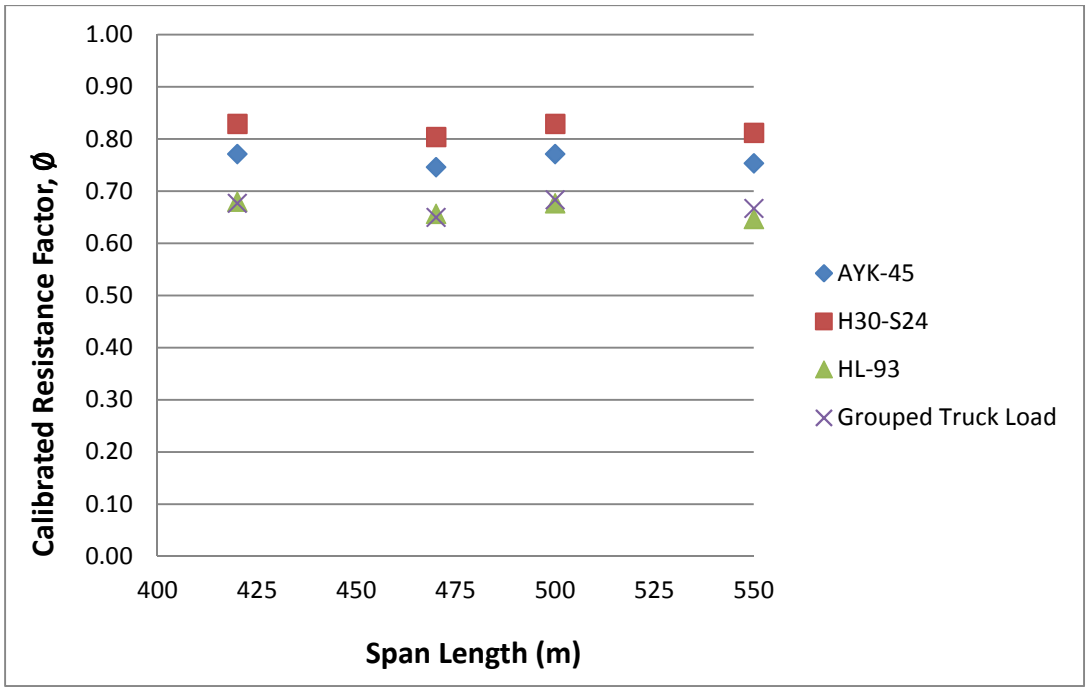

Figure 7-1 Calibrated Resistance Factors Corresponding to β_T=4.30 (Based on Statistical Parameters Obtained from Overall Case for Live Load)

In Figure 7-2 and 7-3, the cross-section dependent study results are presented. Based on these graphs the most conservative truck load is H30-S24 since it the heaviest truck among the live load models of this study. While AYK-45 has a reliability index of 4.30, H30-S24 has a reliability index of 4.22 with the same girder cross-section. However, AYK-45 is more reliable than HL-93 and grouped truck live load model which represents the extreme situation in real life traffic. Furthermore, this study shows that HL-93 truck load and Turkish truck survey data give very close results. It may be concluded that HL-93 truck load is not conservative enough to design special type of bridge like cable-stayed bridges. It may be suitable for only ordinary highway bridges.

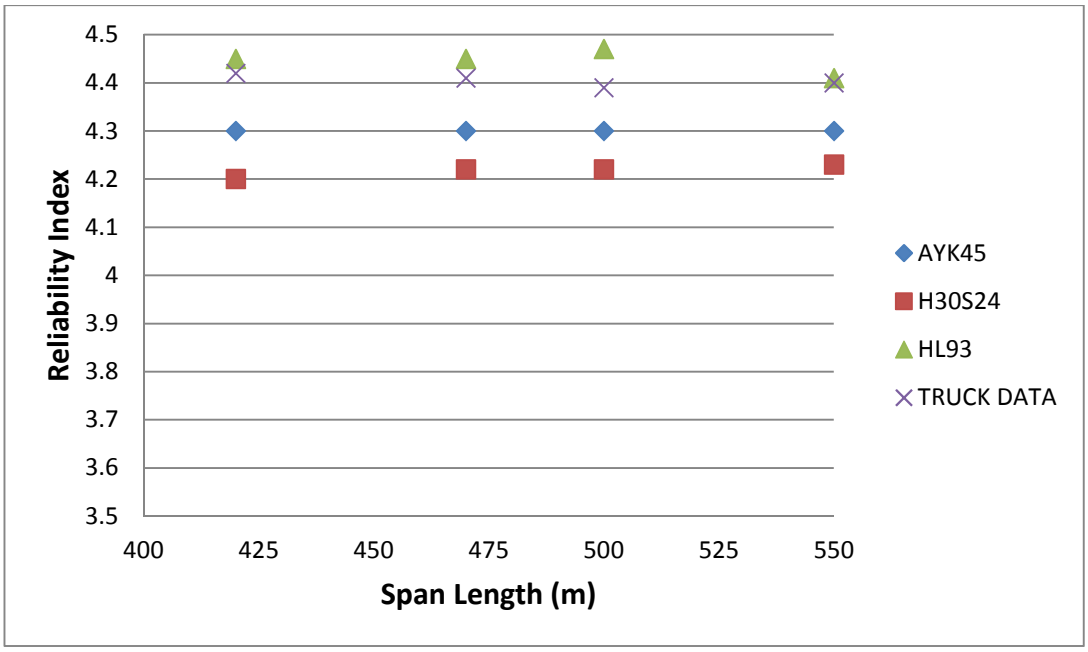

Figure 7-2 Reliability Indices Corresponding to Girder Design Performed for β_T=4.30 for AYK-45, only (Based on Statistical Parameters Obtained from Overall Case for Live Load)

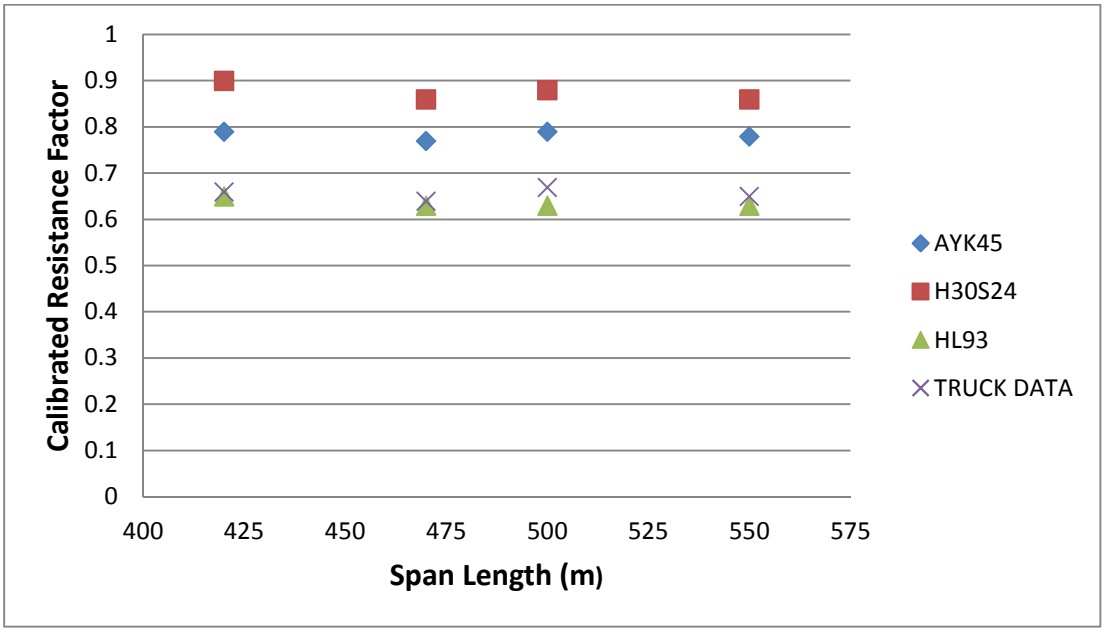

Figure 7-3 Calibrated Resistance Factor Corresponding to Girder Design Performed for β_T=4.30 for AYK-45, only (Based on Statistical Parameters Obtained from Overall Case for Live Load)

7.2 Recommendations for Future Studies

The studied subject in this thesis needs to be repeated for different bridge types, like post-tensioned concrete bridges, reinforced concrete bridges, suspension bridges and arch bridges. Furthermore, this study needs to be expanded for other types of bridge girders. Other than positive moment region failure due to flexure, axial tensile, axial compression, eccentric compression, negative moment region failure due to flexure and shear failure need to be investigated.

Calibrating of design parameters nationally needs to be studied with local data. However, yield strength of steel data is obtained from international sources in this study. Therefore, using local data is very important in future studies.

The calibration process is performed for only live load in this study. However, there are other types of loads taking into consideration for design process, namely wind load, temperature load, earthquake load. Therefore, in future studies these types of loads need to be considered for different limit states.

This study needs to be expanded to other components of bridges rather than girders. As instance to other components of bridges, bracings, piers, pier caps, abutments, foundations, piles may be considered.

REFERENCES

Altay, G., & Güneyisi, E. M. (2008). *Türkiye'de Yapısal Çelik Sektörü ve Yeni Gelişimler.*

American Association of State Highway and Transportation Officials. (2007). *AASHTO LRFD Bridge Design Specifications.* Washington, DC.

American Association of State Highway and Transportation Officials. (2010). *AASHTO LRFD Bridge Design Specifications.* Washington, DC.

Ang, A. H.-S., & Tang, W. H. (1984). *Probability Concepts in Engineering Planning and Design, Vol. 2: Decision, Risk, and Reliability.* John Wiley & Sons Inc.

Argınhan, O. (2010). *Reliability Based Safety Level Evaluation of Turkish Type Precast Prestressed Concrete Bridge Girders Designed in Accordance with the Load and Resistance Factor Design Method, M.Sc. Thesis.* Ankara: The Graduate School of Natural and Applied Sciences, METU.

Barker, R. M., & Puckett, J. A. (2007). *Design of Highway Bridges: an LRFD Approach.* Hoboken, New Jersey: John Wiley & Sons, Inc.

Caner, A. (2011). *Highway and Railroad Infrastructure Lecture Notes*

Castillo, E. (1988). *Extreme Value Theory in Engineering.* Academic Press Inc.

Chen, S.S and et.al. (2005). *NCHRP Report 543: Effective Slab Width for Composite Steel Bridge Members.* Washington, DC: National Academy Press.

Ellingwood, B., Galambos, T. V., MacGregor, J. G., & Cornell, C. A. (1980). *Development of a Probability Based Load Criterion for American National Standard A58.* NPS Special Publication 577.

European Ready Mixed Concrete Organization. (July 2014). *Ready-Mixed Concrete Industry Statistics: Year 2014.*

Fırat, F. K. (2006). Türkiye'de Kullanılan Betonun Kalitesinin İstatistiksel Olarak İncelenmesi. *Yedinci Uluslararası İnşaat Mühendisliğinde Gelişmeler Kongresi, 11-13 Ekim 2006.* İstanbul: Yıldız Teknik Üniversitesi.

Fırat, F. K. (2007). *Development of Load and Resistance Factors for Reinforced Concrete Structures in Turkey, Phd. Thesis.* Ankara: The Graduate School of Natural and Applied Sciences, METU.

Güreş, H. Y. (2013). Çelik Yapı Sektörü 2012 Değerlendirmesi ile 2013 Beklentileri ve Hedefleri.

Haldar, A., & Mahadevan, S. (2000). *Probability, Reliability and Statistical Methods in Engineering Design.* John Wiley & Sons, Inc.

Inyeol, P., Lee, S.H., & Lee, H.S. (2013). Investigation of Design Loads and Load Combinations for Limit State Design of Long Span Cable-Supported Bridge. *IABSE Symposium Report.*

Kesler, C. (1966). Strength. In *Significance of Tests and Properties of Concrete and Concrete-Making Materials, ASTM STP 169A* (pp. 144-159). West Conshohocken, PA: ASTM International.

Koç, A.F. (2013). *Calibration of Turkish LRFD Bridge Design Method for Slab on Steel Plate Girders, M.Sc. Thesis.* Ankara: The Graduate School of Natural and Applied Sciences, METU.

Kun, L., & Qilin, Z. (2012). Research for Calibration and Resistant Factors of LRFD Design of Steel Bridge in China. *Journal of Performance of Constructed Facilities*, Vol. 26, No.2: 212-219.

Li, G. Q., & Li, J. J. (2007). *Advance Analysis and Design of Steel Frames.* John Wiley & Sons, Ltd.

Moses, F. (2001). *NCHRP Report 454: Calibration of Load Factors for LRFR Bridge Evaluation.* Washington, DC: National Academy Press.

Nassif, H. H., & Nowak, A. S. (1995). Dynamic Effect of Truck Loads on Girder Bridges. *Road Transport Technology - 4* (pp. 383-387). Ann Arbor: University of Michigan Transportation Research Institute.

Nowak, A. S. (1999). *NCHRP Report 368: Calibration of LRFD Bridge Design Code.* Washington, DC: National Academy Press.

Nowak, A. S., & Szerszen, M. M. (2000). Structural Reliability as Applied to Highway Bridges. *Prog. Struct. Engng Mater.*, 2:218-224.

T.C. Bayındırlık Bakanlığı, Karayolları Genel Müdürlüğü. (1982). *Yol Köprüleri için Teknik Şartname.* Ankara: Karayolları Genel Müdürlüğü Matbaası.

Türkiye Hazır Beton Birliği. (Nisan 2013). *2012 Yılı Hazır Beton Sektörü İstatistikleri.*

Wang, Y., Zongyu, G., Wang, Z., & Yang, J. (2014). A Case Study of Traffic Load for Long-Span Suspension Bridges. *Structural Engineering International.*